ENERGY TRANSFER IN POLAR POLYATOMIC GASES

By

HENRY ELLIS BASS
II

Bachelor of Science

Oklahoma State University

Stillwater, Oklahoma

1965

Submitted to the Faculty of the Graduate College
of the Oklahoma State University
in partial fulfillment of the requirements
for the Degree of
DOCTOR OF PHILOSOPHY
May 16, 1971

OKLAHOMA STATE UNIVERSITY LIBRARY
AUG 11 1971

ENERGY TRANSFER IN POLAR POLYATOMIC GASES

Thesis Approved:

Thomas G Hunter
Thesis Adviser

Leonid M. Raff

James Lange

D Durham
Dean of the Graduate College

788161

ACKNOWLEDGEMENTS

I take this opportunity to express sincere appreciation to Dr. T. G. Winter for providing the experimental equipment and directing the course of this investigation. His constant encouragement and moral support were instrumental in the culmination of my graduate education. Appreciation is also expressed to Drs. L. M. Raff, and J. N. Lange for serving on the Ph.D. advisory committee.

Particular thanks is extended to Mr. Heinz Hall of the Physics and Chemistry Instrument Shop for designing the ultrasonic instrument used in this investigation and to Mr. Richard Gruhlkey and Mr. Frank Hargrove for constructing the instrument.

I also wish to thank Dr. Landon Evans for suggesting this investigation and for many hours of stimulating discussion on the general problem.

Financial support made available by the National Science Foundation and the National Aeronautical and Space Administration is also gratefully acknowledged. Finally, I wish to express my gratitude to my wife, Ruby, my daughters, Belinda and Christine, and my son, Hank, for their patience and understanding throughout the course of this investigation.

TABLE OF CONTENTS

LIST OF TABLES

LIST OF FIGURES

LIST OF FIGURES (Continued)

LIST OF FIGURES (Continued)

CHAPTER I

INTRODUCTION

Opening Remarks

Probably the most serious failure in the present day kinetic theory of gases is the question of how to treat the internal degrees of freedom in the calculation of transport properties. Because we do not understand the excitation of vibration and rotation, we cannot predict gas viscosity, thermal conductivity, or even the velocity of sound. In the gas phase, energy is transferred from the translational degrees of freedom to the internal degrees of freedom during collisions. Since the dynamics of such encounters determine various properties of the gas, these same properties can be studied to gain some insight into the dynamics of the collisions. Based upon the physical insight obtained from various measurements, a theoretical model of the collision can be formulated. Such a model can be tested by further measurements, and hopefully a model will evolve which will correlate all transport properties.

Landau and Teller (L-T)[1] computed the probability of energy transfer between the vibrational degree of freedom and translation (v-t) during a collision using time dependent perturbation theory and assuming that the intermolecular potential is repulsive varying exponentially with the distance between colliding molecules. Their results indicated that as the static temperature (T) of a system increases, the probability of transferring energy from translation to the vibrational degrees of

freedom should increase as $\exp(T^{-1/3})$. They further found that as the mass of the colliding molecules increases, the probability of energy transfer should decrease. More sophisticated v-t theories give results with the same general characteristics. Although v-t theory has been very successful in predicting most experimentally measured transition probabilities, in the past twenty years different investigators have found evidence that a few molecules do not follow the predictions of Landau-Teller theory.

As early as 1953 it was found that as the static temperature of H_2O/CO_2 mixtures was increased, the CO_2 vibrational transition probabilities for CO_2 - H_2O collisions decreased in direct violation of L-T theory. It was also noted that the calculated transition probabilities were much lower than those measured. For many years, these discrepancies were attributed to some chemical affinity between the CO_2 and H_2O molecules[2]. This explanation was generally accepted until 1967 when Shields and Burks[3] made measurements in CO_2/D_2O mixtures and found a similar temperature dependence and unusually high transition probabilities. Shields and Burks were able to account for the high transition probabilities and the negative temperature dependence using a collision model in which energy was transferred from the vibrational degrees of freedom to the rotational degrees (v-r). This concept of a v-r energy transfer was certainly not new. Millikan and Osborn[4] had already established that the rotational state of colliding molecules affected the probability of transferring energy into the vibrational mode. In addition, Cottrell and several co-workers[5,6] had independently established the presence of v-r energy transfer by comparing the relaxation times of various hydrides with their deuterides. Moore[7] elaborated on their

work and established several criteria for the dominance of v-r energy transfer.

Although the concept of v-r energy transfer was not new, Shields and Burks' use of v-r theory to explain the temperature dependence of CO_2/H_2O and CO_2/D_2O transition probabilities was a significant achievement in the understanding of energy transfer. Recently, Sharma has applied a much more sophisticated theory to the CO_2/N_2[8] and CO_2/H_2[9] systems and has found that v-r exchange is important in determining the temperature dependence of the transition probabilities. The formulation of a fairly reliable v-r theory still left several questions unanswered. One such question is: If v-r transfer leads to the unusual temperature dependence in CO_2/impurity mixtures, why is a similar dependence observed in other molecules which do not meet Moore's criteria for v-r energy transfer? Another question is: Why do some molecules which meet all the criteria for v-r energy transfer follow the temperature dependence predicted by L-T theory? These and other questions prompted this investigation.

Purpose and Scope

The purpose of this investigation was to study the role of v-r energy transfer and intermolecular potentials in determining the temperature dependence of the vibrational transition times. In order to accomplish this objective, it was decided to measure the ultrasonic absorption. Rather than make measurements on a large number of molecules trying to find ones which exhibit the strange temperature dependence desired, a few molecules with varying intermolecular forces and moments of inertia were chosen. This group was chosen to include molecules which

meet Moore's criteria for v-r energy transfer with both small and large dipole moments and molecules which do not meet Moore's criteria but do have large dipole moments. The effect of presumed v-r transfer and dipole moments could then be determined by a process of elimination.

First, a molecule was needed which exchanges energy by v-r but has no dipole moment. This molecule would be used to illustrate the effect of v-r energy transfer on the temperature dependence of the vibrational transition probabilities. Methane was chosen for this molecule. It has no permanent dipole moment and the dominance of v-r energy transfer has been established by Cottrell[5]. Second, a molecule was needed which exchanges energy v-r and has a large dipole moment. By comparing the temperature dependence of the vibrational relaxation time of this molecule with that of CH_4, since both exchange energy v-r, the effect of the dipole moment on such a transfer could be isolated. Two molecules were chosen for this comparison; NH_3 and H_2S. The presence of v-r transfer hasn't been established in these two molecules but both meet Moore's criteria for the dominance of such a process and both have permanent dipole moments of different magnitudes. A fourth molecule was required which has a large dipole moment and exchanges energy v-t. By comparison with H_2S and NH_3, which also have large dipole moments but exchange energy v-r, the effect of the energy transfer process (v-r or v-t) on the temperature dependence of the vibrational transition probabilities could be isolated. Two molecules were also chosen for this comparison; SO_2 and CHF_3.

Many other molecules such as H_2O, D_2S, D_2O, AsH_3, PH_3, and SbH_3 could have been used in place of H_2S and NH_3. The latter were chosen for a variety of reasons. AsH_3 and PH_3 are deadly and highly explosive.

D_2O and D_2S are expensive, and H_2O requires special gas handling equipment if reliable results are to be obtained.

Once the above molecules were selected, a secondary investigation of interest was decided upon; an investigation of the temperature dependence of the rotational relaxation times of polyatomic polar molecules. Actually, this investigation was a bonus since the rotational relaxation times had to be determined in the course of the vibrational experiment anyway. Four of the molecules selected have large dipole moments and their relaxation times were used to determine the applicability of Zeleznik's[10] theory of r-t energy transfer to polyatomic polar molecules. Evans[11] confirmed that this theory gives acceptable results for two diatomic polar molecules and although Zeleznik's theory is only derived for the diatomic case, he has generalized it to include polyatomics.

Discussion of the Remainder of the Thesis

The necessary theory for understanding the experimental results is presented in Chapter II. The chapter starts with a few basic definitions which relate the experimentally determined relaxation times to the theoretically calculated collision numbers. Next, the experimental method along with capabilities, and limitations is discussed. The equations used to reduce the experimental data and assumptions made are presented. Finally, the different types of energy transfer theories are discussed with special emphasis placed on the temperature and mass dependence of the calculated transition probabilities.

The experimental data is presented in Chapter III. The method used to extract relaxation times from experimental absorption data and the

method used for error analysis are discussed. Next the experimental results are given along with a brief discussion of previous results on the gas and reasons for any discrepancies.

The conclusions from this investigation are given in Chapter IV. The experimental results of Chapter III are examined in light of the theory presented in Chapter II and conclusions as to the applicability of this theory are drawn. The appendicies contain information on the experimental method and a derivation of the equations which relate ultrasonic absorption and velocity to molecular constants and relaxation times. This derivation is a consolidation and expansion of the work of several authors.

CHAPTER II

THEORY

Definitions

When experimentally determining the probability of transferring either rotational or vibrational energy during a molecular collision, there are two problems which must be solved. First, a suitable experimental method must be devised which measures some quantity which is dependent upon the dynamics of the collision. Secondly, the experimental results must be analyzed to give parameters which can be theoretically calculated to confirm or disprove particular collision models. In ultrasonic absorption measurements, the quantities measured are the received signal strength and path length. These quantities can be used to calculate the coefficient of absorption at various pressures. Ideally, theoretical calculations based on an assumed collision model would yield absorption coefficients as a function of pressure. In practice, a more indirect method is used to relate theory to experiment.

Ultrasonic absorption can be related to the vibrational and rotational relaxation times using the theory given in the next section. Usually, rather than relaxation times, theoretical calculations give the probability of transferring a quantum of energy during a collision (P_{10}). In order to relate P_{10} to the relaxation time β, the collision frequency must be determined. If this latter quantity is called M, then for an energy transfer process where only one mode is gaining and losing

energy[12],

$$\beta = (MP_{10})^{-1}(1-\exp(-h\nu/kT))^{-1} \quad (1)$$

where ν is the frequency of vibration. For rotational energy transfer, the exponential factor is omitted. This form is somewhat different from that used by Herzfield and Litovitz[13] who omit the exponential factor and instead include this factor in the theoretical expressions for P_{10}. The collision number, Z, is $1/P_{10}$. There are many theories for obtaining P_{10} assuming various models for the collision, however, for polar molecules the term M is very poorly defined. Most investigators obtain M using a "hard spheres" collision model and experimental viscosity values. This method gives

$$M = 1.271\ P/\eta \quad (2)$$

where η is the viscosity and P is the pressure. This expression is probably not very accurate for molecules which interact via long range angle dependent forces. It does, however, represent the best available expression for the collision frequency and gives results which are directly comparable to the work of previous investigators.

Calculating P_{10} using one model, calculating M using a "hard spheres" model and then comparing experimental collision numbers to theoretical ones is very discomforting. An alternative method was used by Raff and Winter[14] when calculating velocity dispersion due to rotational relaxation. This method relates theoretically derived rate constants directly to velocity dispersion thus eliminating the need for a collision frequency. This method is far superior to that outlined above provided the theoretical expression for the rate constants is correct. If these constants are not accurately known, it is often more

convenient and just as meaningful to relate experiment and theory to one quantity, Z, and then see how this quantity varies with physical parameters both theoretically and experimentally. Hopefully, this process will allow incorrect collision models to be eliminated making a more exact comparison between experiment and theory possible.

Experimental Determination of Relaxation Times Using Ultrasonics

Prior to measuring relaxation times acoustically, several factors affecting the use of ultrasonic absorption and velocity dispersion data to obtain relaxation times had to be considered. First, the decision had to be made whether to place emphasis on absorption measurements or velocity measurements. Several authors[15,16] have pointed out that absorption measurements are best suited for the analysis of multiple relaxation processes. Since this investigation involved such processes, the decision was made to emphasize absorption data.

There are several types of instruments which can be used to measure ultrasonic absorption[(12)]. The two most common are the ultrasonic interferometer and the ultrasonic spectrometer. The interferometer consists of a sending transducer and a reflector or receiving transducer. Standing waves are set up between the sender and reflector whenever the pathlength is an integral number of half-wavelengths. The wavelength is measured by moving the reflector or transducer and observing the input impedance of the transmitter or the received signal strength. When a standing wave condition is reached, the current through the transducers changes sharply giving a series of voltage spikes as a function of path length. The absorption is determined by measuring the magnitude of these spikes. The interferometer is characterized by highly accurate velocity

measurements. Accurate absorption coefficients can also be obtained provided the sending transducer and reflector are held parallel with a high degree of precision[12].

An ultrasonic spectrometer is very similar in design to an interferometer. The primary design difference is the reduced requirement on transducer parallelism. The spectrometer operates with path lengths large enough so that all reflected waves are absorbed before reaching the receiving transducer, i.e., out of the standing wave region. In this region, the absorption is related simply to the path length and observed signal strength. The spectrometer, then, is characterized by precise absorption measurements which makes it ideally suited for this investigation. Accurate velocity measurements can be made, however, the accuracy is not comparable to that of an interferometer due to the shorter path length variation experimentally attainable.

Consider an ultrasonic spectrometer consisting of a sending transducer and a receiving transducer separated by a distance x. Let α be the absorption coefficient. An acoustic wave transmitted from the sender will be partially received by the receiving transducer and partially reflected. The reflected part may also be partially reflected back to the receiver where it will add to the originally received wave with a phase factor determined by the velocity and x. This reflected wave will have travelled a path length 2x greater than the original wave. In order to assure that the recorded signal at the transducer is not affected by a reflected wave, the reflected signal should be very small compared to the direct signal. A 10% reflected wave, i.e., I(reflected)/I(original) = .1 will make the recorded signal vary by plus or minus 10%, depending on the phase angle between the two signals. An error of 20% will be

introduced into the absorption measurement. In order to achieve a 10% reflected wave, αx must be equal to 1.15 which means that the intensity at the separation which just meets the 10% criterion has been attenuated about 10 db before attenuation measurements can begin. At high f/P values, 10 db may represent the entire signal.

At first glance, it might appear that as the absorption increases, the minimum allowable rod separation decreases accordingly thus allowing absorption measurements at very high attenuations out of the standing wave region. In fact, the acoustic signal introduced into the gas decreases as the pressure is decreased due to the acoustic mismatch at the gas-transducer boundary. This effect adds to the increase in attenuation at high f/P values. At very high values of f/P, the absorption no longer increases with decreasing pressure. The observed signal, however, continues to decrease due to the increased impedance mismatch. At zero pressure, the attenuation is zero, however, the impedance mismatch is infinite allowing no signal to be introduced into the gas.

One way of overcoming the problem of standing waves is to use a pulsed signal. A short pulse train is transmitted and before the reflected wave can reach the receiver, the pulse is terminated. The original wave can then be observed separately from the reflected wave provided the pulse length does not allow a standing wave, and provided the time between pulses allows time for all reflections to be absorbed or received. The pulse method also allows separation of the acoustic signal which travels a short distance through the gas and the mechanical signal which travels a greater distance through the base of the instrument. A pulsed spectrometer was used in this investigation.

The use of absorption data to analyze relaxation processes is very

limited. The longest relaxation time which can be measured using this technique is governed by the diameter of the transducers and quartz coupling rods available. In order to generate plane waves for which the theory is applicable the wavelength of sound in the crystal must be much less than the diameter of the face of the crystal. Quartz rods are only available up to about 1" in diameter which means the frequency must be about 1 MHz. f/P values less than 1 MHz can be obtained by pressurizing the system. Pressurization is limited by safety requirements, construction of the instrument, and characteristics of the gas used, i.e., vapor pressure, reactivity, etc.

The shortest relaxation time which can be measured is determined by the classical absorption of the gas compared to the relaxation absorption at the f/P for maximum relaxation absorption. If the relaxation absorption is less than 10% of the total measured absorption, it will be less than the experimental error at high f/P values and will be masked in the experimental scatter. A statistical analysis of many data points may give reliable results even when the relaxation absorption is slightly less than the experimental scatter. A more quantitative discussion is given in the section on experimental error.

To illustrate the above situation, consider a relaxation process where the relaxing specific heat is 3/2·R (rotational relaxation of a polyatomic molecule) and the relaxation time is 10^{-10} sec. At 100 MHz, let us say the classical absorption is 1,000 db/inch. The relaxation absorption at this frequency would be much less than 10 db/inch since the maximum which occurs around 200 MHz is only about 10 db/inch. If the relaxation time were 10^{-9} seconds, the relaxation peak could be observed and the relaxation time measured. Although the numerical values

used here are hypothetical, they are of the correct order of magnitude.

It is shown in Appendix C that the experimental absorption can be related to the relaxation times of the various processes present by the expression

$$\frac{k^2}{\omega^2} = \frac{\rho_o}{B_T}\left\{\frac{\bar{C}_v + \sum_{i=1}^{n}\frac{C_i'}{1+i\omega\tau_i}}{\bar{C}_p + \sum_{i=1}^{n}\frac{C_i'}{1+i\omega\tau_i}}\right\} - \frac{\rho_o}{B_T}\left\{\frac{\bar{C}_v + \sum_{i=1}^{n}\frac{C_i'}{1+i\omega\tau_i}}{\bar{C}_p + \sum_{i=1}^{n}\frac{C_i'}{1+i\omega\tau_i}}\right\} \cdot$$

$$\left\{\frac{1}{\bar{C}_v + \sum_{i=1}^{n}\frac{C_i'}{1+i\omega\tau_i}} - \frac{1}{\bar{C}_p + \sum_{i=1}^{n}\frac{C_i'}{1+i\omega\tau_i}}\right\} iWk^2 - i\omega \cdot \frac{4}{3}\eta\frac{\rho_o}{B_T^2} \qquad (3)$$

$$\left\{\bar{C}_v + \sum_{i=1}^{n}\frac{C_i'}{1+i\omega\tau_i}/\bar{C}_p + \sum_{i=1}^{n}\frac{C_i'}{1+i\omega\tau_i}\right\}^2$$

where $k^2 = (\omega/v - i\alpha)^2$

α = coefficient of absorption

ρ_o = static density = m/v

$B_t = \rho_o(\partial P/\partial\rho)T = RT/M$

$\bar{C}_v$ = constant volume specific heat of translation = 3/2 R

$\bar{C}_p$ = constant pressure specific heat of translation = 5/2 R

C_i' = specific heat of ith internal mode

ω = angular frequency of acoustic wave

$W = \nu m/\rho_o\omega$

λ = thermal conductivity

m = mass

τ_i = relaxation time of ith internal mode

The specific heat of rotation was set equal to 3/2 R. Using the Euken approximation (17) λ was set equal to $\eta/m \{1 + \frac{9}{4} R [\bar{C}_v + \sum_{i=1}^{n} \frac{C'_i}{1+i\omega\tau_i}]\}$. When only one vibrational relaxation time was observed, which indicated vibration relaxed in series, C_{vib}/R was set equal to $C_p/R-4$ (18).

Following the example of McCoubrey (12), the measured vibrational relaxation time τ_{vib} was related to the relaxation time of the lowest vibrational mode β_{vib} by the expression

$$\beta_{vib} = \tau_{vib} \cdot \frac{C_s}{C_{vib}} \tag{4}$$

where the Plank-Einstein relation was used to calculate C_s;

$$C_s = R(\theta/T)^2 e^{\theta/T}/(e^{\theta/T} - 1)^2 \tag{5}$$

where θ = characteristic temperature of vibration. Shields (19) has examined the accuracy of Equation 4 and has found it to be acceptable provided $\bar{v}$-$\bar{v}$ transfer is at least as fast as v-t. The rotational relaxation time, $\tau_{rot} = \beta_{rot}$. Using these equations and Equation 1 and 2, the transition probability can be calculated from the absorption data. A detailed description of the method used in these calculations is given in Chapter III.

Vibration-Translation Energy Transfer

Since 1950, a great deal of work on theoretical calculations of v-t transition probabilities has been published. The most noted of the early works was due to Landau and Teller (1). This theory employs time de-

pendent perturbation theory to calculate the transition probabilities. Using this theory, if $|C_k|^2$ = probability that an oscillator will be in the state k at time t, then

$$\frac{dC_k}{dt} = -\frac{i}{h}\sum_{\ell=1}^{N} C_\ell V_{k\ell} \exp[it(Ek - E\ell)/h] \qquad (6)$$

where $V_{k\ell} = \langle\psi_k^{o}|H'(t)|\psi_\ell^{o}\rangle$

ψ_i^{o} = unperturbed eigen function of the oscillator in state i

$H'(t)$ = perturbing Hamiltonian

E_i = energy of the vibrator in quantum state i.

The semi-classical approximation is next made by assuming that $H'(t)$ can be expressed in terms of the time varying coordinates obtained by solving the classical equations of motion. Once this approximation is made, Equation 6 which represents N coupled differential equations can be solved numerically for special cases or further assumptions can be made to arrive at an analytical solution. Landau and Teller assumed that the oscillator was initially in state m so $c_m(t=0) = 1$ and $c_1(t=0) = 0$ for $1 \neq m$. For this case, Equation 6 can be written as

$$\dot{c}_k = -\frac{i}{h} V_{km} \exp[2\pi i\nu t] \qquad (7)$$

where $h\nu = E_k - E_m$.

The differential equations are no longer coupled. Following the treatment of Landau and Teller, V is written as $V = xF(t)$ where $F(t)$ is the perturbing force due to an incoming atom or molecule and x is the displacement of the oscillator. Equation 7 then becomes

$$c_k^2 = \frac{1}{h^2} |X_{mk}|^2 \left| \int_{-\infty}^{\infty} F(t) \exp[2\pi i \nu t] dt \right|^2 \qquad (8)$$

where $X_{mk} = \langle \psi_m^o | X | \psi_k^o \rangle$

In order to arrive at an analytical form for the probabilities, Landau and Teller assumed an exponential form of the intermolecular potential

$$V(r) = \lambda \exp(-\alpha r) - \mu \exp(-\tfrac{1}{2} \alpha r). \qquad (9)$$

and were able to show that

$$P_{10} = (4\pi/\sqrt{3}) \, NB \, r_o^2 \, v^* \exp\left(-3y^* + \frac{h\nu}{2kT}\right) \qquad (10)$$

where $y^* = (2\pi^4 \, mv^2/\alpha^2 \, kT)^{1/3}$

$B = 32\pi^4 \, m^2 \nu / h\alpha^2 M)$

$v^* = (4\pi^2 \, kT\nu/\alpha M)^{1/3}$

M = reduced mass of the oscillator.

Equation 10 is due to Cottrell, Dobbie, McLain, and Read (6) and differs from Landau and Teller's result in the pre-exponential term and the symmetrization term, $\exp(\frac{h\nu}{2kT})$. These two terms are important for calculations, however, the general behaviour of the transition probability is governed by the $\exp(-3y^*)$ term. Equation 10 has been used and misused by many investigators. Due to its simple form, it can easily be applied to most systems and as a result, it has become common practice to apply this theory to any vibrational energy transfer process without considering the limitations imposed by the small perturbation assumption and the form of the intermolecular potential.

At reasonable temperatures, the exponential term of Equation 10 will dominate the temperature dependence of the transition probabilities. Obviously, for this simple expression, since $\alpha > 0$, the transition probabilities will always increase with temperature. Widom and Bauer (2) have shown that a negative temperature dependence can be introduced via the pre-exponentail term, but their treatment of the CO_2 - H_2O system using this treatment has been shown to be incorrect (3).

Slawsky, Schwartz, and Herzfield (20) have developed a quantum mechanical treatment of vibrational energy transfer. This treatment uses the method of partial waves. McCoubrey has shown that for most molecules, this treatment gives the same result as the simpler Landau-Teller Theory. Shin (21,22) has elaborated on the method of SSH and has demonstrated the importance of the angle dependent dipole-dipole and dipole-quadrapole forces in determining the transition probabilities. His final expression for the probability of transferring one quantum of vibrational energy during a collision is

$$P(T,\text{angles}) = \frac{24\pi}{19}\left(\frac{x}{kT}\right)^{3/2} A \exp\left[-\frac{19x}{7kT} + \frac{1}{42}\left(\frac{\Gamma(\frac{1}{12})}{\Gamma(7/12)}\right)^2 \frac{Dx}{kT} + \frac{1}{2\sqrt{2}}\right.$$

$$\left(\frac{\Gamma(\frac{1}{12})\Gamma(\frac{4}{12})}{\Gamma(\frac{7}{12})\Gamma(\frac{10}{12})}\right)\left(\frac{\mu^2}{D\sigma^3}\right)\left(\frac{D^{3/4}\, x^{1/4}}{kT}\right)g + \frac{3(4)^{2/3}}{448}\,\frac{\Gamma(\frac{1}{12})\Gamma(\frac{3}{12})}{\Gamma(\frac{7}{12})\Gamma(\frac{9}{12})}\,\frac{\mu Q}{D\sigma^4} \qquad (11)$$

$$\left.\frac{D^{2/3}\, x^{1/3}}{kT}h + \frac{19}{2}\left(\frac{13}{1596}\right)^2\left(\frac{\Gamma(\frac{1}{12})}{\Gamma(\frac{7}{12})}\right)^4 \frac{D}{kT} - \frac{D}{6kT} + \frac{\Delta}{2kT}\right]$$

where $X = \left[\frac{\Gamma(\frac{19}{12})}{\Gamma(\frac{1}{12})}\,\frac{(4D)^{1/2}\, 2\pi m_r \sigma\, \Delta kT}{h}\right]^{12/19}$

and the potential energy V is given by

$$V = 4D[(\sigma/r)^{12} - (\sigma/r)^{6} - (\sigma/r)^{8}\, t^*g - (\sigma/r)^{4}\, u^*h] \qquad (12)$$

$$t^* = \mu^2/4D\sigma^3 \qquad u^* = 3\mu Q/8D5^4$$

$$g = \cos\theta_1 \cos\theta_2 - \sin\theta_1 \sin\theta_2 \cos\phi$$

$$h = \tfrac{1}{2}(\cos\theta_1 - \cos\theta_2)(\text{ð}\sin\theta_1 \sin\theta_2 \cos\phi - 3\text{ć}os\,\theta_1 \cos\theta_2 - 1)$$

θ_1 and θ_2 are the angles of inclination of the molecular axis to the line of centers. ϕ is the relative azimuthal angle. μ is the dipole moment and Q is the quadrapole moment. Δ is the energy transferred $= h\nu$ where ν is the frequency of vibration.

The probability may be divided into an angle dependent part and an angle independent part

$$P(T,\text{angles}) = P_{LJ}(T) \times f(T,\text{angles}). \qquad (13)$$

f(T,angles) can be expressed as

$$f(T,\text{angles}) = \exp(\alpha g + \beta h). \qquad (14)$$

Averaging over all possible angles, Shin found that

$$\langle f \rangle = \frac{\exp(22)}{16(\alpha^2-\beta^2)} \qquad (15)$$

This treatment is different from those theories which use

$$V = \text{Leonnard Jones} + \delta^*/r^3$$

where δ^* is a constant related to the dipole moment squared, (23) since the angle dependence of the dipole-dipole contribution is accounted for. Shin's method applied to H_2O predicts a negative temperature dependence of the transition probabilities in tentative agreement with the experi-

mental work of Fujii (24).

Before using Shin's formalism to calculate transition probabilities, several limitations should be discussed. First, there is an ill defined pre-exponential factor A in Equation 11. Second, the possibility of v-r energy transfer is not considered. Third, the angle dependence has been averaged over all possible angles but has not been summed over all rotational states. At low temperatures, the colliding molecules may not experience the average potential interaction but may feel preferred orientation during the collision. Finally, the vector nature of the dipole forces hasn't been fully considered. The transition probability in Equation 11 is a maximum when $\theta_1 = \theta_2 = 0$ irregardless of the molecule under consideration. For diatomic molecules, this condition seems reasonable but for polyatomic molecules, there is no guarantee that when $\theta_1 = \theta_2 = 0$, the molecule will be aligned for the most efficient transfer of energy.

Although Shin's method leaves much to be desired, it is at least a first attempt to account for the angle dependence of the intermolecular potential. The effect of this dependence on the transition probabilities in Ammonia is given in Figure 1. The limitations of this method mentioned above are only given to point out that quantitative agreement with experiment should not be expected. The important characteristic of this method, i.e., the negative temperature dependence of the vibrational transition probabilities, is observed in some molecules. The above explanation is the only explanation available for this temperature dependence if one assumes a v-t energy transfer process.

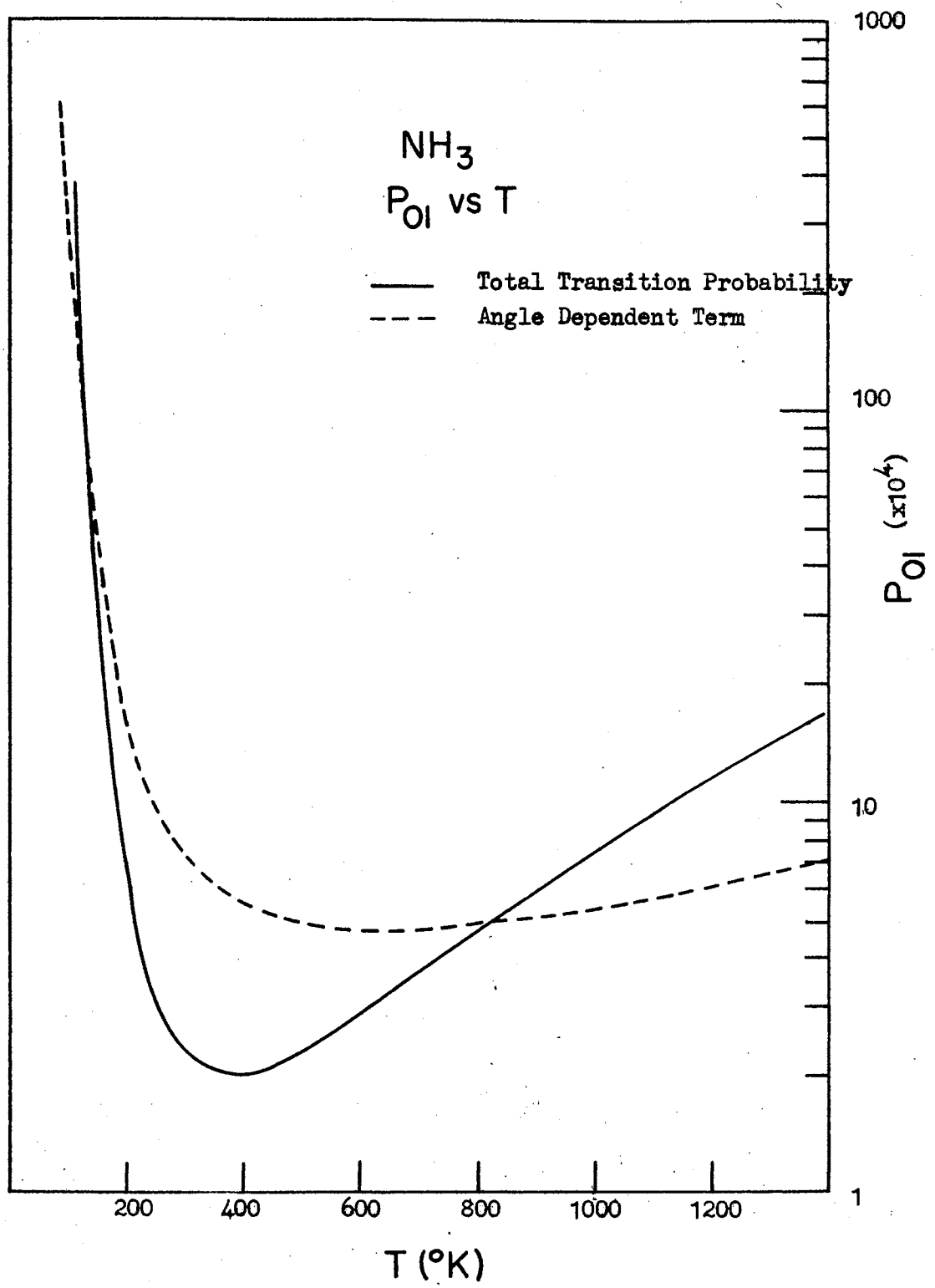

Figure 1. Effect of Angle Dependent Potential Terms on Energy Transfer in Ammonia

Rotation-Translation Energy Transfer

There is no general, simple theory for R-T energy transfer analagous to the Landau-Teller theory for V-T exchange. Some work has been done for non-polar diatomic molecules with excellent agreement with experimental data (14). The multi-level character of the rotational energy makes a more general treatment extremely difficult. Although a calculation of the transition probabilities involved in rotational relaxation is at present not possible, the qualitative dependence of the collision number on certain molecular parameters can be predicted. One way of determining how the collision number should depend on the dipole moment, moment of inertia, and temperature is given by Zeleznik (10). His method is primarily concerned with treatment of thermal conductivity data and as a result, he assigns one collision number to the process. Although exact collision numbers can not be obtained, certain ratios of special interest can be calculated. First, the dependence of collision number on moment of inertia and dipole moment can be written as

$$\frac{Z(1,T)}{Z(2,T)} = \frac{N_1}{N_2}\left(\frac{\mu_2\sigma_1}{\mu_1\sigma_2}\right)^4 \frac{\theta_{11}(\xi_2^2)}{\theta_{11}(\xi_1^2)} \tag{16}$$

where μ = dipole moment

σ = molecular diameter

$\xi^2 = \frac{16}{5}\pi\frac{(I/M)\eta}{(\pi mkT)^{1/2}}$

η = coefficient of viscosity

I = moment of inertia

$\theta_{11}(\xi^2)$ = function given in tabular for in Zeleznik's paper.

The temperature dependence can be expressed as

$$\frac{Z(1,T)}{Z(1,T_o)} = \left(\frac{T}{T_o}\right)^3 \left[\frac{\eta_1(T_o)}{\eta_1(T)}\right]^2 \frac{\theta_{11}(1,T_o)}{\theta_{11}(1,T)} \qquad (17)$$

Evans found agreement with experiment ( ) is impressive for two diatomic molecules considering the questionable manner in which Z has been assigned to τ's found acoustically. Latter work by Hill and Bass (25) indicates that the dipole dependence of the above expression isn't valid for NO which has a small dipole moment.

Vibration-Rotation Energy Transfer

Cottrell and co-workers (5,6) first found that some molecules seem to exchange energy between vibration and rotation rather than between vibration and translation. They came to this conclusion by comparing the relaxation times of several hydrides to their deuterides. V-T theory predicts that the deuteride should have a noticably shorter relaxation time due to a smaller oscillator frequency, however, for some molecules they found that the hydrides had relaxation times approximately equal to the deuterides. This behaviour was later observed in other molecules by different investigators.

The importance of v-r energy transfer wasn't fully appreciated or accepted until Moore (7) demonstrated that a qualitative v-r theory could account for the short relaxation times of a large number of molecules. In his paper, Moore established several criteria which he considered necessary if v-r transfer was to be more efficient than v-t processes. One of these is that $I/d^2 < M$ where I is the moment of inertia, d is the distance from the center of mass to the peripheral atom of the rotator, and M is the reduced mass of the oscillator. Fol-

lowing his argument, for molecules with a low moment of inertia (particularly hydrides) the rotational velocity may exceed the translational velocity. In this case, I determines the rotational velocity, hence the transition probabilities. Moore replaced the reduced mass of the colliding pair in the Landau-Teller expression with I/d^2 and the translational relative velocity with the rotational velocity ωd. With these substitutions and the exponential potential used before for L-T theory, he found that

$$P_{10} = \frac{1}{Z_{10}} = \frac{1}{Z_o} \frac{17.1\, I^{13/6}\, \nu^{4/3}}{d^{13/3}\, T^{1/6}\, M\alpha^{7/3}} \exp\left[-1.78 \left(\frac{\nu^2}{d^2 \alpha^2 T}\right)^{1/3} + \frac{0.719\nu}{T}\right] \quad (18)$$

where ν = vibrational frequency of the oscillator (cm^{-1})

Z_o = steric factor

Moore found impressive agreement between Z_{10}'s calculated from Equation (18) and those derived experimentally for molecules where $I/d^2 < M$.

The very simple form of the intermolecular potential and the very simple collision model Moore uses casts some doubts on his conclusions. One can not, however, overlook the fact that he was able to account for the anomalously high transition probabilities of some 25 molecules. The large number of molecules for which Moores theory holds is in itself some justification for accepting, at least in part, his physical picture of the collision.

Shield's and Burks (3) have developed a somewhat more realistic model of v-r energy exchange. They assume that the time dependent force acting on the oscillator is

$$F(t) = F_o\, e^{(-\alpha t)^2} \cos\,(2\omega' t + \phi) \quad (19)$$

where ω' is the angular frequency of the rotor, and ϕ is a phase angle. F_o and α are adjustable parameters and will be discussed later. Using this form for the perturbation, they find:

$$P_{10} = \left(\frac{\pi |F_o|^2}{4h\omega M\alpha^2}\right)\left[1 + \frac{4kT}{I\alpha^2}\right]^{-1/2} \exp\left[\frac{-I\omega^2}{\gamma kT + 2I\alpha^2} + \frac{h\omega}{2kT}\right] \qquad (2b)$$

where ω is now the angular frequency of the oscillator, I is the moment of inertia, and the other parameters are defined above.

Shields has applied the above equation to CO_2/H_2O-D_2O-H_2S-D_2S (26) mixtures with excellent results both in magnitude and temperature dependence. Setting $F_o = 24\varepsilon/\sigma$ where ε and σ are the Leonnard - Jones potential parameters, gives good agreement with experiment for the above molecules. Shields used a value of α equal to $\alpha_o/\sqrt{\mu}$ where α_o is the same for all molecules of the same type and μ is the reduced mass of the colliding molecules. For the above molecules, $\alpha_o = 1.184 \times 10^{14}$ sec^{-1} gives the best agreement with experiment.

The combined success of Moore and Shields in accounting for the high transition probabilities and later the temperature dependence of these probabilities leaves little doubt that v-r energy exchange is important in some molecules. More recent calculations by Sharma (8,9) further supports this observation.

CHAPTER III

EXPERIMENTAL RESULTS

Discussion of the Experimental Apparatus

Two instruments were used in this investigation. The first instrument used has been adequately described by Hill[27]. The second instrument is similar to the one built by Hill but eliminates many of the problems encountered with the older spectrometer. The electrical systems were the same for the two instruments. The gas handling systems were similar except all tubing used with the new spectrometer was 3/8" and 1/2" stainless steel. The stainless steel tubing offered greater safety at elevated pressures. The large diameter tubing allowed a much better pump rate than was possible with the previous instrument.

The test chamber of the new spectrometer is 304 Stainless Steel heavy wall tubing which provides excellent resistance to the corrosive gases used in this investigation, except SO_2, and can withstand temperatures up to 1,000°C. The tube is surrounded by a three zone Linberg furnace which is controlled automatically with a thermocouple mounted in the center of the furnace. The operator simply dials in a temperature and the controller keeps the temperature constant to within 1°C.[28] The temperature profile in the tube is controlled by changing the power into the end zones. This profile is monitered by a series of thermocouples spread along the tube. Since stainless steel is only a fair conductor of heat, the temperature profile inside the tube should be much

flatter than on the outside. The magnitude of the temperature within the tube was measured by inserting Argon and measuring the velocity. By comparing this velocity with tabulated values, the temperature could be found to within 3% at room temperature and to within 1% at 1,000°C. More accuracy could possibly have been obtained but was not considered necessary.

The base of the new spectrometer is designed in such a manner that the rods maintain their alignment at all pressures thus alleviating one of the primary weaknesses of the previous instrument. The rod holders are designed to ease changing the rods and the instrument is permanently aligned so periodic rod alignment was not required. Rod alignment was checked twice during the series of measurements and no corrections were necessary.

The experimental absorption in Helium near room temperature is given for the old instrument in Figure 2 and for the new instrument in Figure 3. Both these graphs are based on the decrease in signal between only two points so they represent the worst possible experimental case, thus the deviations from the theoretical lines should be the greatest encountered experimentally. The two instruments give approximately the same scatter for Helium. Figure 4 gives the absorption in Argon measured with the new spectrometer. The excellent agreement with theory is partly fortuitous and partly due to the larger mass of Argon which leads to larger absorption. Generally, measurements of large coefficients of absorption were more accurate than low values except at f/P's above 100 MHz.

With the exception of the large mechanical coupling, the new instrument worked well. The mechanical coupling created no problem for

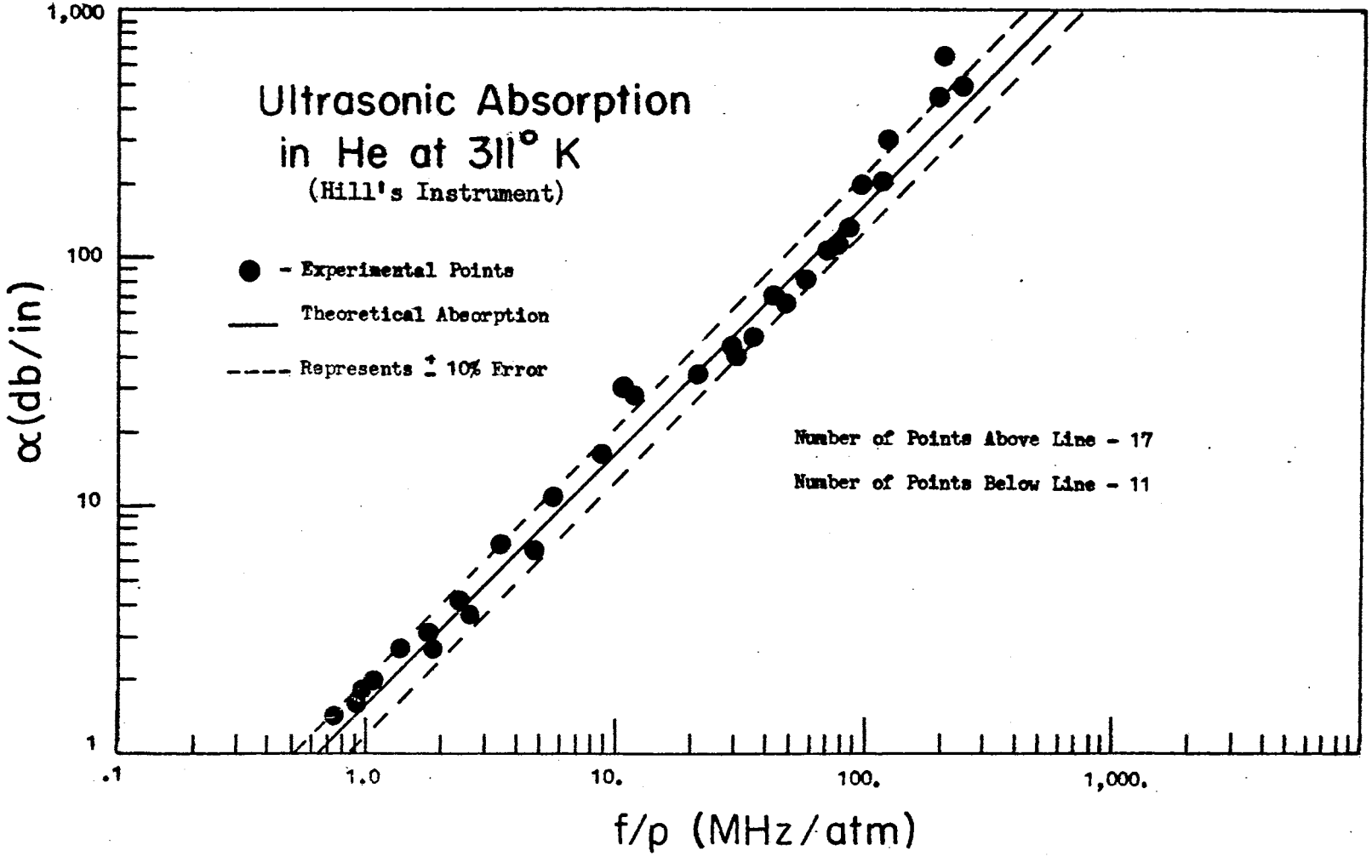

Figure 2. Typical Absorption Data Using Hill's Instrument

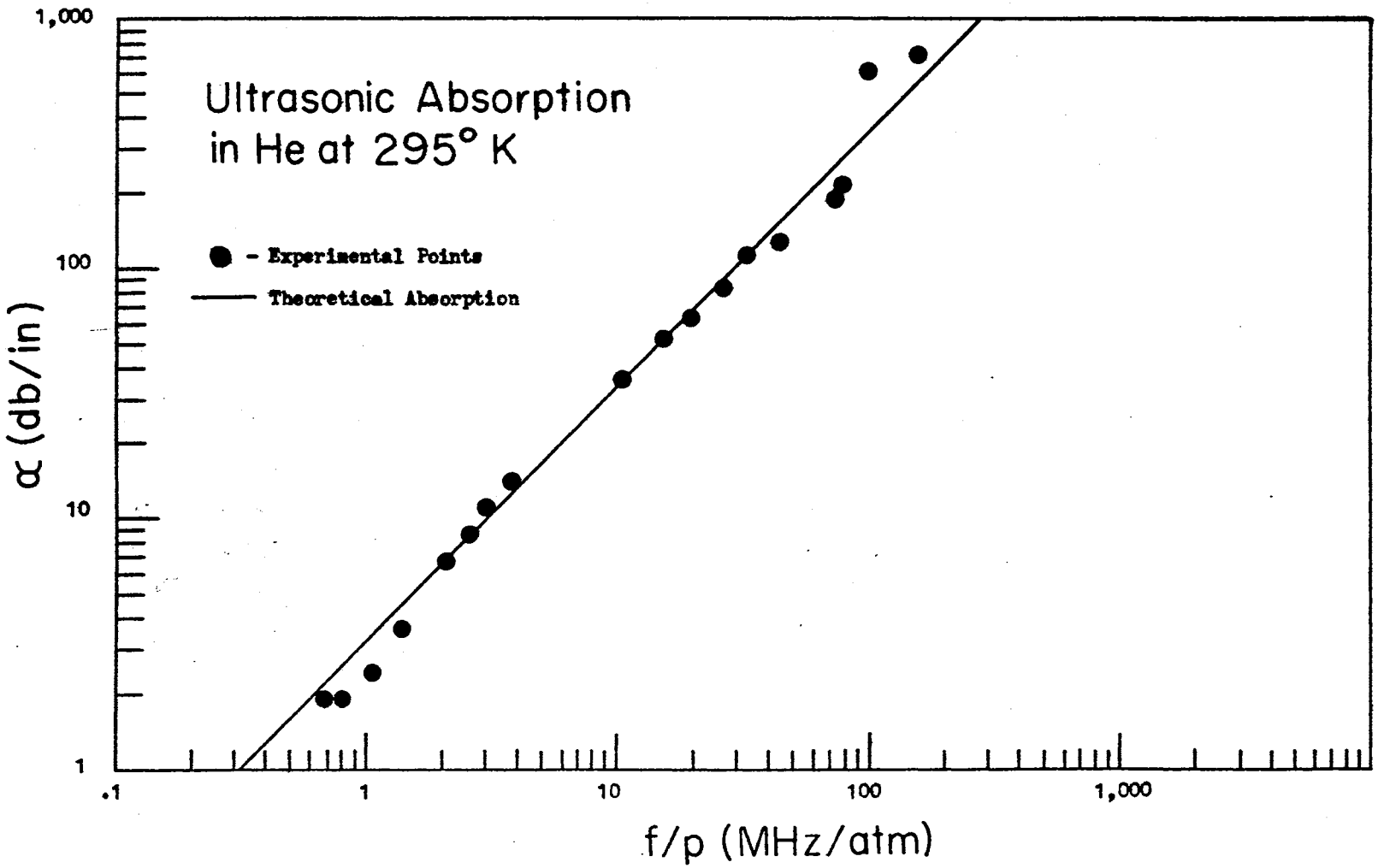

Figure 3. Ultrasonic Absorption in Helium Using the New Instrument

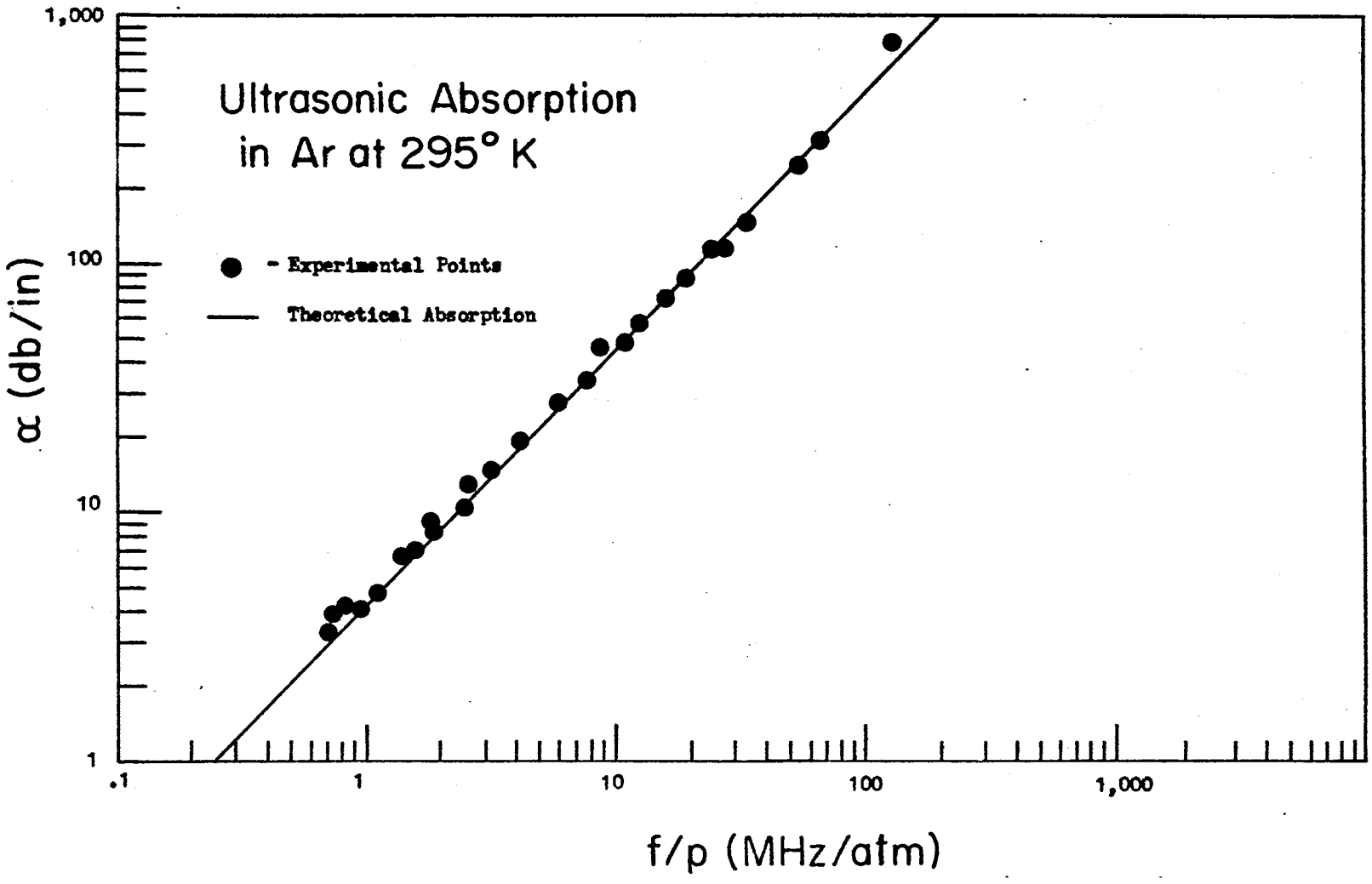

Figure 4. Ultrasonic Absorption in Argon Using the New Instrument

the pulsed operation so long as the Pulse Repetition Frequency (PRF) was kept below 30 c.p.s. This low PRF made the signal difficult to detect on the scope and at low pressures, the signal became extremely eratic. In the future, a boxcar integrator could be used to overcome this problem and improve the accuracy at high values of f/P keeping in mind the argument in Chapter II.

Dissassembly of the apparatus is very straightforward. No special precautions need to be taken except when handling the quartz rods. These rods are very expensive and very easy to chip. Whenever a rod was chipped, the chipped end was cut off with a glass saw and then lapped down by hand using sandpaper of varying coarseness. While sanding off the end, the rod was mounted in a machine block which kept the surface to be ground perpendicular to the length of the rod. The error in flatness was less than .0001 inch when the above procedure was followed.

Method of Analyzing Data

Ultrasonic absorption and dispersion were measured in Sulphur Dioxide, Ammonia, Fluoroform, and Hydrogen Sulfide at several temperatures to obtain the vibrational and rotational relaxation times. In addition, the absorption data collected by Hill for Methane was reanalyzed to obtain relaxation times and collision numbers which could be readily compared to the other relaxation times obtained in this investigation. The SO_2 data was taken with the instrument designed by Hill. All other measurements were made with the new spectrometer.

In order to extract the relaxation times from experimental data, an iterative procedure was used. First, a likely set of τ's were used to calculate the classical absorption using Equation (3) which was sub-

tracted from the measured absorption to obtain the experimental internal absorption. These same τ's were then used to calculate a theoretical internal absorption curve. The square of the difference between the theoretical curve and the experimental internal absorption was summed over all experimental points. The τ's were then incremented a small amount and the process repeated over a predetermined range of τ's. The set of τ's which give the smallest error were chosen as the "best" τ's.

In practice, if two or more relaxation times are to be extracted from the experimental data, the range of search for τ can not be made very large due to limited computer time. To overcome this problem, the range on each τ was first made large as was the increment by which it was changed. The first run gave a close estimate of the correct relaxation times. The interval was then decreased along with the increment so that the total number of points at which the error was computed remained constant. This process was repeated until the desired accuracy in τ was achieved. This method of analyzing the data works well provided the error decreases continuously toward the correct value of τ over a range larger than the increment used. If this criteria is met, the true minimum will be found in the presence of many minima. When the error fluctuates rapidly with the τ's, a relative minimum may be selected instead of the true minimum. Normally, if a large number (20-70) of data points are obtained, the error will converge rapidly to give the best τ's.

The experimental velocity data was used only to check the temperature and to insure that dissociation was not taking place. When the gas began to dissociate, the velocity would rapidly increase with temperature as shown in Figure 5 for Ammonia. When the temperature of the gas

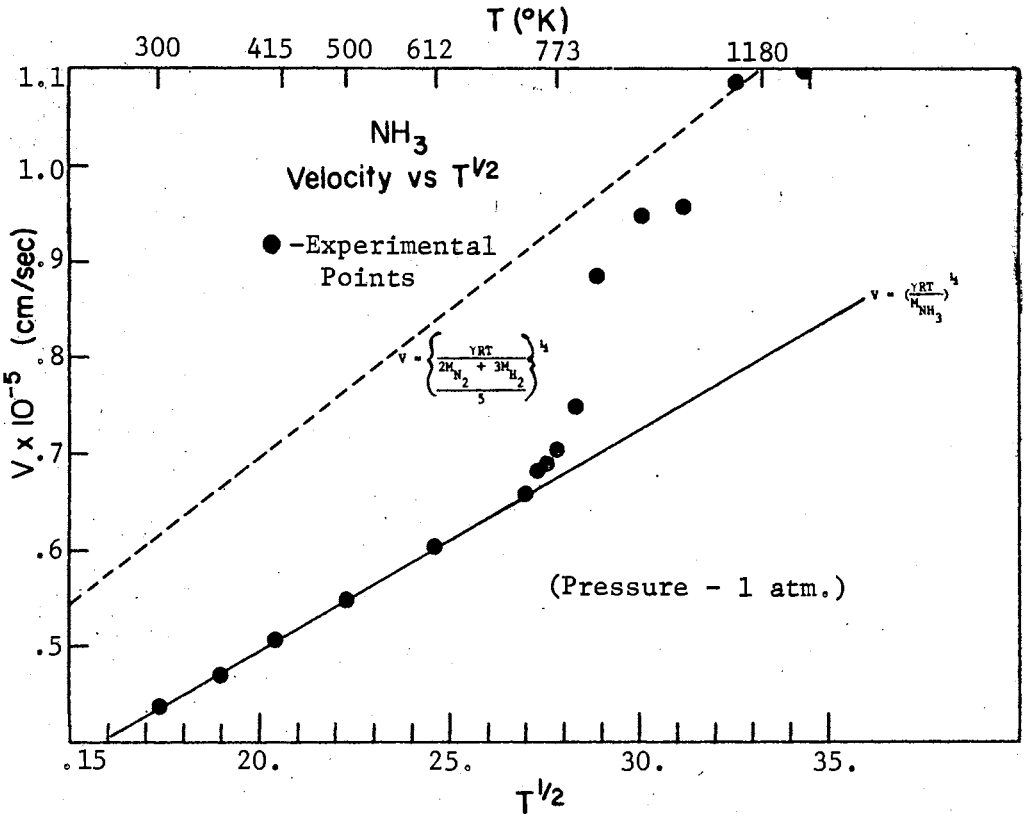

Figure 5. Variation of Velocity with Temperature in NH_3 While the Gas is Dissociating

was not in equilibrium with the test chamber and furnace, the velocity would increase as a function of time.

The experimental absorption can be measured with a maximum error of 10%. Relating this experimental error in absorption to an error in relaxation times is very difficult. The error in τ with a fixed error in absorption depends upon the relaxation strength (specific heat) of the process being observed, the separation of different relaxation peaks, and the amount of the relaxation curve covered in the experiment. A numerical method was employed to compute the experimental error in τ. This was done as follows. First, a set of experimental points were selected from the theoretical curve corresponding to the "best" set of τ's. The points were made to correspond in f/P to those measured experimentally. Next, an error between $\pm$ 10% was randomly assigned to the simulated points to get a simulated data set. This process was repeated until five simulated data sets were obtained. The data sets were then processed as though they had been collected experimentally giving five sets of "best" τ's.

This method of error analysis has been applied to Ammonia and Hydrogen Sulfide. These molecules represent quite different relaxation strengths and relaxation peak separation. For Ammonia, the simulated data sets were used to obtain a feel for the variation of the error with the number of data points collected. To do this, a fixed number of simulated points were removed systematically from each of the simulated data sets so that the whole range of f/P was still covered. The results are given in Figure 6. The complete results of the error analysis are given in Table I. The maximum % error obtained is the maximum variation between the "best" τ's for the real experimental data and the "best" τ's

TABLE I

RESULTS OF ERROR ANALYSIS

No. of Data Points	Max. % Error in τ_{rot}	Avg. % Error in τ_{rot}	Max. % Error in τ_{vib}	Avg. % Error in τ_{vib}
		Ammonia at 27°C		
39	18	8	60	26
29	27	15	76	44
20	27	14	80	32
10	30	19	73	52
5	41	27	96	72
		Ammonia at 500°C		
37	30	20	23	13
		Hydrogen Sulfide at 25°C		
30	10	5	17	8
		Hydrogen Sulfide at 400°C		
30	15	6	11	6

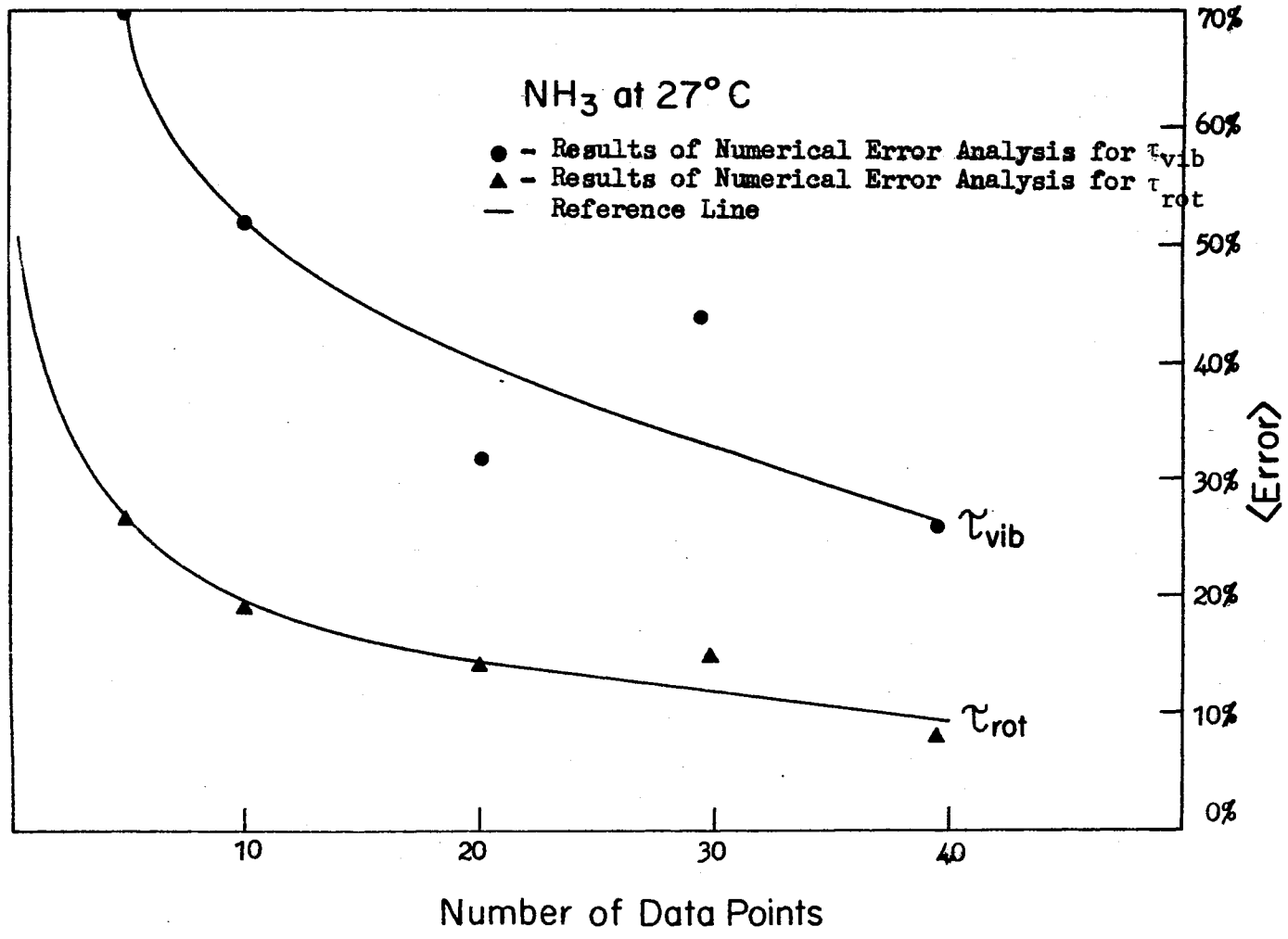

Figure 6. Results of a Numerical Error Analysis at the Relaxation Times in Ammonia

for the simulated experimental data. This maximum % error is assumed to be the experimental error.

Methane

Several investigators[12] have measured the vibrational and rotational relaxation times of CH_4, however, the most complete set of data was obtained by Hill and Winter[29]. Their data was analyzed using the method outlined in the previous section to obtain relaxation times and collision numbers which would be consistent with the numbers obtained for other gases. The analysis was made assuming all vibrational modes relax in series with each other and in parallel with rotation.

Methane is a symmetric top molecule. The H atoms form the base of a pyramid and the Carbon atom forms the apex. The lowest frequency vibration ($\theta = 1881^{o}$) is the doubly degenerate bending mode. The gas used was Matheson CP Grade with a stated minimum purity of 99.9%. The rotational energy is given by $E_{rot} = J(J + 1)A_o$ where $A_o = 5.249$ cm^{-1}. In the energy range $300^{o}K \pm 50^{o}K$, there is one rotational energy level. This represents the lowest density of states of any molecule included in this investigation.

The analysis of the experimental absorption data yielded rotational and vibrational relaxation times which are smaller than those published by Hill and Winter obtained from fitting both velocity and absorption data visually. Both methods give reasonable agreement with previous results as shown in Figure 7. An error analysis was not made but due to the high vibrational specific heat, τ_{vib} for Methane should be more accurate than τ_{vib} for H_2S while the $\tau_{rot's}$ should be of comparable accuracy. The experimental absorption data along with the "best" theoreti-

cal curves are given in Figures 10 through 13. The 1073°K vibrational peak is not as large as predicted. This is probably due to either an error in the specific heat used or an error in temperature. The former is most probable since the measured velocity is close to that calculated. The relaxation times calculated using Equation 3 and the collision numbers are presented in Figures 7 through 9. The straight lines are only given for visual reference. The molecular parameters used to analyze the data are given in Table II.

The vibrational collision numbers for Methane behave with temperature as predicted by v-t theory. At 298°K, SSH theory gives $\beta = 1.38$ μsec.[30] compared with $\beta = 1.26$ μsec. found in this investigation. At 574°K, SSH theory predicts $\beta = .246$ μsec. compared to $\beta = .273$ μsec. found experimentally demonstrating that v-t theory can predict both the magnitude and the temperature dependence of the relaxation times for CH_4. It should be pointed out, however, that v-r theory gives equally good results hence measurements on CH_4 alone can not determine the process which is dominate. This determination has been made by comparing β for CH_4 to β for CD_4. v-t theory gives $\beta(CH_4)/\beta(CD_4) = 2$ at room temperature while v-r theory predicts this ratio will be 1/2. Cottrell and Matheson[5] have shown experimentally that this ratio is about 1/2 in excellent agreement with v-r theory. Methane also meets Moore's criteria for v-r energy transfer, $M \cong 5 \times I/d^2$.

Methane was quite a good choice as a molecule which probably exchanges energy v-r but has no dipole moment. The experimental results indicate that in the absence of angular dependent potential terms, v-t theory and v-r theory must have approximately the same temperature dependence. Furthermore, this temperature dependence must be of the form $\exp-(kT)^{1/3}$.

Since the effect of angle dependent terms seems negligible in CH_4 energy transfer, one might expect CH_4 rotational collision numbers to follow the general pattern established by Raff and Winter[14] for non polar diatomic molecules. That is, as the rotational energy level spacing increases, ln z becomes less dependent upon temperature. The energy level density in CH_4 is larger than that for H_2 and D_2 yet smaller than that for O_2 and N_2. From the above argument, one would expect dz/dT for CH_4 to be greater than the corresponding ratio for H_2 or D_2 but less than this ratio for O_2 or N_2. This prediction is confirmed by the experimental results (see Figure 51).

TABLE II

EXPERIMENTAL RESULTS AND MOLECULAR PARAMETERS FOR METHANE

Thermodynamic Properties of Methane (31)

Mass = 16 a.m.u. Frequency = 1.065 MHz

T (^{o}K)	$\eta \times 10^{3}$ (poise)	γ	C_p/R
298	.120	1.311	4.313
573	.217	1.200	6.106
773	.264	1.160	7.428
1073	.301	1.125	8.988

Vibrational Frequencies

ν_1 (cm^{-1})	ν_2 (cm^{-1})	ν_3 (cm^{-1})	ν_4 (cm^{-1})
2916	1534	3019	1306

Rotational Wavenumbers (32)

$A_o = B_o = C_o = 5.249\ cm^{-1}$

Experimental Results for Methane

T (^{o}K)	$\tau_{vib} \times 10^{7}$ (sec)	$\beta_{vib} \times 10^{7}$ (sec)	Z_{vib}	$\tau_{rot} \times 10^{9}$ (sec)	Z_{rot}
298	17.8	12.6	13,000	.77	8.3
573	4.4	2.7	1,600	1.4	8.3
773	2.7	1.5	720	2.3	11.
1073	1.9	.90	378	4.2	18.

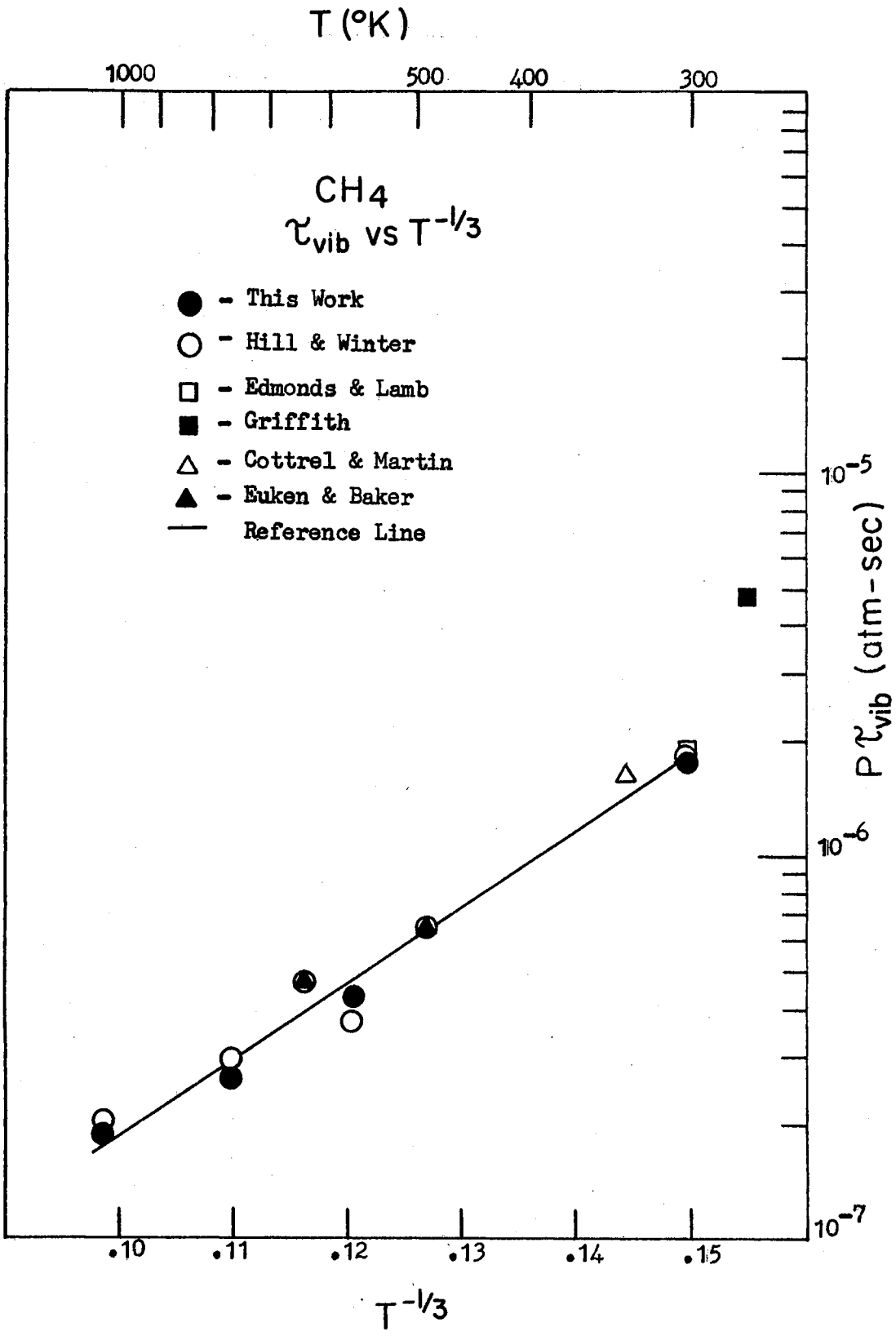

Figure 7. Vibration Relaxation Times in Methane

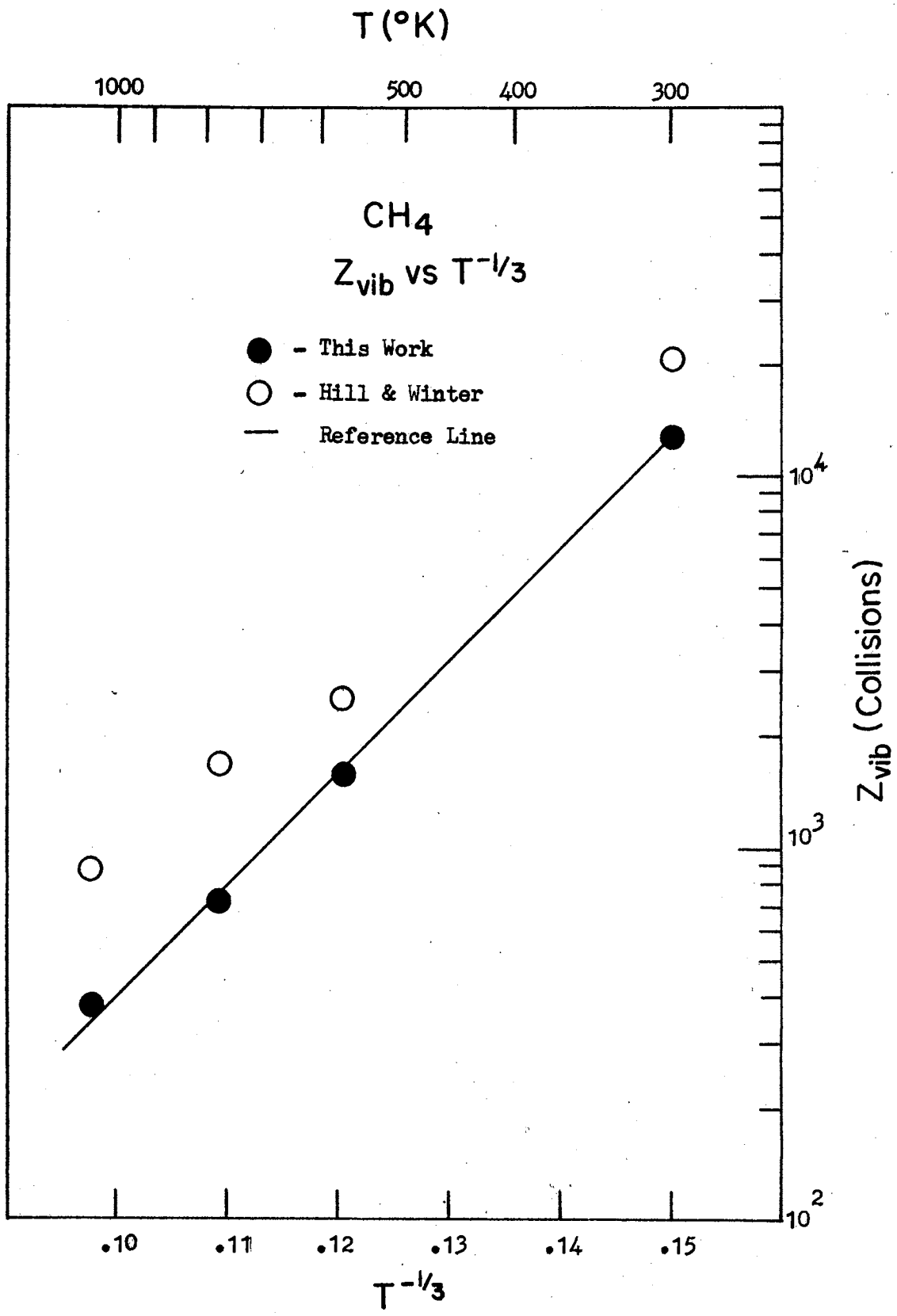

Figure 8. Vibration Collision Numbers in Methane

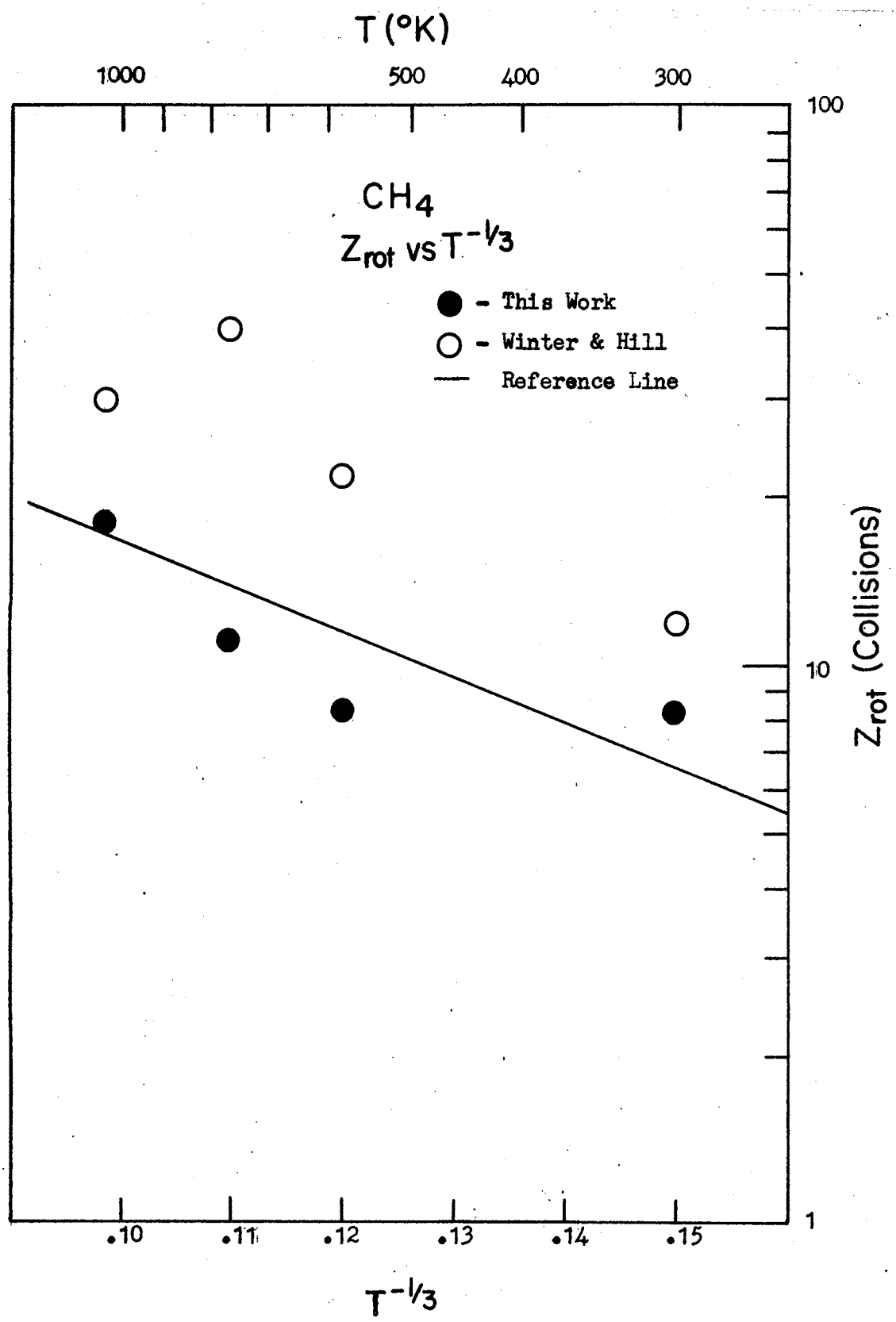

Figure 9. Rotational Collision Numbers in Methane

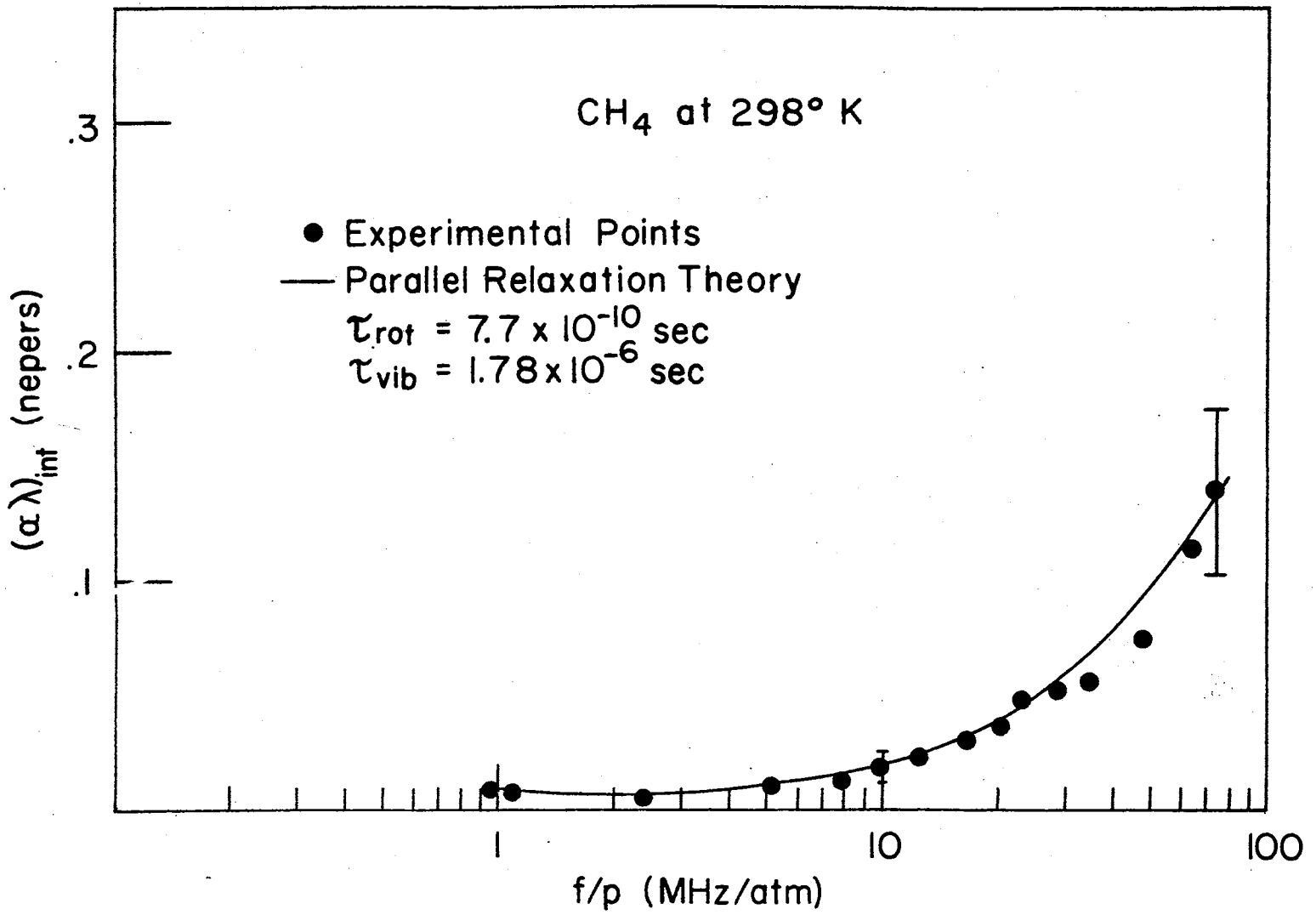

Figure 10. Absorption in Methane at 290°K With Parallel Relaxation Curve

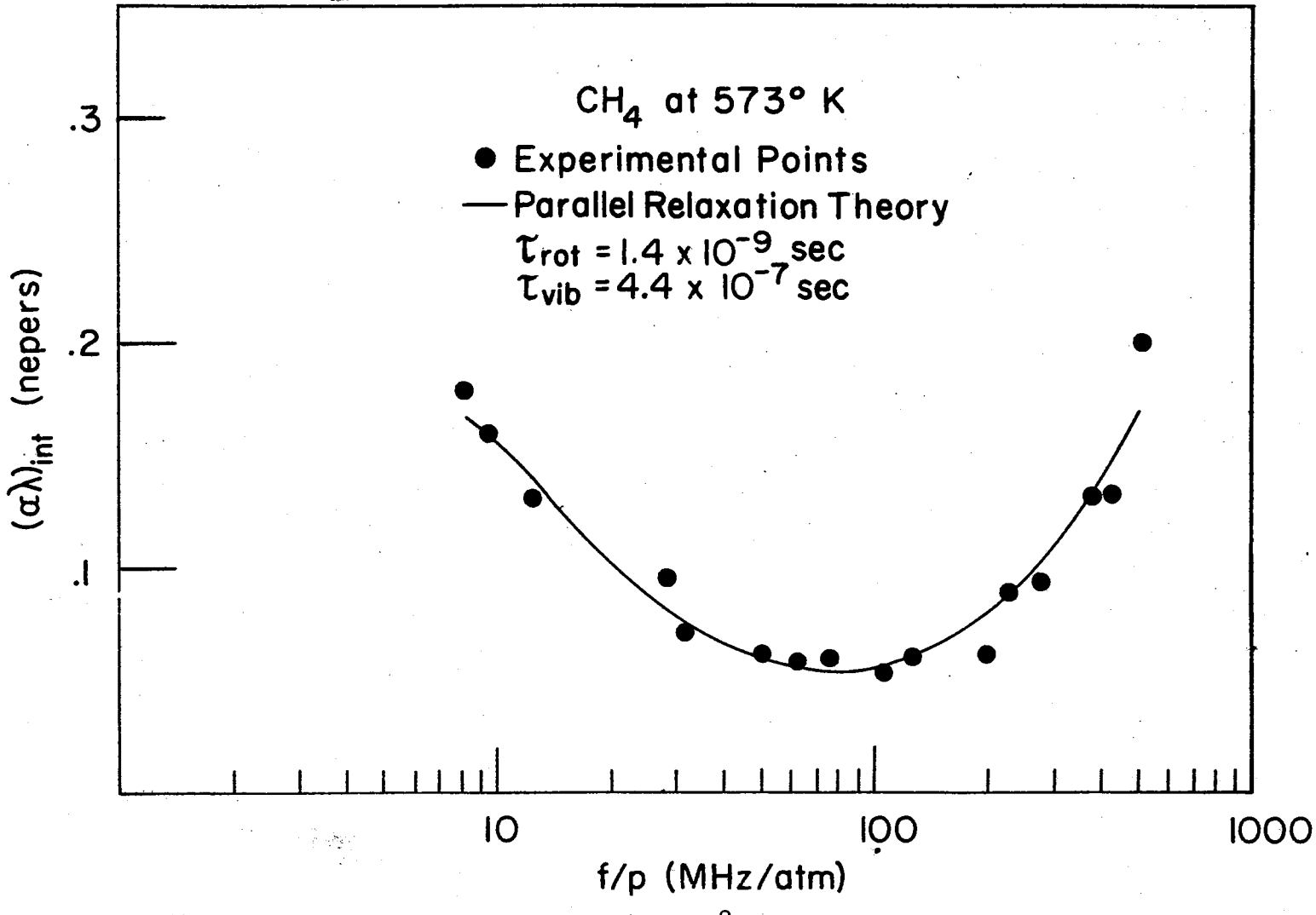

Figure 11. Absorption in Methane at 573°K With Parallel Relaxation Curve

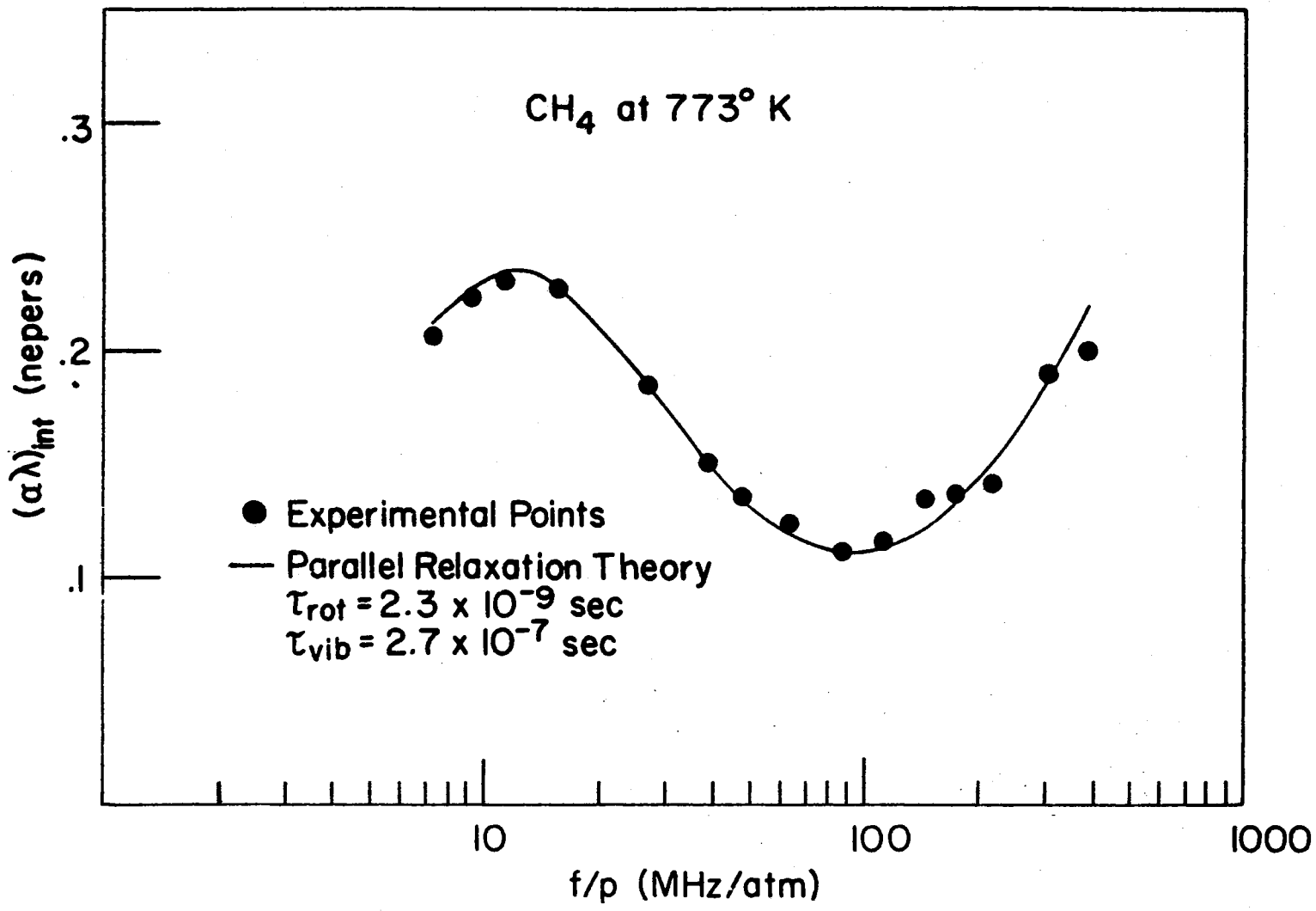

Figure 12. Absorption in Methane at 773°K With Parallel Relaxation Curve

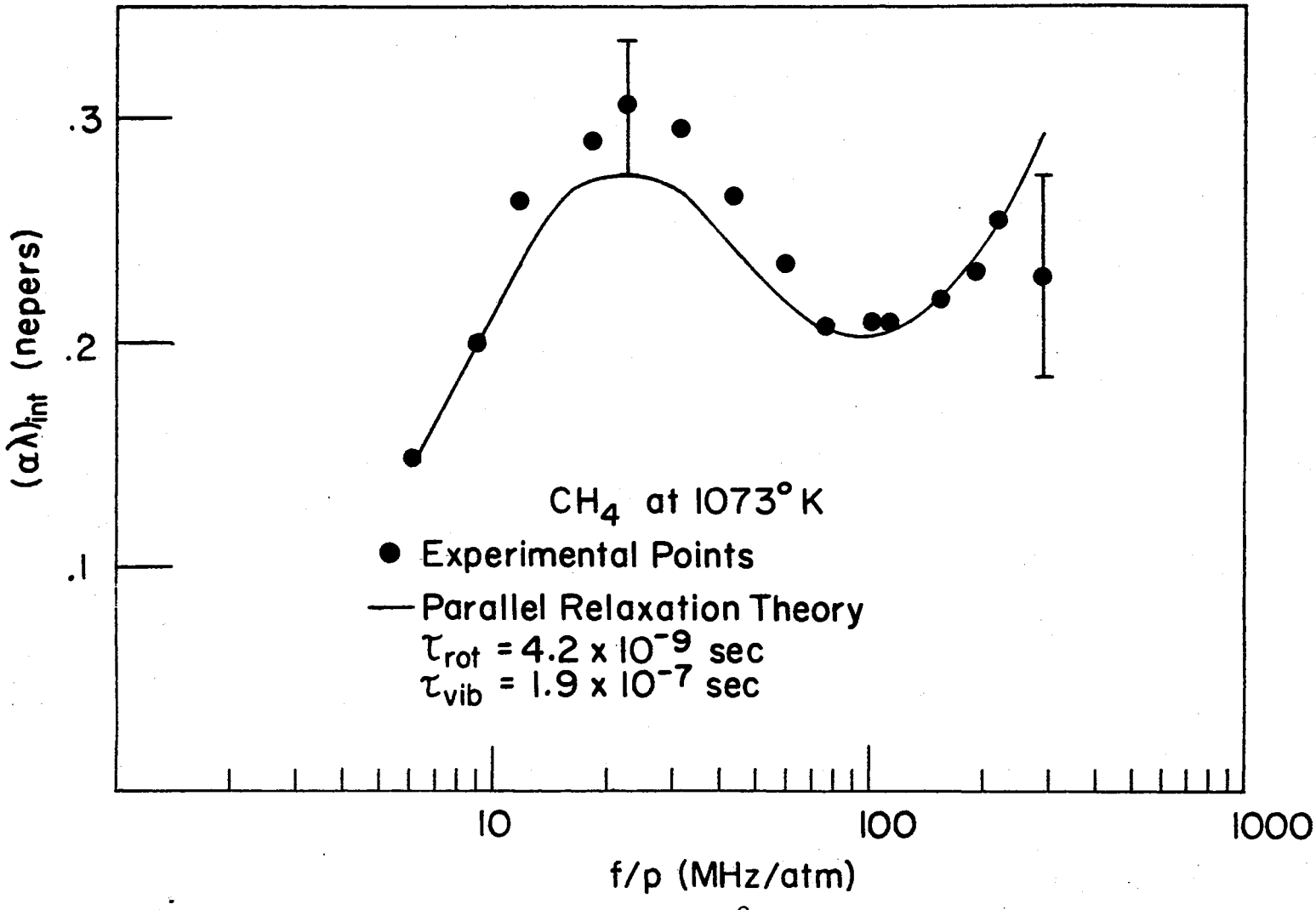

Figure 13. Absorption in Methane at 1073°K With Parallel Relaxation Curve

Hydrogen Sulfide

Previous attempts to measure the vibrational relaxation time of Hydrogen Sulfide have been unsuccessful. Geide (33) measured room temperature absorption and dispersion in the f/P range 1 MHz to 100 MHz and concluded the vibration relaxation must lie below 1 MHz at room temperature. Shields (34) measured absorption and dispersion in the f/P range 100 KHz to 1.2 MHz and concluded the vibrational relaxation must lie above 1.2 MHz. Geide was able to observe the beginning of the rotational relaxation peak and assigned a collision number of 30 to it. Recent thermal transpiration measurements (35) indicate Z_{rot} at room temperature should be about 4.

The H_2S molecule forms an isosceles triangle with the S atom at the apex. The lowest vibrational mode ($\theta = 1704^{\circ}$) is the bending mode where the H atoms move together like sicssors with the S atom at the apex remaining fixed. The other two modes are the stretching modes where the H atoms move along the valence bands either in phase ($\theta = 3760^{\circ}$) or out of phase ($\theta = 3781^{\circ}$). The rotational energy is a very complicated function of the three moments of inertia. Wang (36) has calculated the energy levels and in the energy range $300^{\circ}K \pm 50^{\circ}$, there are 27 allowed energy levels. Other molecular constants required to analyze the absorption data are given in Table III. Experimental viscosity values are only available to $200^{\circ}C$. Higher temperature values are from calculations by Krieger (37).

Since previous investigators were unable to observe vibrational relaxation at room temperature, these measurements were started at $383^{\circ}K$. At room temperature, $C_{vib} = .118R$ but at $383^{\circ}K$, $C_{vib} = .238$ thus the absorption due to vibrational relaxation should be much larger at $383^{\circ}K$

than at 298°K. The 383°K absorption data shows a definite peak due to vibrational relaxation occurring at about 5 MHz/atm.

A mass spectrometer analysis of the gas showed less than 2% N_2 as the only detectable impurity. Such an impurity should affect τ_{vib} by less than 1%. This analysis along with the excellent stability in pressure indicated no dissociation was occurring at 573°K. A dissociation would have introduced an excess of H_2 into the gas, and if this occurred, the rotational relaxation of the H_2 present could be confused as a vibrational relaxation since the rotational relaxation time of H_2 is in the region where vibrational relaxation of H_2S seems to occur. At 773°K, the H_2S began to dissociate as indicated by a very slight increase in pressure when the gas system was filled with H_2S and then isolated. This increase in pressure was accompanied by a small increase in velocity. All measurements were made a 673°K and below.

At room temperature, the absorption due to vibrational relaxation is so small that if higher temperature results were not available, this absorption would have been attributed to an error in viscosity. The viscosity values, although unreliable, could not account for the excess absorption at higher temperatures. The failure of the theoretical curve to match the experimental points at low values of f/P at 573°K and 673°K may be due to an error is viscosity. Such an error would make the relaxation times obtained too large.

When Geide measured absorption in H_2S, he was observing vibrational relaxation but had no way of knowing this since vibrational relaxation contributes such a small absorption. The presence of vibrational relaxation could account, at least in part, for the high collision number Geide obtained for rotation. The effect of disregarding the vibrational

absorption is illustrated with the experimental data and "best" theoretical curves in Figures 16 through 20. At the two lowest temperatures, disregarding the vibrational relaxation results in a fair fit to experimental data but this fit is poor at higher temperatures. The relaxation times obtained by disregarding vibrational relaxation are consistently higher than the actual rotational relaxation times.

Figures 14 and 15 give the vibrational and rotational collision numbers along with rotational collision number due to Geide and thermal conductivity measurements. The vibrational collision numbers at first increase, then decrease with temperature. Such behaviour has been observed by Corran (38) et. al. for other molecules but their results are not nearly so conclusive. The change in Z_{vib} with temperature can be duplicated to a fair degree using Equation 20 with $F_o = 7.55 \times 10^{-5}$ dynes and $\alpha = 4.7 \times 10^{13}$ sec^{-1}. This value of F_o is about twice that predicted from the Lennard-Jones potential parameters given by Mason and Monchick (23). If H_2S is considered to be similar to the CO_2/H_2S system, α should be about 3×10^{13} sec^{-1}. In an H_2S/H_23 collision, the relative angular velocities must be considered, where in an H_2S/CO_2 collision, only the rotation of the H_2S molecule is important. It is not too surprising then that the value of α is quite different for the two situations. The use of v-r theory is further supported by recent measurements on D_2S by Shields (26) who found $\tau(D_2S) = 4.8 \times 10^{-8}$ sec. v-t theory predicts $\tau(H_2S)/\tau(D_2S) = 1$, v-r predicts this ratio will be .25, and experimentally the ratio is about .5.

If one interprets this slightly high experimental ratio to be indicative of the presence of v-t transfer to a small degree, the high temperature behaviour is easily explained. Assuming v-t is present but

TABLE III

EXPERIMENTAL RESULTS AND MOLECULAR PARAMETERS FOR HYDROGEN SULFIDE

Thermodynamic Properties of Hydrogen Sulfide

Mass = 34.08 a.m.u. Frequency = 1.00 MHz

T (^{o}K)	$\eta \times 10^{3}$ (poise)	γ	C_p/R
298	.1288	1.324	4.118
383	.1723	1.309	4.238
473	.2113	1.287	4.477
573	.2376	1.275	4.643
683	.2717	1.259	4.851

Vibrational Frequencies (32)

ν_1 (cm^{-1})	ν_2 (cm^{-1})	ν_3 (cm^{-1})
2611	1183	2626

Rotational Wavenumbers (32)

A_o (cm^{-1})	B_o (cm^{-1})	C_o (cm^{-1})
10.37	8.991	4.732

Experimental Results for Hydrogen Sulfide

T (^{o}K)	$\tau_{vib} \times 10^{8}$ (sec)	$\beta_{vib} \times 10^{8}$ (sec)	Z_{vib}	$\tau_{rot} \times 10^{9}$ (sec)	Z_{rot}
298	3.0	2.7	273	.8	8.0
383	5.0	5.6	417	1.1	8.2
473	9.0	7.2	426	1.8	11.
573	5.5	4.3	215	2.7	15.
683	4.0	3.2	138	3.6	17.

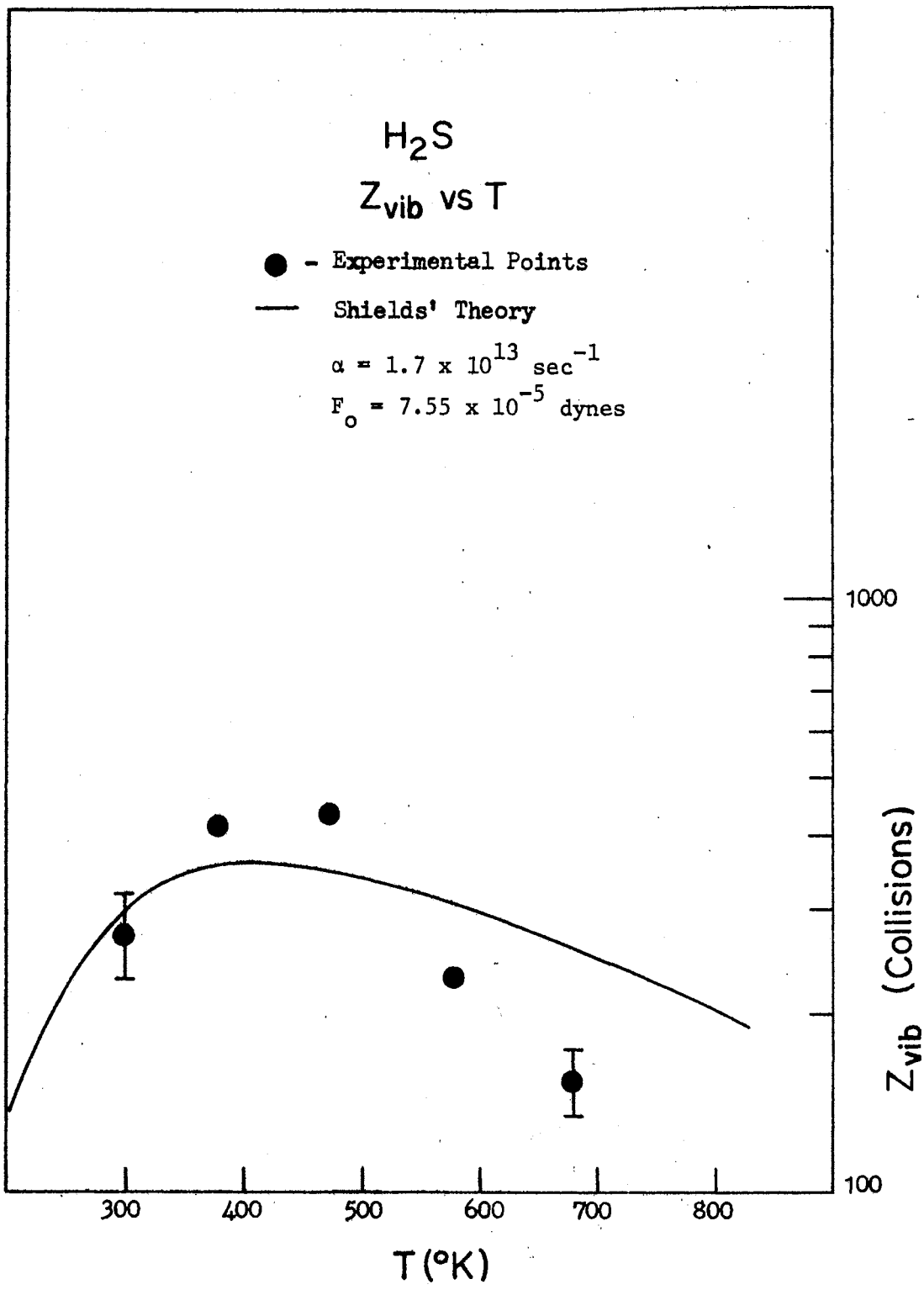

Figure 14. Vibrational Collision Numbers in Hydrogen Sulfide

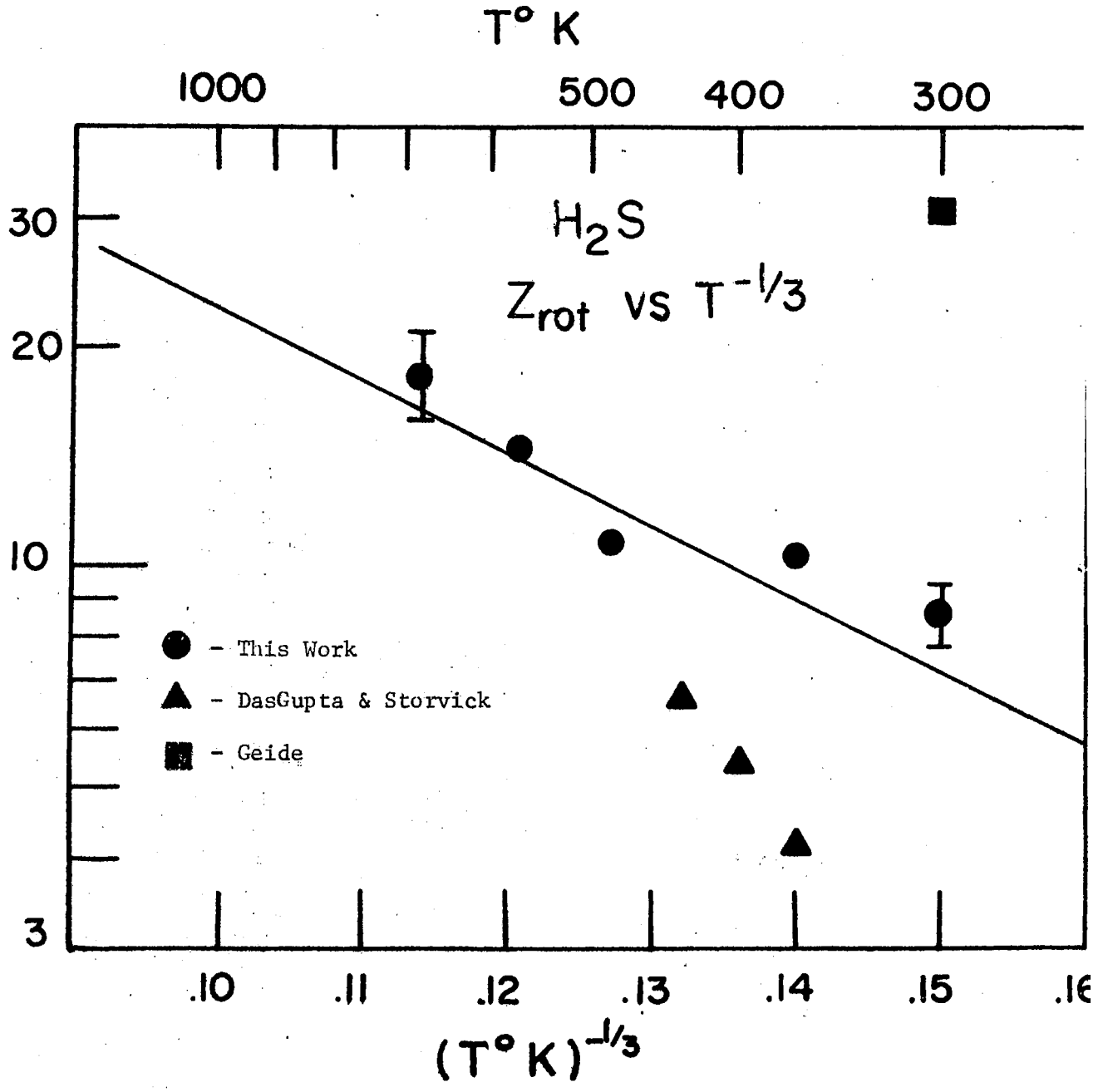

Figure 15. Rotational Collision Numbers in Hydrogen Sulfide

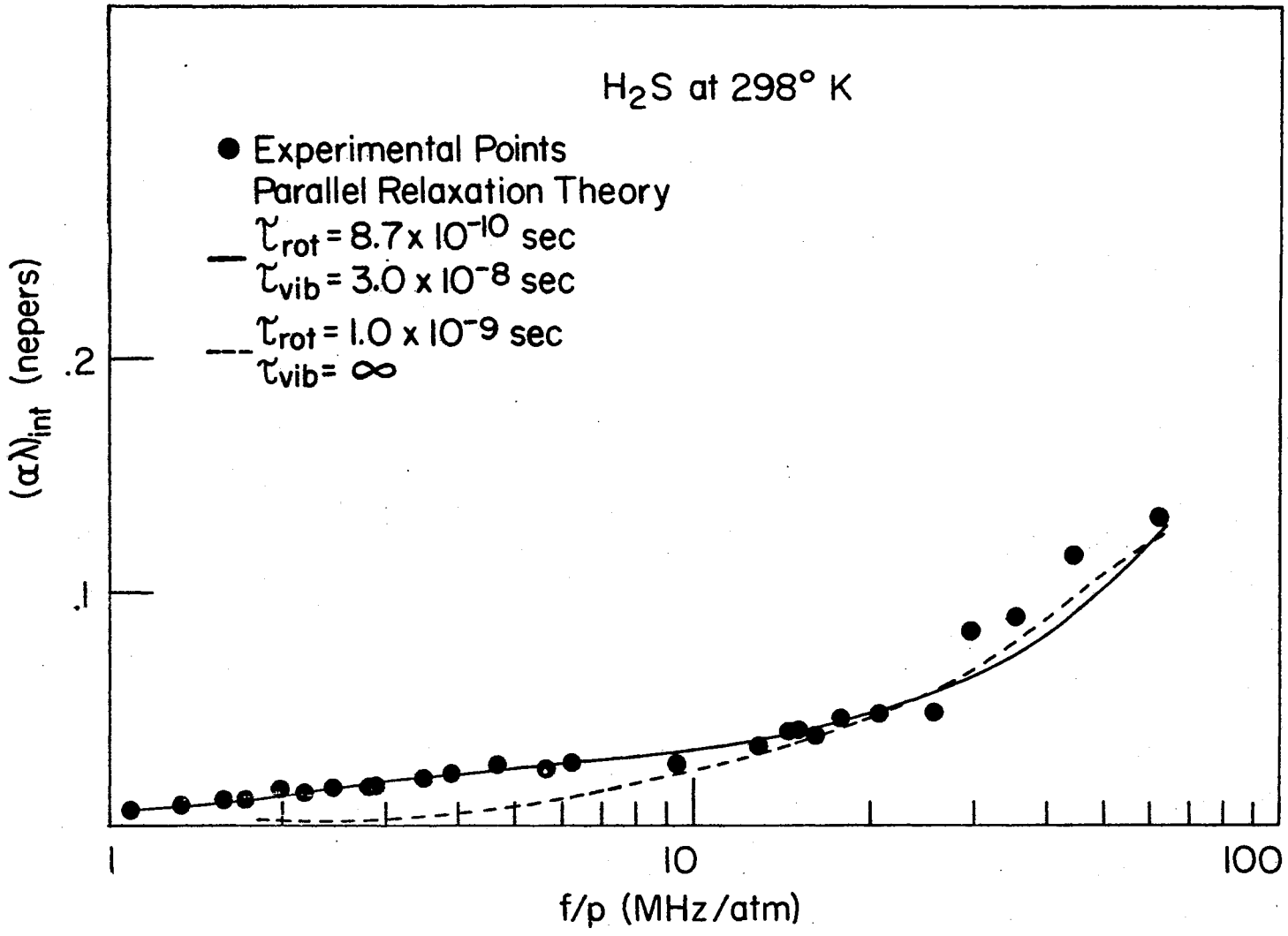

Figure 16. Absorption in Hydrogen Sulfide at 298°K With Parallel Relaxation Curves

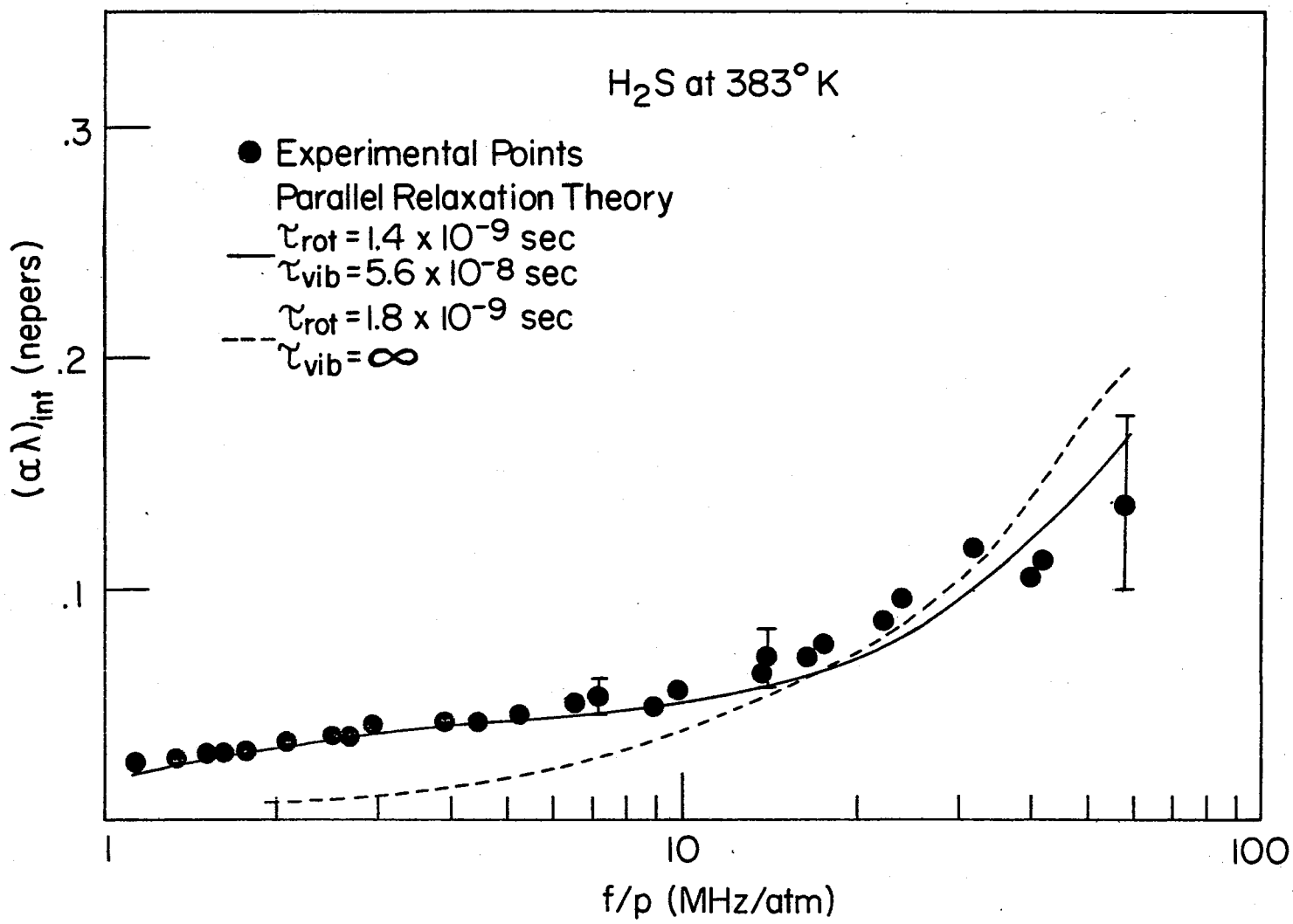

Figure 17. Absorption in Hydrogen Sulfide at 383°K With Parallel Relaxation Curve

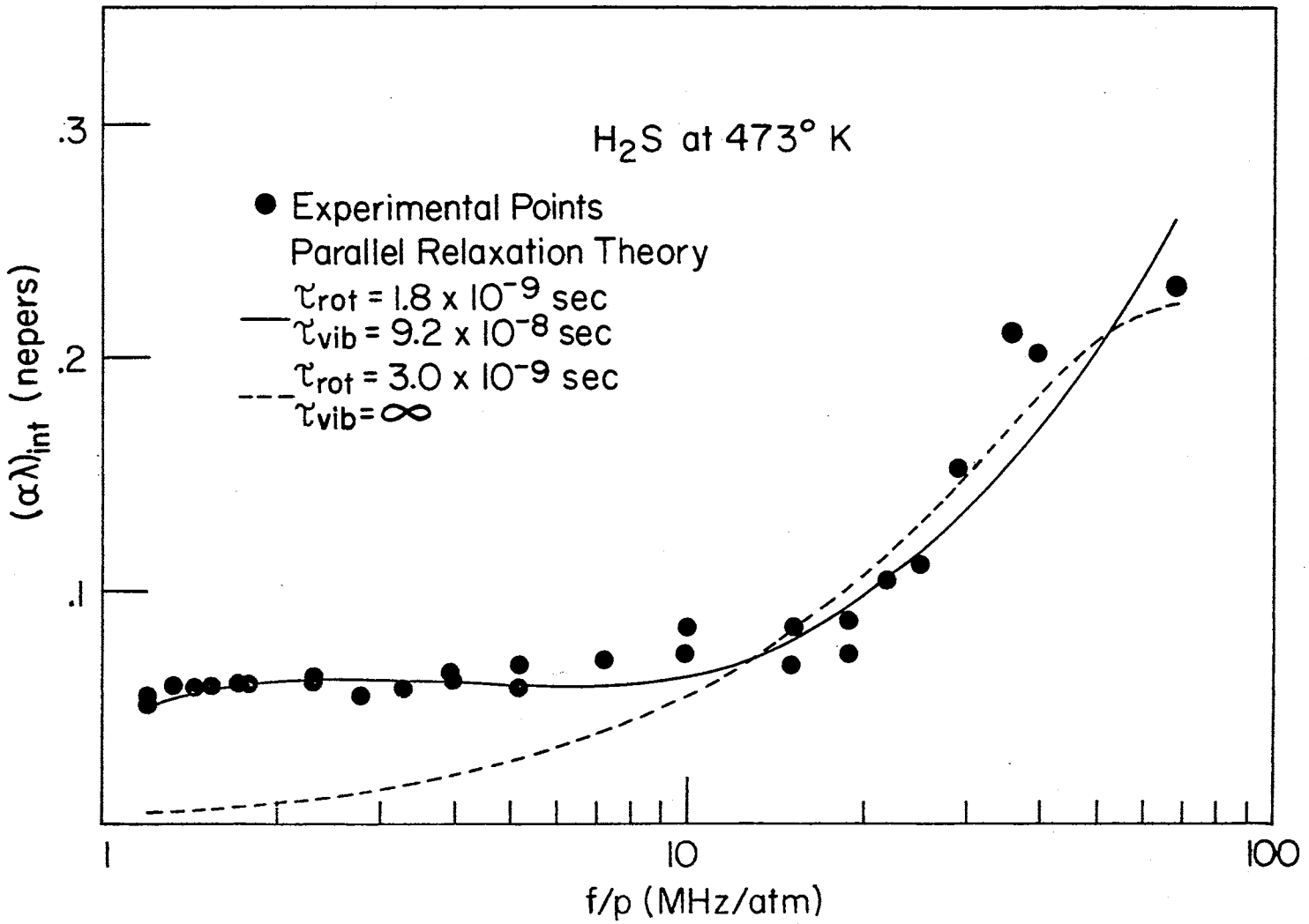

Figure 18. Absorption in Hydrogen Sulfide at 473°K With Parallel Relaxation Curves

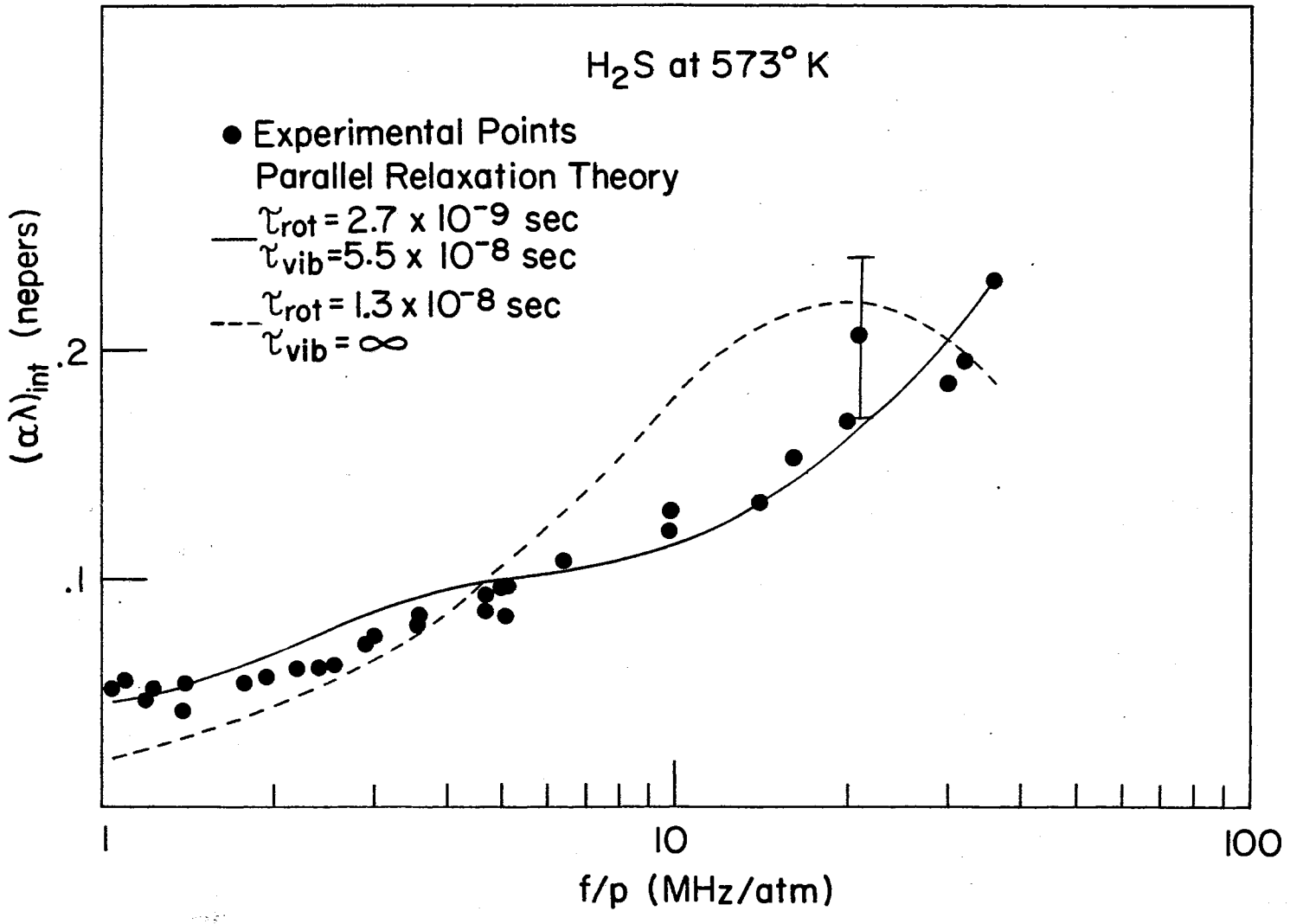

Figure 19. Absorption in Hydrogen Sulfide at 573°K With Parallel Relaxation Curves

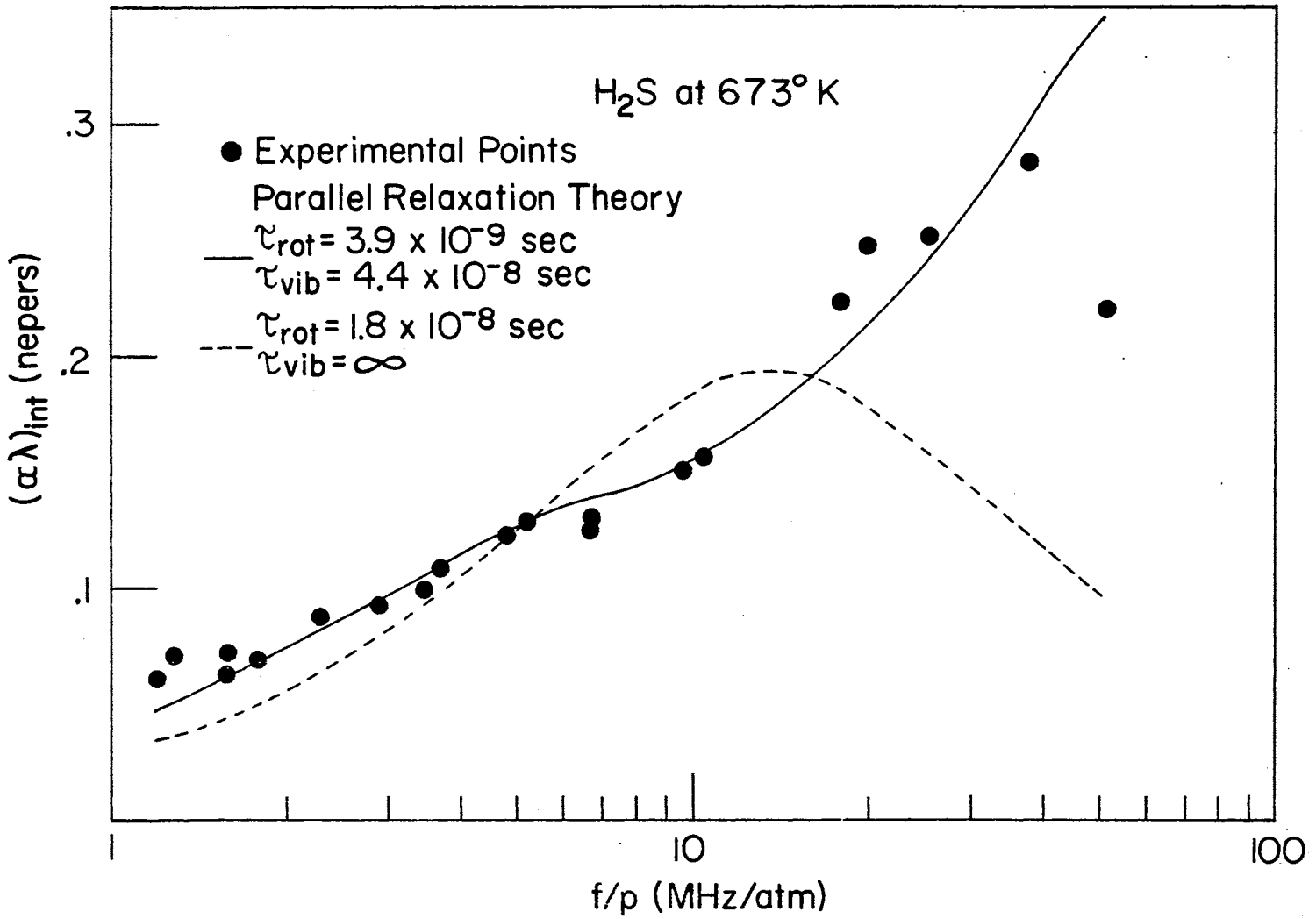

Figure 20. Absorption in Hydrogen Sulfide at 673 With Parallel Relaxation Curves

not dominant at room temperature and recognizing that the collision numbers for v-t processes decrease with temperature, there should be some temperature where the decreasing v-t collision numbers overtake the increasing or almost constant v-r collision numbers. When this happens, the collision number should vary with T approximately as predicted by v-t theory. Such a behaviour is noted in H_2S. At low temperatures v-r theory is followed and at high temperatures, v-t theory is followed.

Ammonia

Previous work on Ammonia has yielded vibrational relaxation times which differ by two or three orders of magnitude. Cottrell and Matheson (39) and Strauch and Decius (40) critically evaluated those relaxation times extracted from experimental velocity data and found that the investigators had failed to correct adequately for gas imperfections. As a result, the only valid relaxation times in the literature are those of Jones, Lambert, Saskena, and Stretton (41), Petralia (42), and Keller (43). The measurements made by Jones, et. al. cover by far the greatest range of f/P so they should be best suited for obtaining relaxation times. He and his co-workers found that vibration and rotation relax together (they assigned one τ to both processes) with a relaxation time of .735 nsec. at room temperature. They further found that the vibrational relaxation times calculated from SSH theory increase with rising temperature due to the effect of attractive forces becoming less important with rising temperature.

The NH_3 molecule forms a pyramid with the Nitrogen atom at the apex and the three Hydrogen atoms as the base. The lowest frequency

vibration ($\theta = 1368^{o}K$) corresponds to the inversion of the Nitrogen atoms. Since NH_3 is a symmetric top, $E_{rot} = J(J + 1)A_o + K^2 (B_o - A_o)$ (44) where $A_o = 6.24\ cm^{-1}$, and $B_o = 9.941\ cm^{-1}$. In the energy range $300^{o}K \pm 50^{o}K$ there are 28 allowed energy levels. Other molecular constants required for analysis of the experimental data are given in Table IV.

Ultrasonic absorption was measured in the temperature range $300^{o}K$ to $1180^{o}K$. Above $773^{o}K$, the gas dissociated and the resulting relaxation times were unreliable. A mass spectrometer sample collected at $953^{o}K$ showed a 20% Nitrogen impurity while a sample collected at room temperature had only a .5% impurity. The measured absorption below $773^{o}K$ was too high to be accounted for by rotational relaxation alone, hence two relaxation times were assigned the process and the values of these parameters were extracted using the method previously discussed. The internal absorption found experimentally was spread out more than it would have been if both rotation and vibration were relaxing together so both relaxation times were varied to fit the experimental data. The vibrational relaxation time at room temperature differed significantly from Jones' value due to the different methods used to analyze the data. The rotational relaxation times are comparable.

The experimental absorption data is presented in Figures 24 through 29. The error bars on the absorption curves give an indication of the large error in internal absorption which is induced by only a 10% error in the total measured absorption. The curves for $C_{vib} = 0$ are not exact but do give an indication of the magnitude of the rotational contribution to the internal absorption curve. The measured absorption clearly can not be accounted for by rotational relaxation alone. For f/P values

TABLE IV

EXPERIMENTAL RESULTS AND MOLECULAR PARAMETERS FOR AMMONIA

Thermodynamic Properties of Ammonia (31,37)

Mass = 17.03 a.m.u. Frequency = 1.00 MHz

T (^{o}K)	$\eta \times 10^{3}$ (poise)	γ	C_p/R
300	.1031	1.303	4.303
415	.1470	1.270	4.687
490	.1791	1.251	5.010
612	.2194	1.224	5.419
773	.2726	1.196	6.025
953	.3250	1.182	6.642

Vibrational Frequencies (32)

ν_1 (cm^{-1})	ν_2 (cm^{-2})	ν_3 (cm^{-1})	ν_4 (cm^{-1})
3337	949.8	3444.	1628.

Rotational Wavenumbers (32)

A_o (cm^{-1})	B_o (cm^{-1})
6.24	9.941

Experimental Results for Ammonia

T (^{o}K)	$\tau_{vib} \times 10^{9}$ (sec)	$\beta_{vib} \times 10^{9}$ (sec)	Z_{vib}	$\tau_{rot} \times 10^{9}$ (sec)	Z_{rot}
300	2.5	1.8	22	.92	11
415	3.2	2.0	17	1.2	10
490	4.0	2.1	15	1.4	10
612	5.8	2.7	14	4.0	23
773	7.5	2.9	11	4.7	22

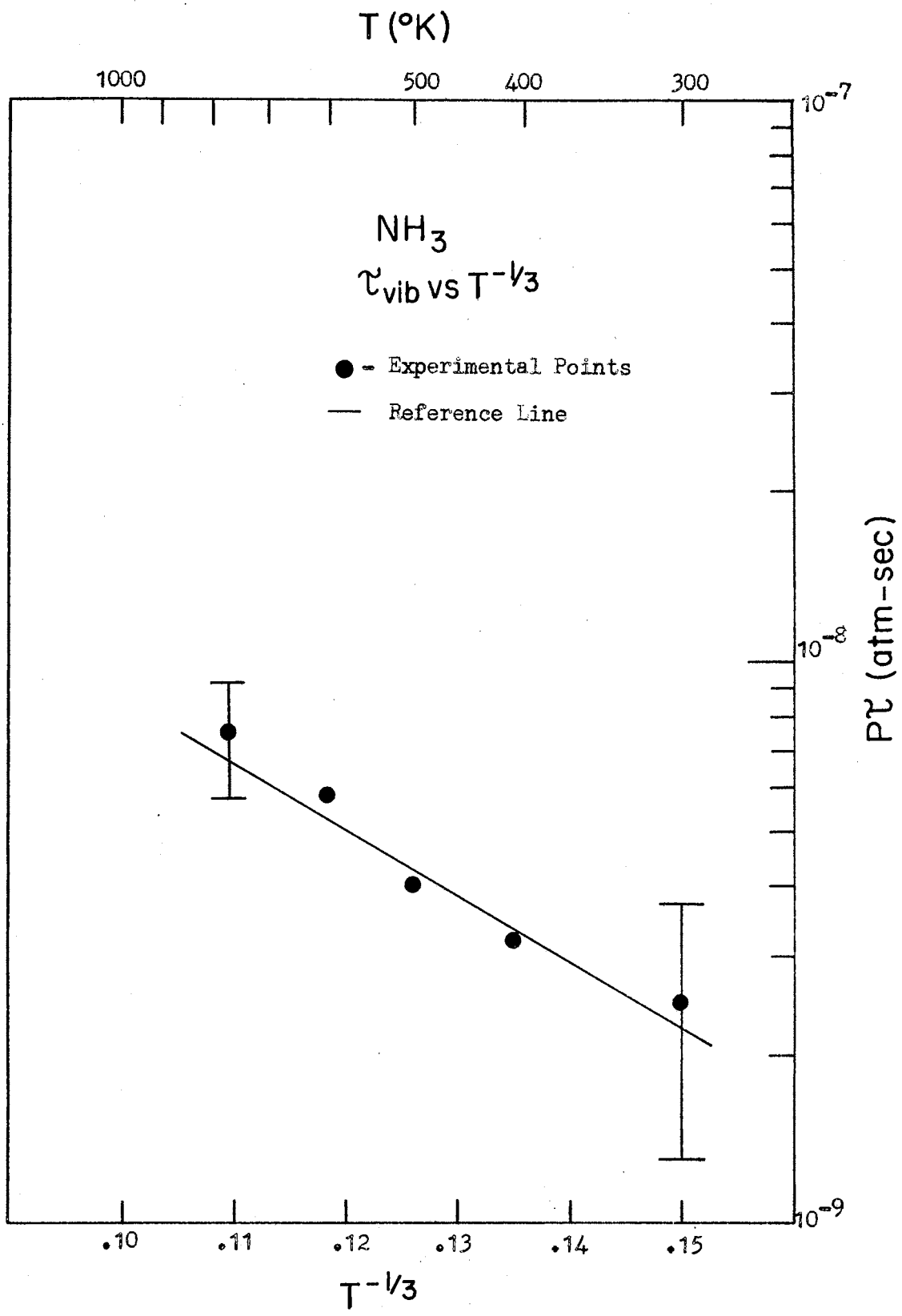

Figure 21. Vibrational Relaxation Times in Ammonia

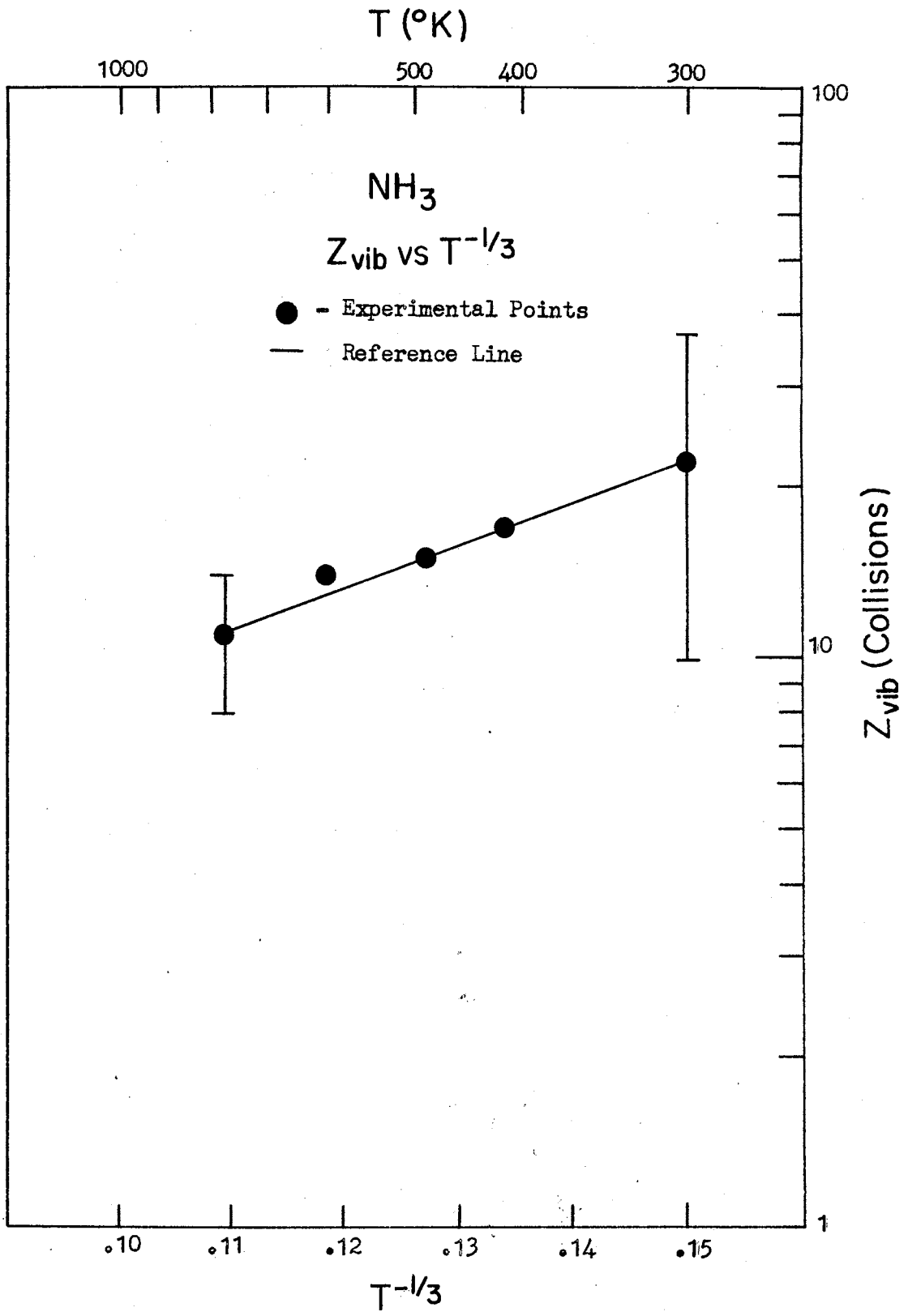

Figure 22. Vibrational Collision Numbers in Ammonia

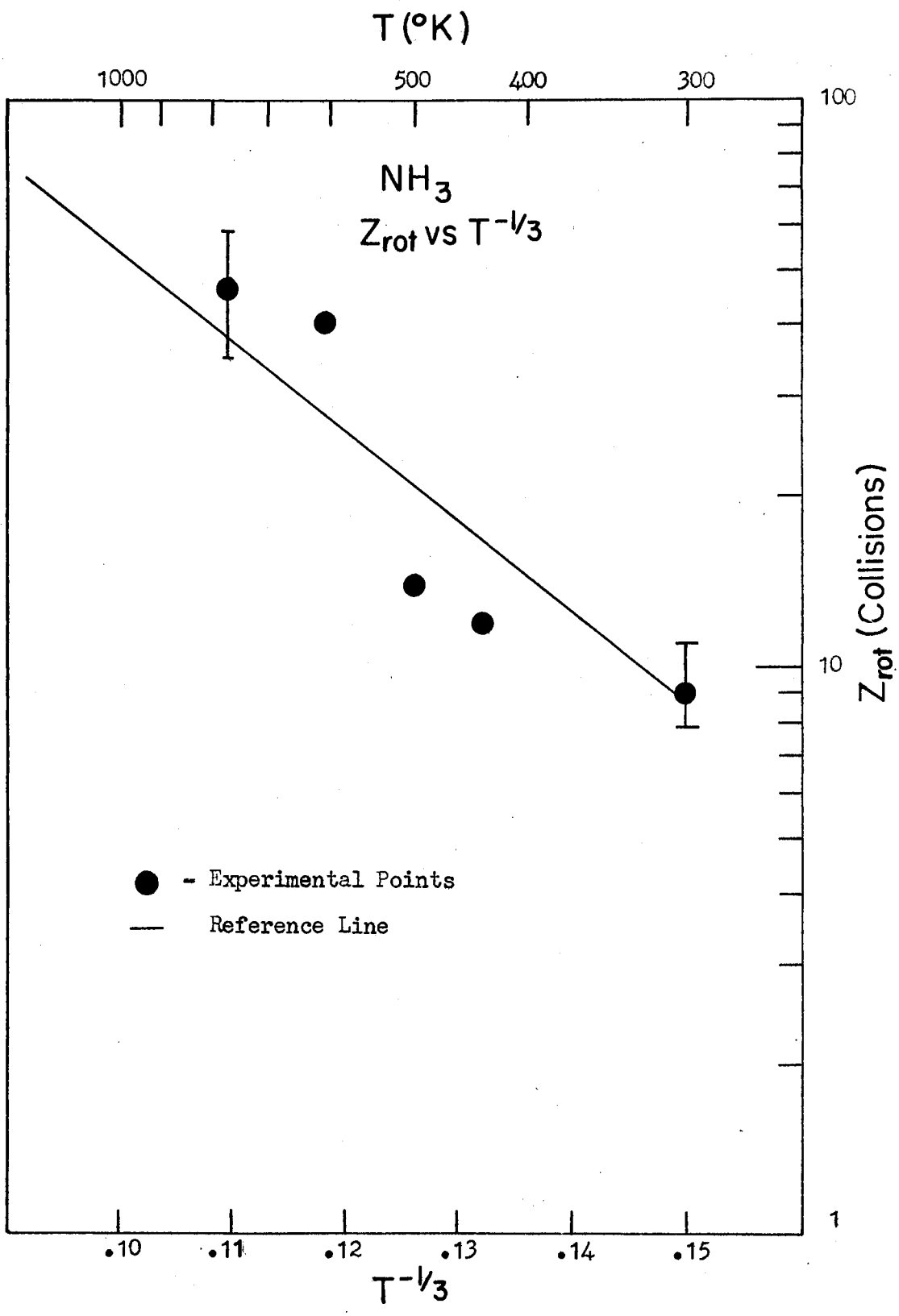

Figure 23. Rotational Collision Numbers in Ammonia

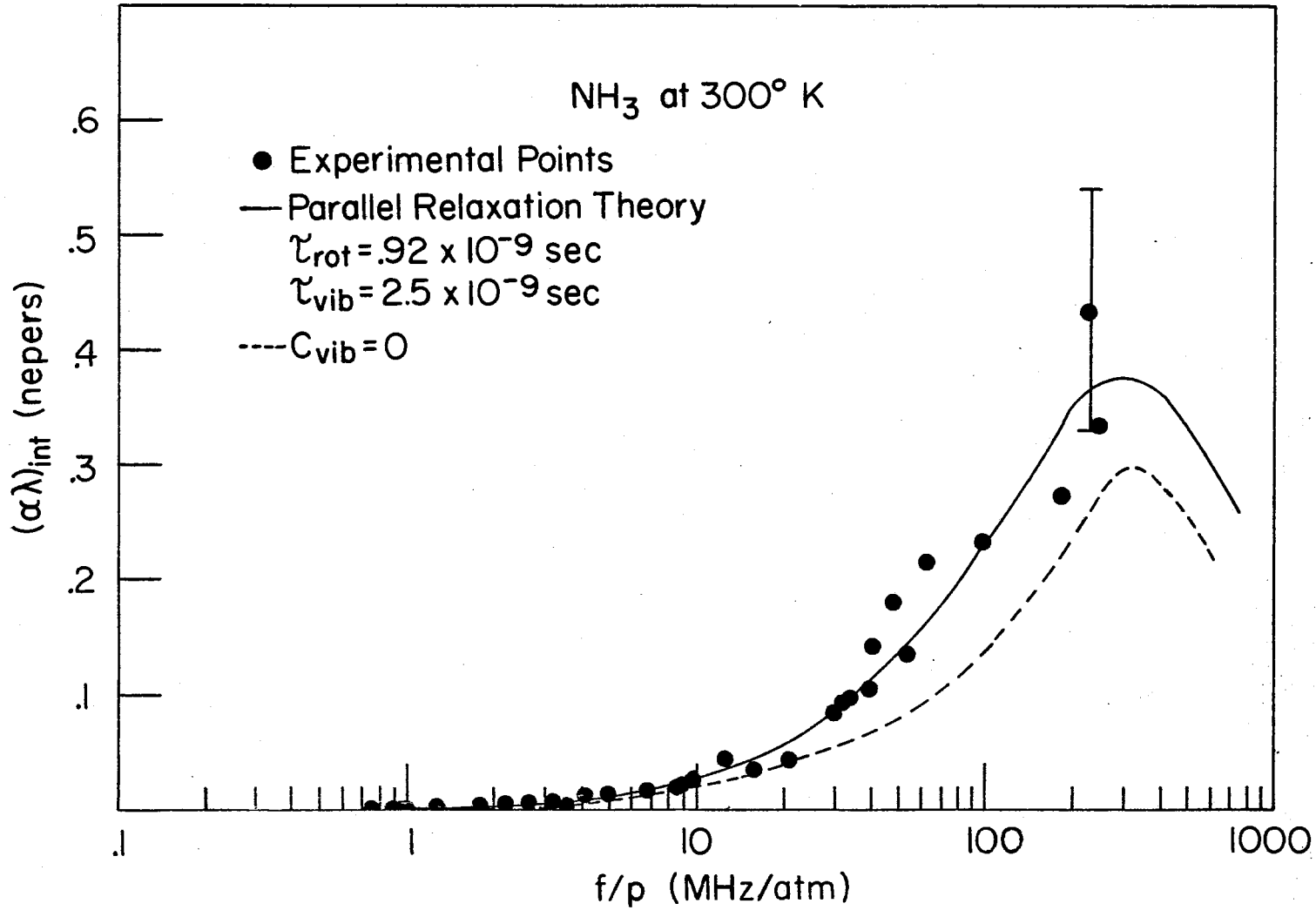

Figure 24. Absorption in Ammonia at 300°K With Parallel and Single Relaxation Curves

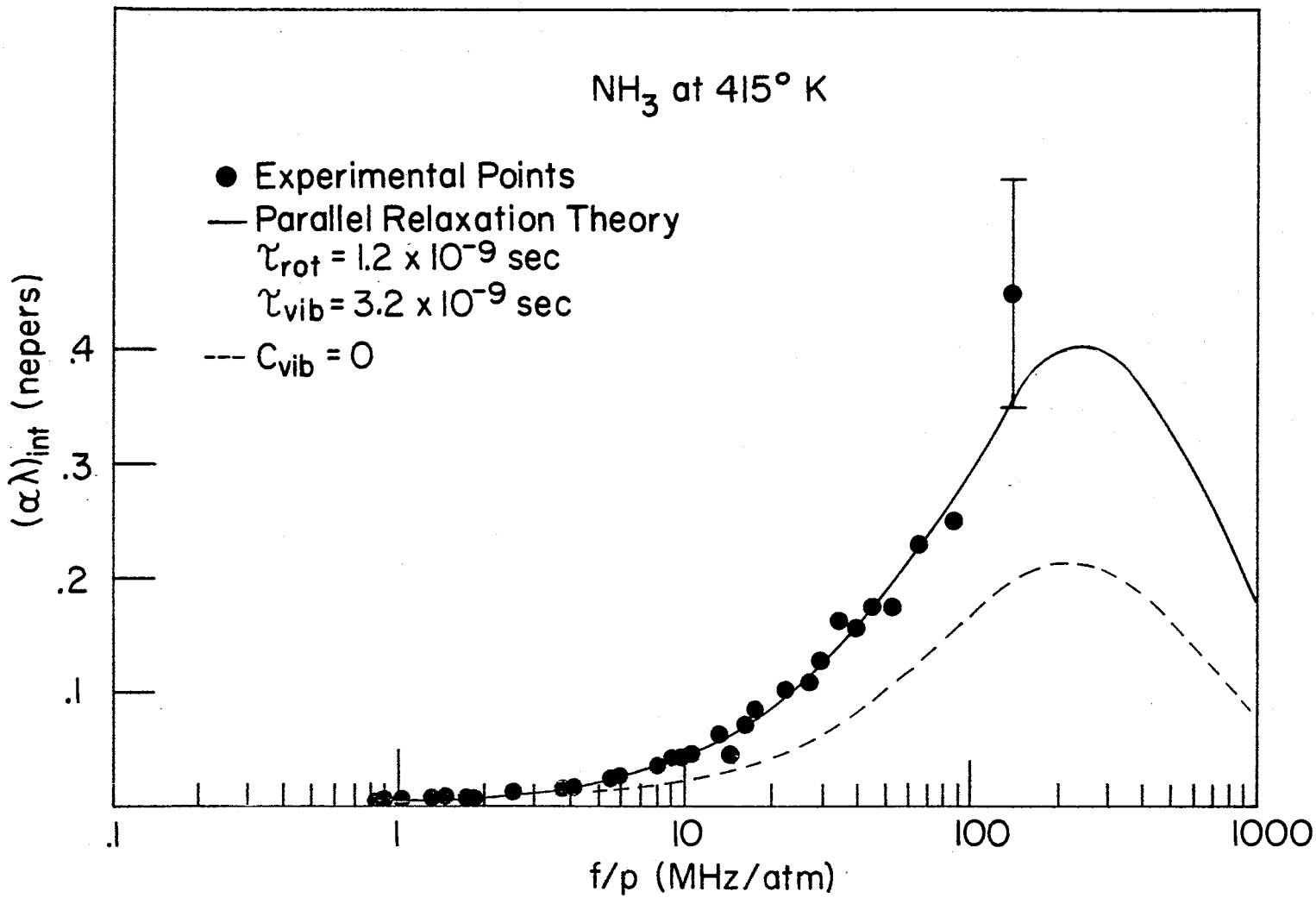

Figure 25. Absorption in Ammonia at 415°K With Parallel and Single Relaxation Curves

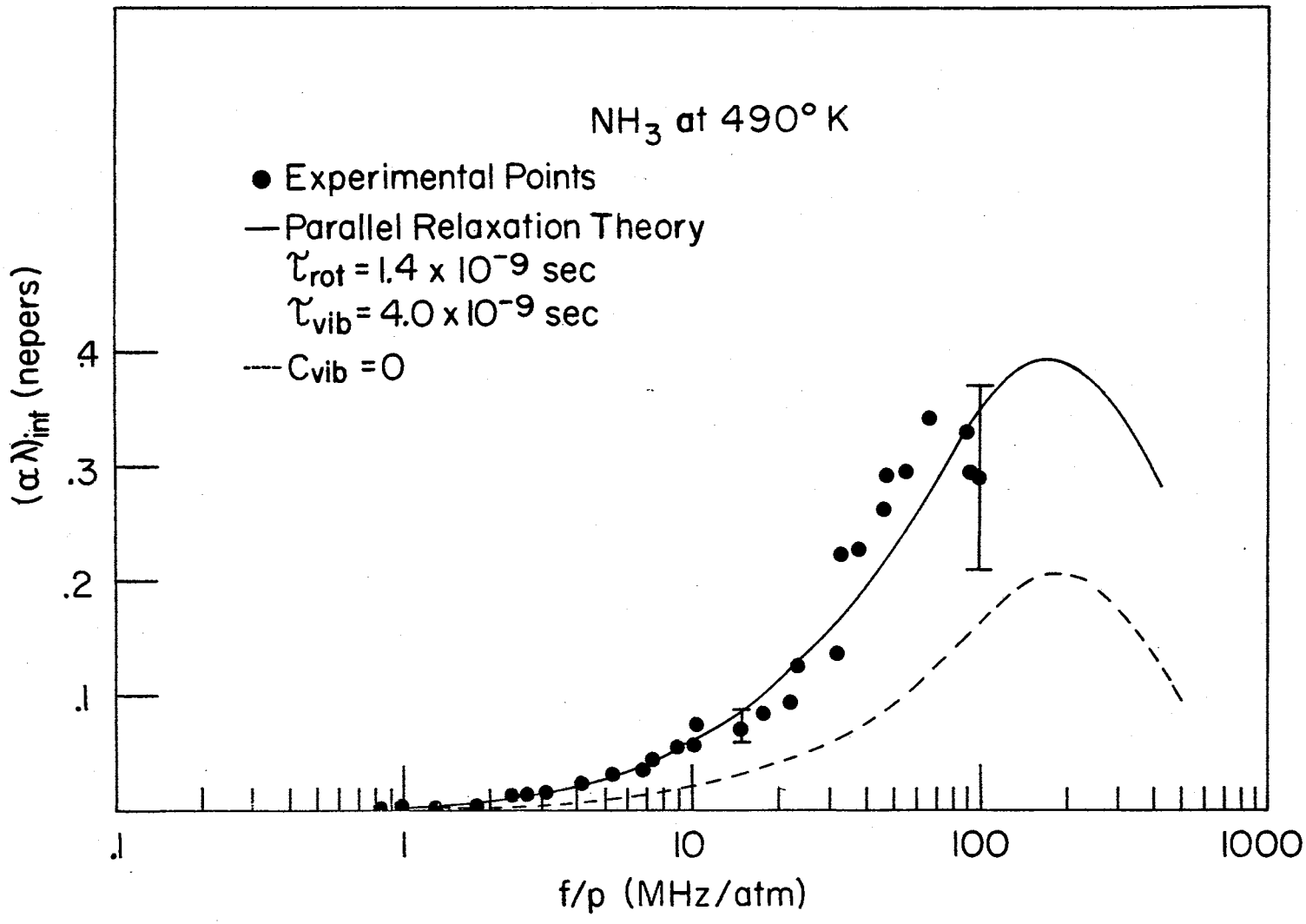

Figure 26. Absorption in Ammonia at 490°K With Parallel and Single Relaxation Curves

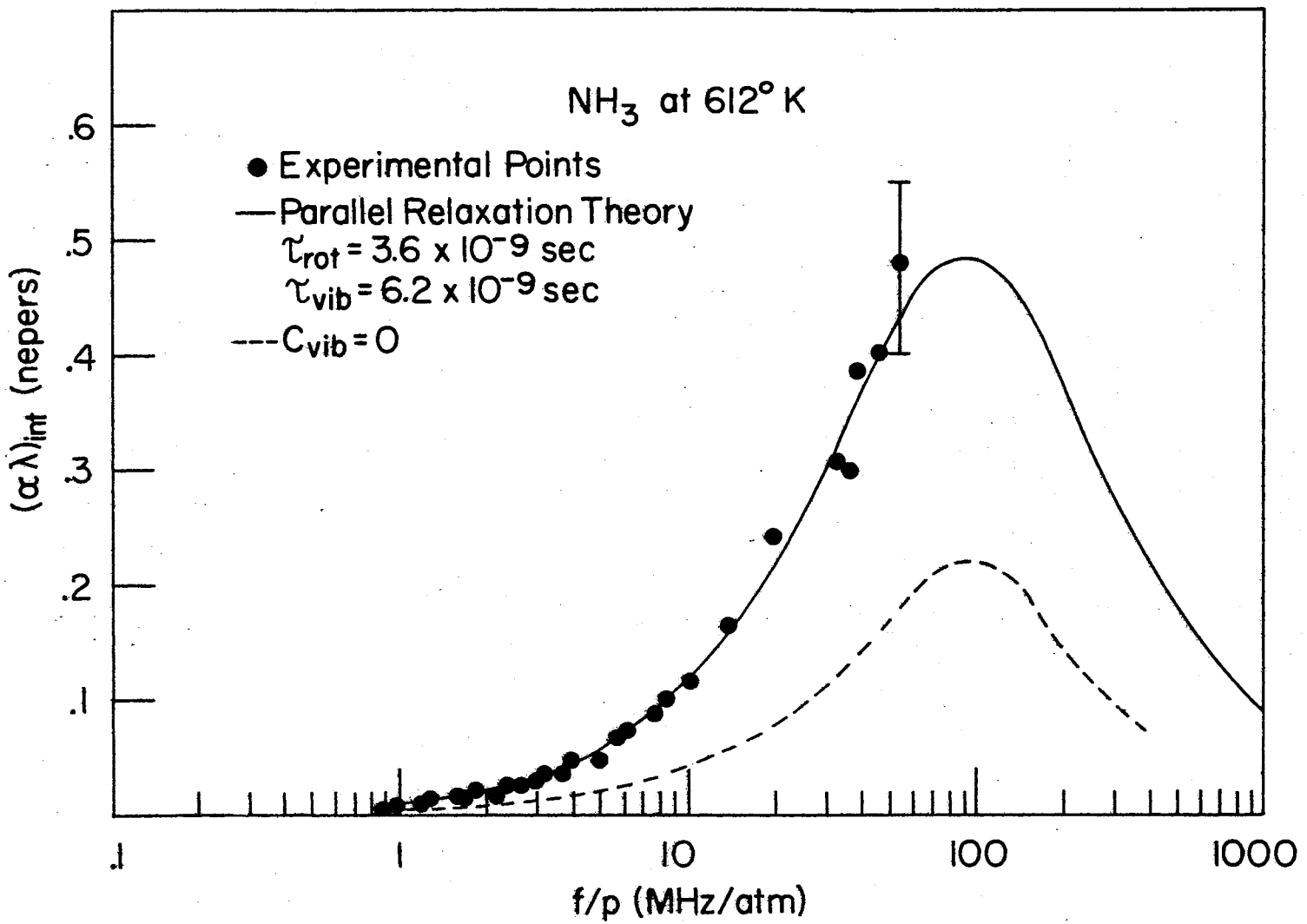

Figure 27. Absorption in Ammonia at 612°K With Parallel and Single Relaxation Curves

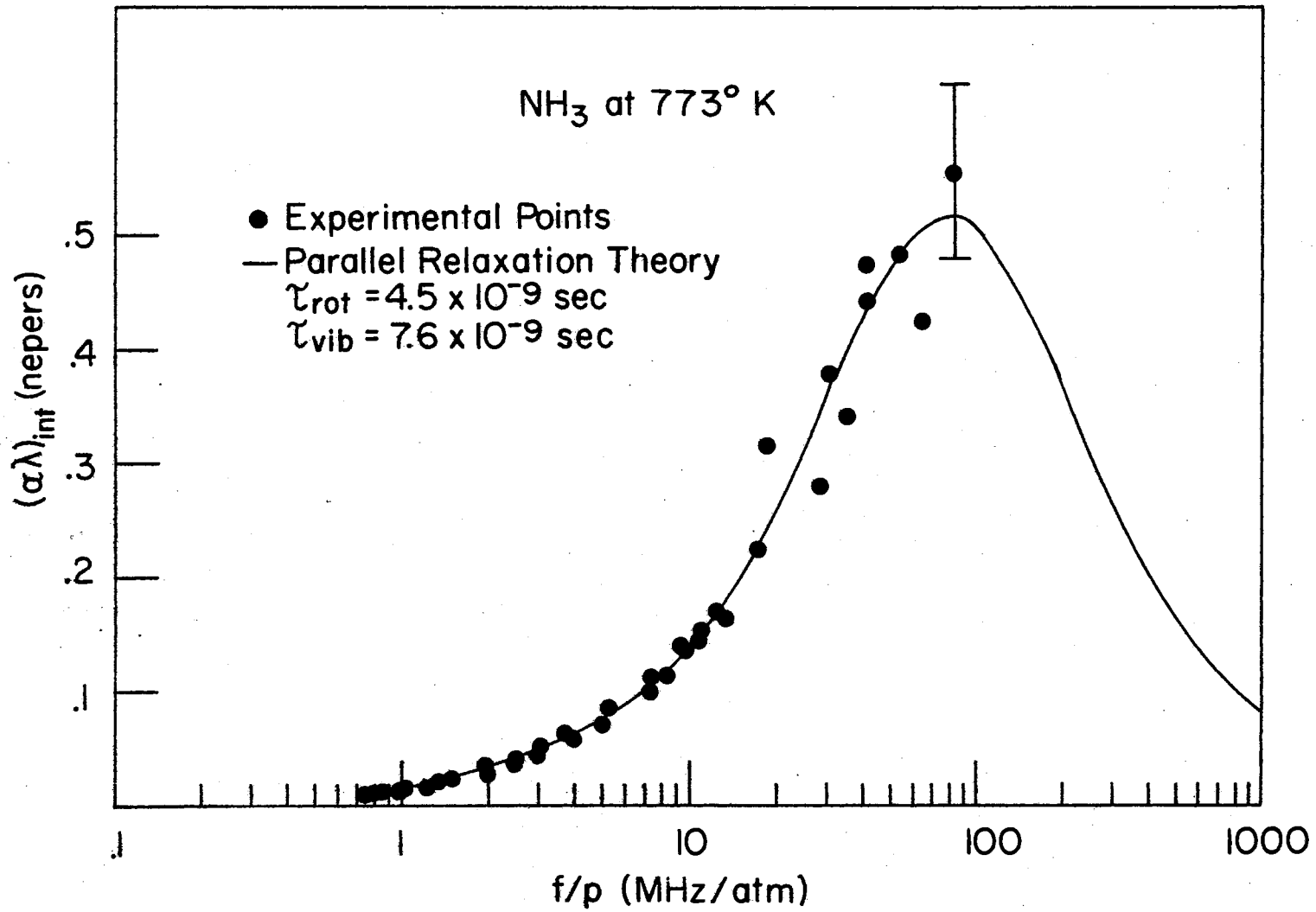

Figure 28. Absorption in Ammonia at 773°K With Parallel Relaxation Curves

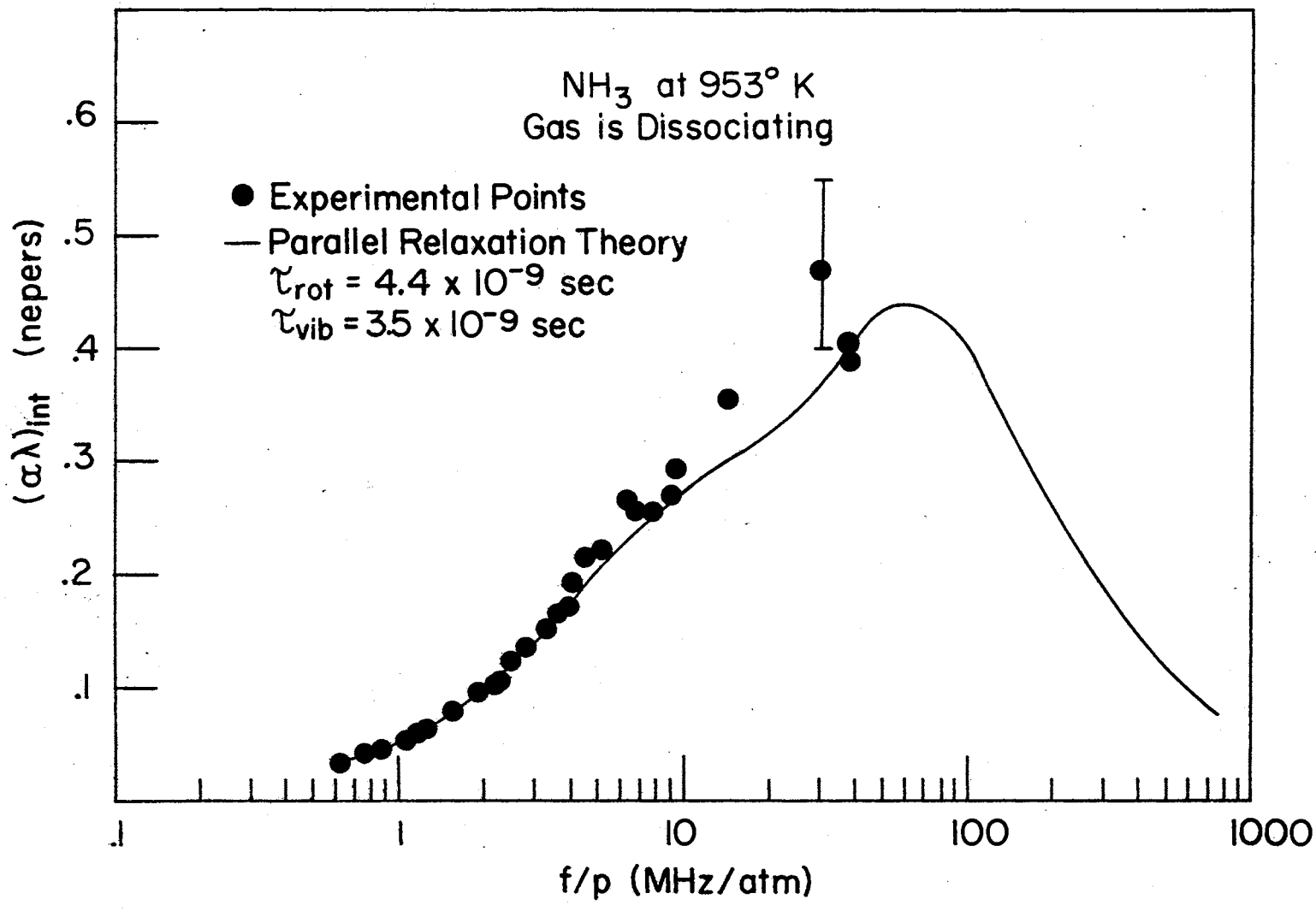

Figure 29. Absorption in Dissociating Ammona at 953°K With Parallel Relaxation Curve

above 100 MHz/atm., the experimental error in absorption may very well exceed 10%. The collision numbers derived from absorption measurements are given in Figures 22 and 23. Again, the straight lines represent the general temperature dependence predicted by L-T theory. The vibrational relaxation times increase with increasing temperature as predicted by SSH Theory (Figure 21). The error bars on the relaxation times and collision numbers are derived from the numerical error analysis described previously. Even though the vibrational relaxation times increase rapidly with temperature, the collision numbers decrease. This is due to the increasing importance of the 2344^{o} mode at higher temperatures.

Cottrell and Matheson (39) found Z_{vib} for ND_3 to be about 90. This investigation yielded a Z_{vib} for NH_3 at room temperature of 23 hence $P_{10}(NH_3)/P_{10}(ND_3) \cong 4$. This compares to a ratio of .8 calculated using v-t theory and a ratio of 1.3 using v-r theory. The large difference between experiment and theory could be attributed to two factors. First, Cottrell and Matheson have pointed out that the inversion of the NH_3 molecule might be very easy to excite. Second, the large probabilities obtained from either v-r or v-t theory demonstrates that the small perturbation approximation upon which these theories are based is no longer valid.

Sulphur Dioxide

Several investigators have measured the vibrational relaxation times of SO_2. Lambert and Salter (45) and later Shields (15) found that the dispersion and absorption due to vibrational relaxation could not be represented with a single relaxation time. Lambert and Salter suggested that the lowest energy mode relaxes separately from the two higher

modes which relax together in series. Shields found that the experimental data could be reproduced by a theoretical curve assuming either three series processes or the two higher modes in series and the lowest mode in parallel with these. By assuming different relaxation times, he found that the two treatments could be made mathematically equivalent, therefore, acoustic measurements in pure SO_2 can not differentiate between the two processes. The only rotational collision numbers available in the literature were derived from experimental thermal conductivity and thermal transpiration data (10,35).

The SO_2 molecule forms an isoceles triangle. The lowest vibrational mode($\theta = 745^{o}$) is the vibration of the 0 atoms like scissors with the S atom at the apex. The other two modes ($\theta_2 = 1656^{o}$ and $\theta_3 = 1956^{o}$) are due to the 0 atoms moving along the valence bonds either in phase or out of phase. A relaxation time τ_1 was assigned to the lowest energy mode and a relaxation time $\tau_{2,3}$ was assigned to the other two modes. These were assumed to relax in parallel with rotation and in parallel with each other. The results of this analysis are given in Figures 35 through 43. The experimental data was also analyzed assigning a single relaxation time to vibrational relaxation.

The analysis of the absorption data using three relaxation times compares favorably with the results of Shields. At low and high temperatures the vibrational relaxation peak was in the range of the instrument so the relaxation times obtained are quite accurate. At intermediate temperatures, the accuracy of the relaxation times was degraded since the entire absorption peak could not be observed. The shape of the absorption peak is critical when separating two relaxation pressures.

During his analysis, Shields required the relaxation times obtained

by a least squares fit to be proportional to the concentration of Argon thus restricting the choice of 100% SO_2 relaxation times. This very probably accounts for the difference in relaxation times obtained by Shields and those found in this investigation. The analysis based on a single relaxation time for vibration gives τ at first increasing then decreasing with temperature, an unusual phenomena. A correct analysis based on two relaxation times shows the relaxation time of the lowest vibrational mode increases with temperature; however, the collision numbers decrease with increasing temperature but not exponentially with $T^{-1/3}$ as predicted by L-T theory. The relaxation time of the highest energy vibrational modes behaves classically as does the associated collision numbers.

The rotational energy levels are given approximately by the relation $E_{rot} = J(J + 1)(A_o + B_o) + K^2 (A_o - \frac{1}{2}(B_o + C_0)$ (44) where $A_o = 2.024$ cm^{-1}, $B_o = .3442$ cm^{-1} $C_o = .2935$ cm^{-1}, $J \doteq 0,1,2,\ldots,$ and $K \doteq 0,1,\ldots,J$. In the energy range $300^oK \pm 50^oK$ there are approximately 30 energy levels. This energy level density is slightly greater than NH_3 and H_2S. The rotational relaxation times increase with increasing temperature as do the rotational collision numbers. These results are compared with the results of Das Gupta and Storvich (35) in Figure 34. The excellent agreement between thermal transpiration numbers and acoustic numbers is the first such agreement observed. In the past, thermal conductivity measurements in SO_2 have yielded rotational collision numbers from 1 to 3 some increasing and some decreasing with temperature (10). The change in Z_{rot} with temperature is much less than one would predict based on the density of rotational energy states and large dipole moment. In view of this discrepancy, the ultrasonic velocity was examined to deter-

TABLE V

MOLECULAR PARAMETERS FOR SULPHUR DIOXIDE

Properties of Sulphur Dioxide (31)

Mass = 64,066 a.m.u. Frequency = 1.01 MHz

T (^{o}K)	$\eta \times 10^{3}$ (poise)	γ	C_p/R
290	.1177	1.266	4.761
298	.1310	1.263	4.796
418	.1833	1.230	5.343
528	.2342	1.210	5.773
662	.2352	1.198	6.045
668	.2775	1.198	6.056
792	.3202	1.188	6.315
901	.3545	1.183	6.469
1090	.4156	1.179	6.588

Vibrational Frequencies (32)

ν_1 (cm^{-1})	ν_2 (cm^{-1})	ν_3 (cm^{-1})
1151	517.7	1362

Rotational Wavenumbers (32)

A_o (cm^{-1})	B_o (cm^{-1})	C_o (cm^{-1})
2.024	.3442	.2935

mine if a different result would have been obtained using velocity data. This examination showed that if velocity were used, all the relaxation times would have been increased slightly but the slope of ln Z_{rot} vs $T^{-1/3}$ would remain essentially unchanged.

A sample of the SO_2 used was taken from the ultrasonic instrument and analyzed in a mass spectrometer. The analysis indicated a 2% N_2 impurity. This same impurity was found in several other samples and may be a result of the sampling method. The error introduced by this impurity if the impurity is actually present can be estimated using Equation 2.118 from Cottrell and McCoubrey (12).

$$\frac{1}{\tau} = \frac{A}{\tau_{AA}} + \frac{B}{\tau_{AB}}$$

where τ is the observed relaxation time, A is the mole fraction of SO_2, B is the mole fraction of N_2, τ_{AA} is the actual relaxation time in SO_2, and τ_{AB} is the relaxation time of a gas in which only N_2 - SO_2 collisions occur. This latter quantity can be estimated using the results of Shields for SO_2/Ar mixtures as about 25 x 10^{-7} sec. hence the impurity should introduce an error in τ of about .4% which is insignificant.

Neither v-t or v-r theory can predict the odd temperature dependence of Z_1. Corran, Warburton, Lambert and Salter (38) have explained this behaviour in a qualitative manner. They assert that the observed temperature dependence is the result of preferred alignment during collisions due to long range dipole-dipole forces. As the temperature increases, such a preferred alignment should become less important due to more rapid rotations of the molecules. This explanation is further supported by this investigation. Referring to Figure 32 note that at high

TABLE VI

EXPERIMENTAL RESULTS FOR SULPHUR DIOXIDE

T (^{o}K)	$\tau_1 \times 10^8$ (sec)	Z_1	$\tau_{2,3} \times 10^7$ (sec)	$\beta_2 \times 10^7$ (sec)	Z_2
290	4.6	460	6.9	4.4	4,900
298	5.1	460	6.4	4.1	3,900
418	6.7	390	3.2	1.7	1,200
528	8.7	360	3.3	1.7	870
662	8.0	290	2.8	1.5	700
668	8.3	260	2.6	1.4	540
792	9.3	230	2.2	1.1	360
901	8.9	180	1.8	.90	240
1090	8.9	140	1.5	.76	160

T (^{o}K)	$\tau_{rot} \times 10^{10}$ (sec)	Z_{rot}
290	3.4	3.7
298	3.0	3.3
418	5.0	3.7
528	7.0	3.9
662	10.	5.4
668	13.	6.2
792	12.	4.8
901	13.	4.7
1090	20.	6.0

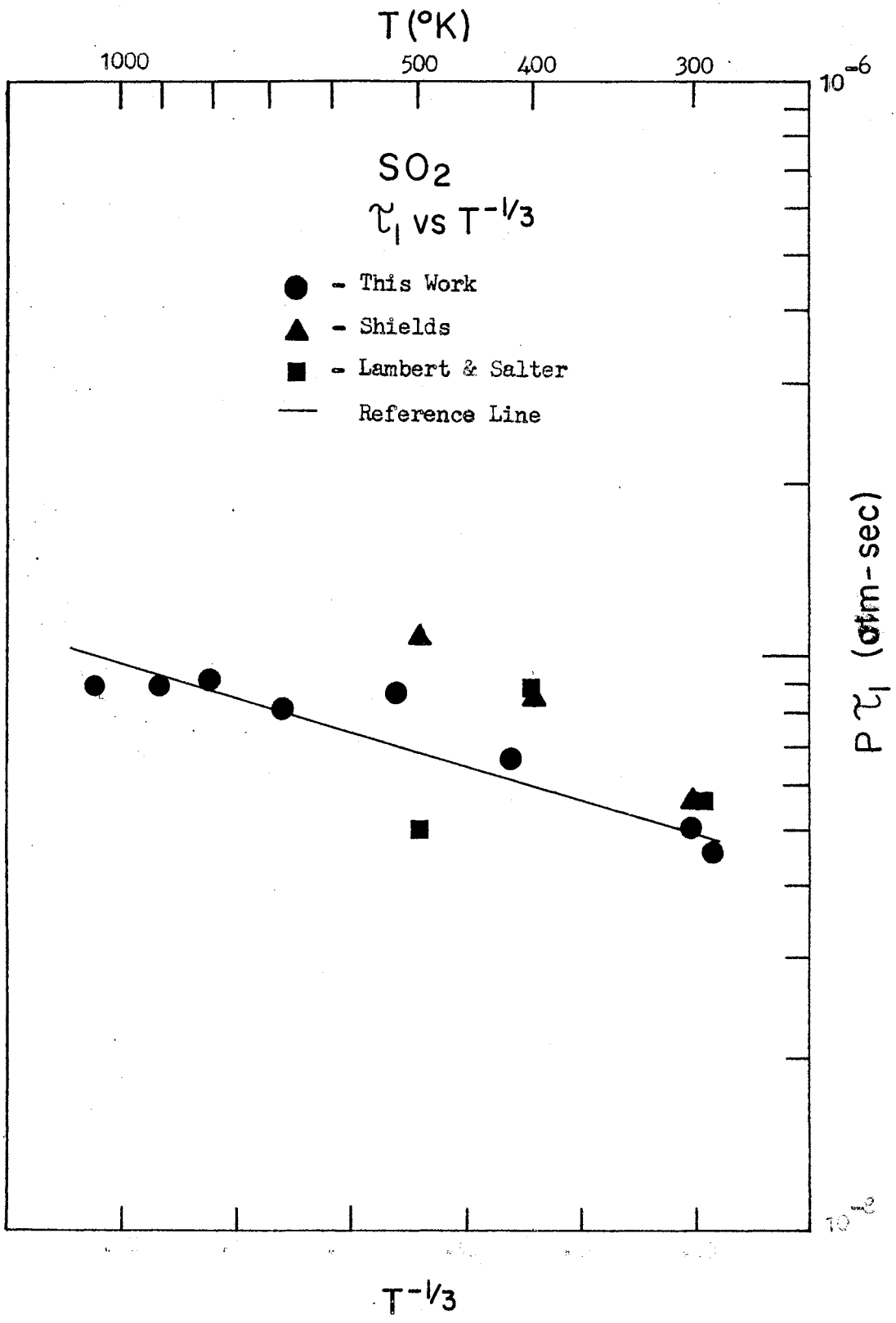

Figure 30. Vibrational Relaxation Times at the Lowest Energy Mode in Sulphur Dioxide

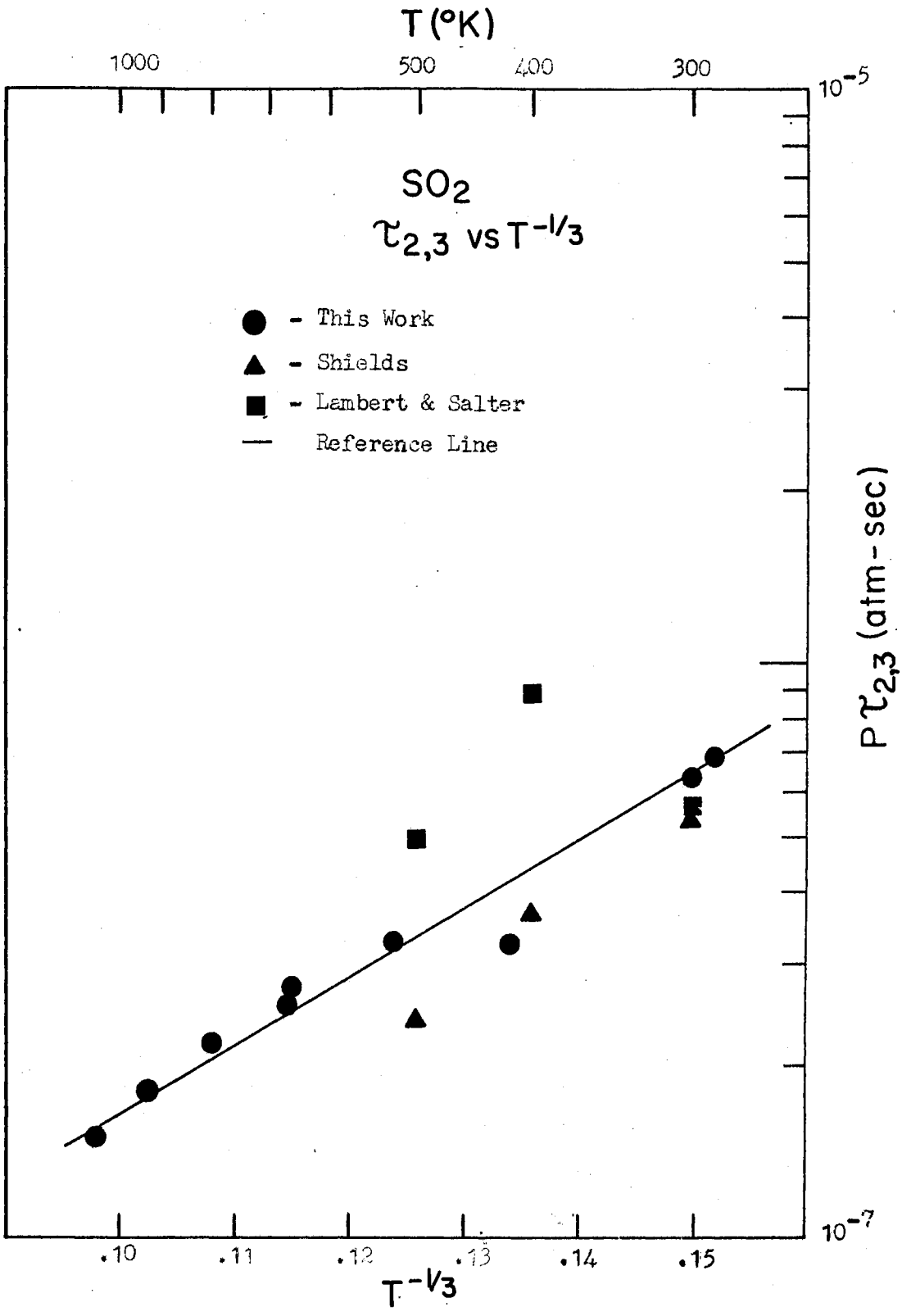

Figure 31. Vibrational Relaxation Times of the Highest Energy Modes in Sulphur Dioxide

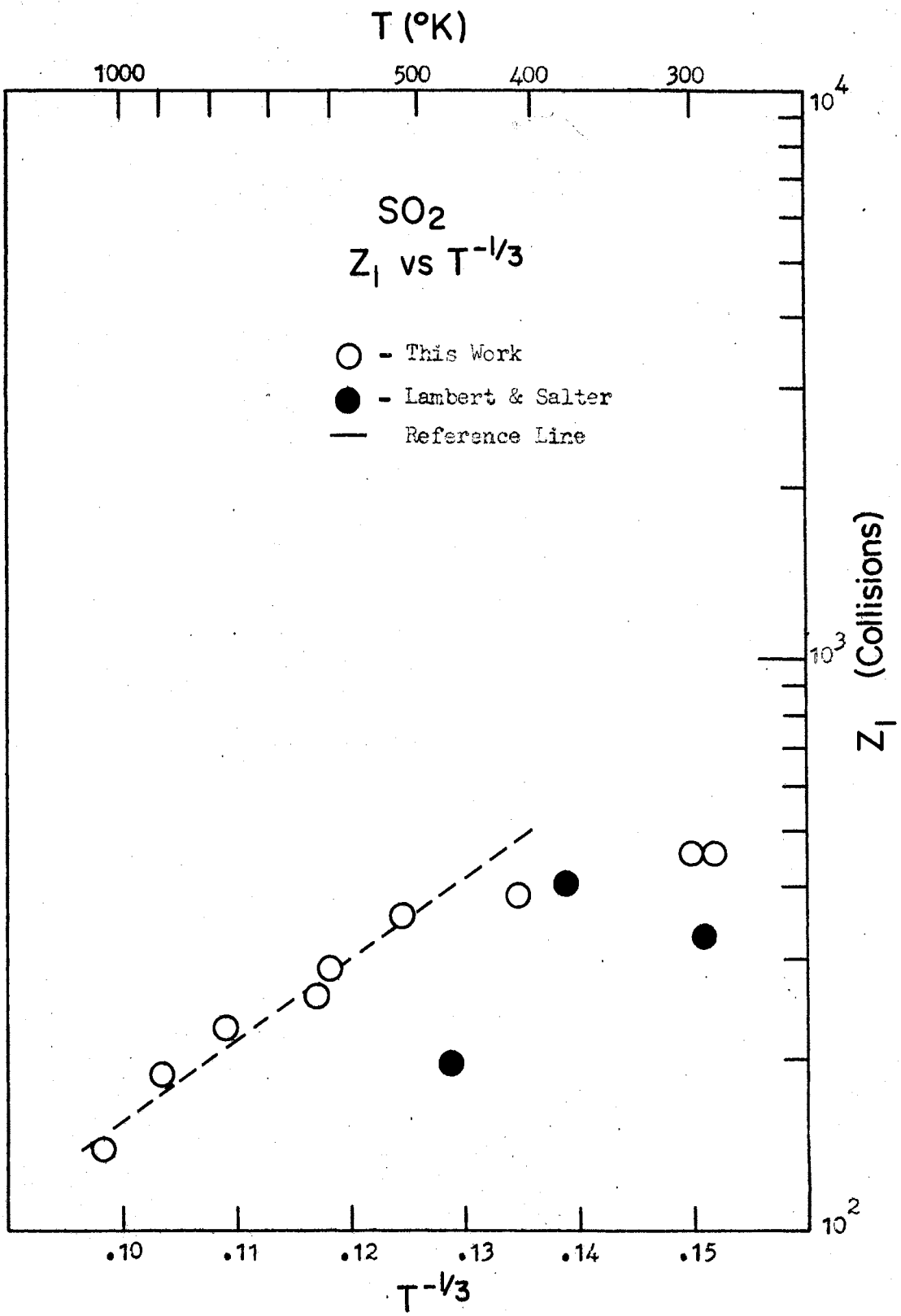

Figure 32. Vibrational Collision Numbers for the Lowest Energy Mode in Sulphur Dioxide

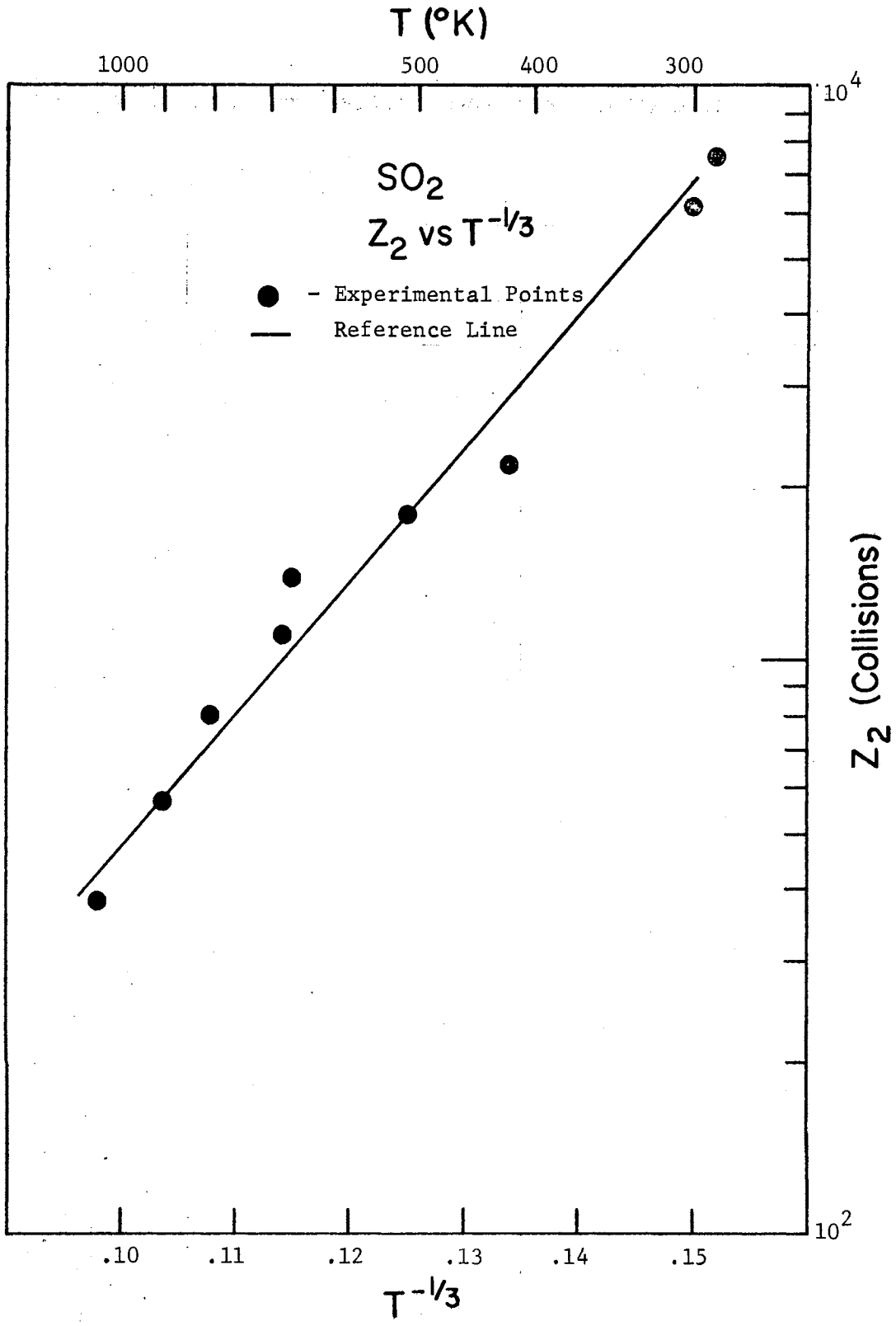

Figure 33. Vibrational Collision Numbers for the Highest Energy Modes in Sulphur Dioxide

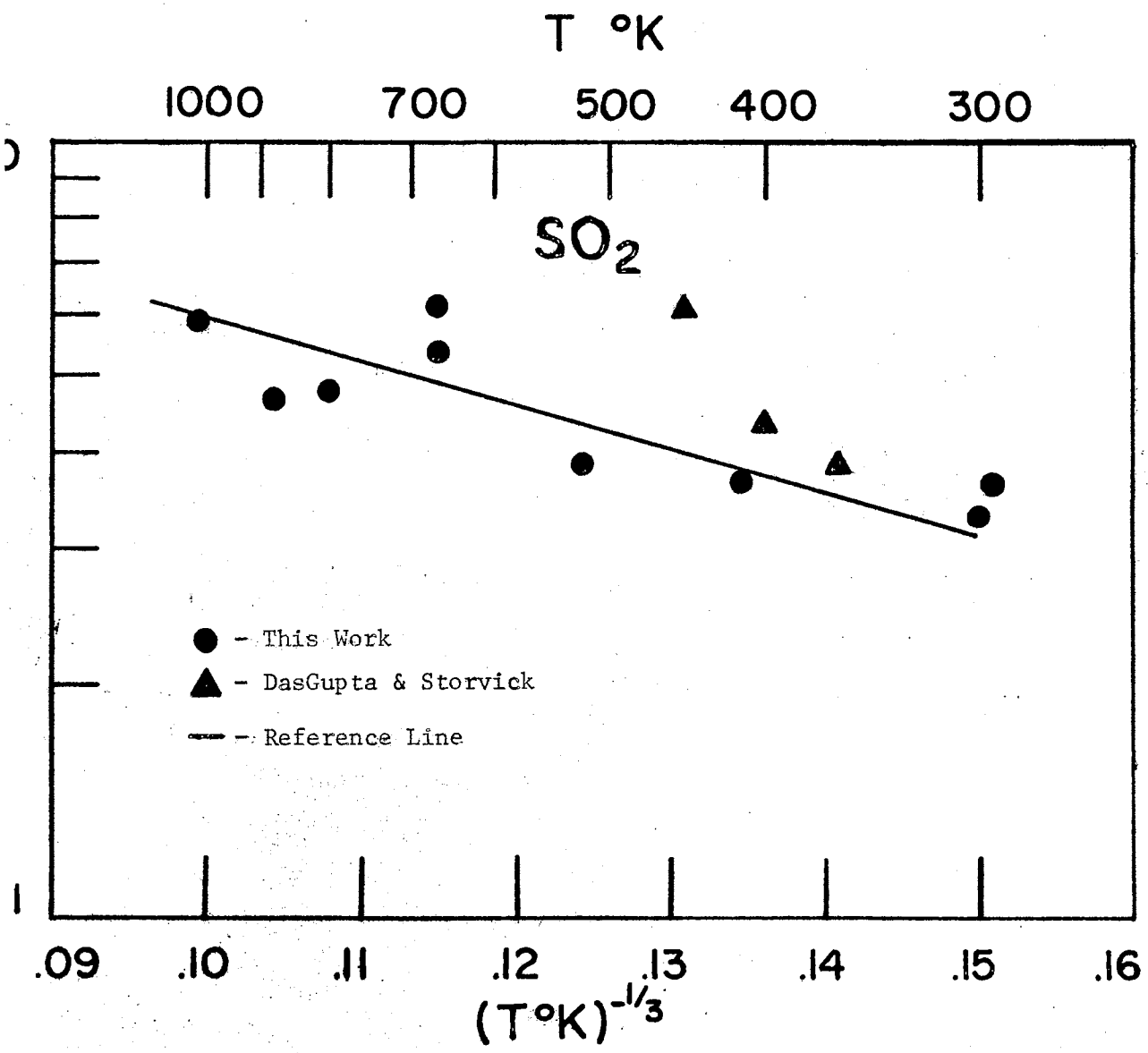

Figure 34. Rotational Collision Numbers in Sulphur Dioxide

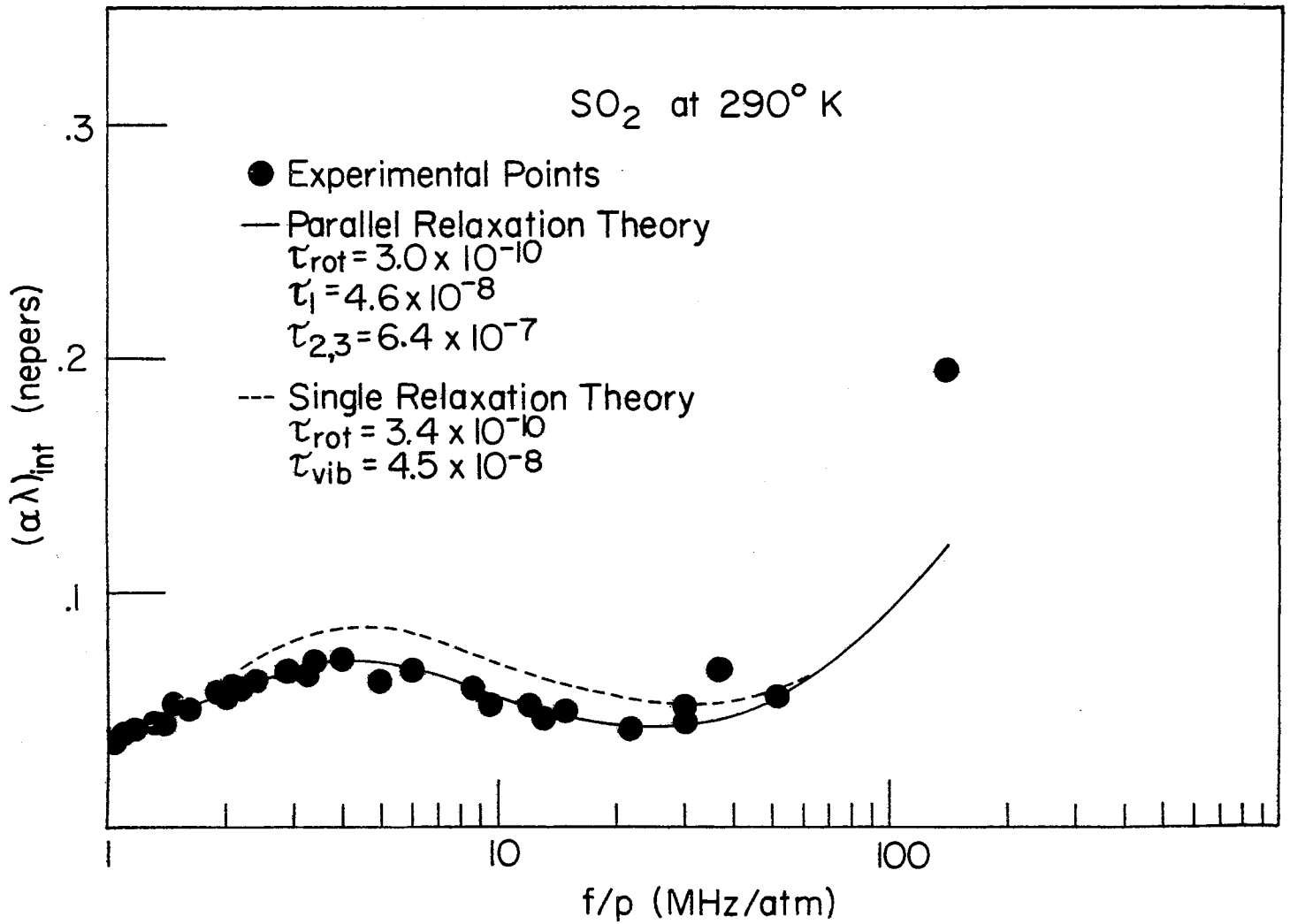

Figure 35. Absorption in Sulphur Dioxide at 290°K With Parallel and Single Relaxation Curves

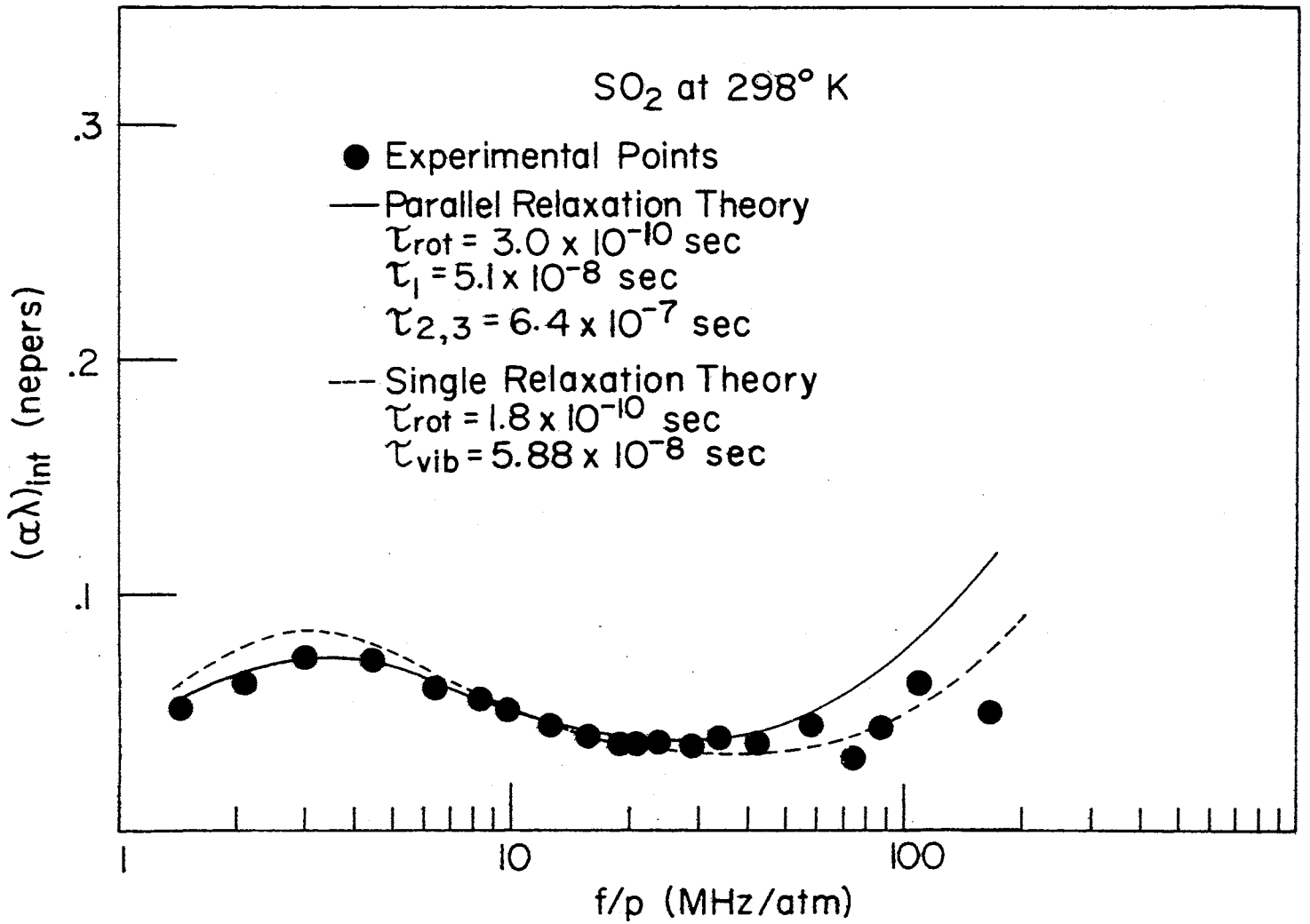

Figure 36. Absorption in Sulphur Dioxide at 298°K With Parallel and Single Relaxation Curves

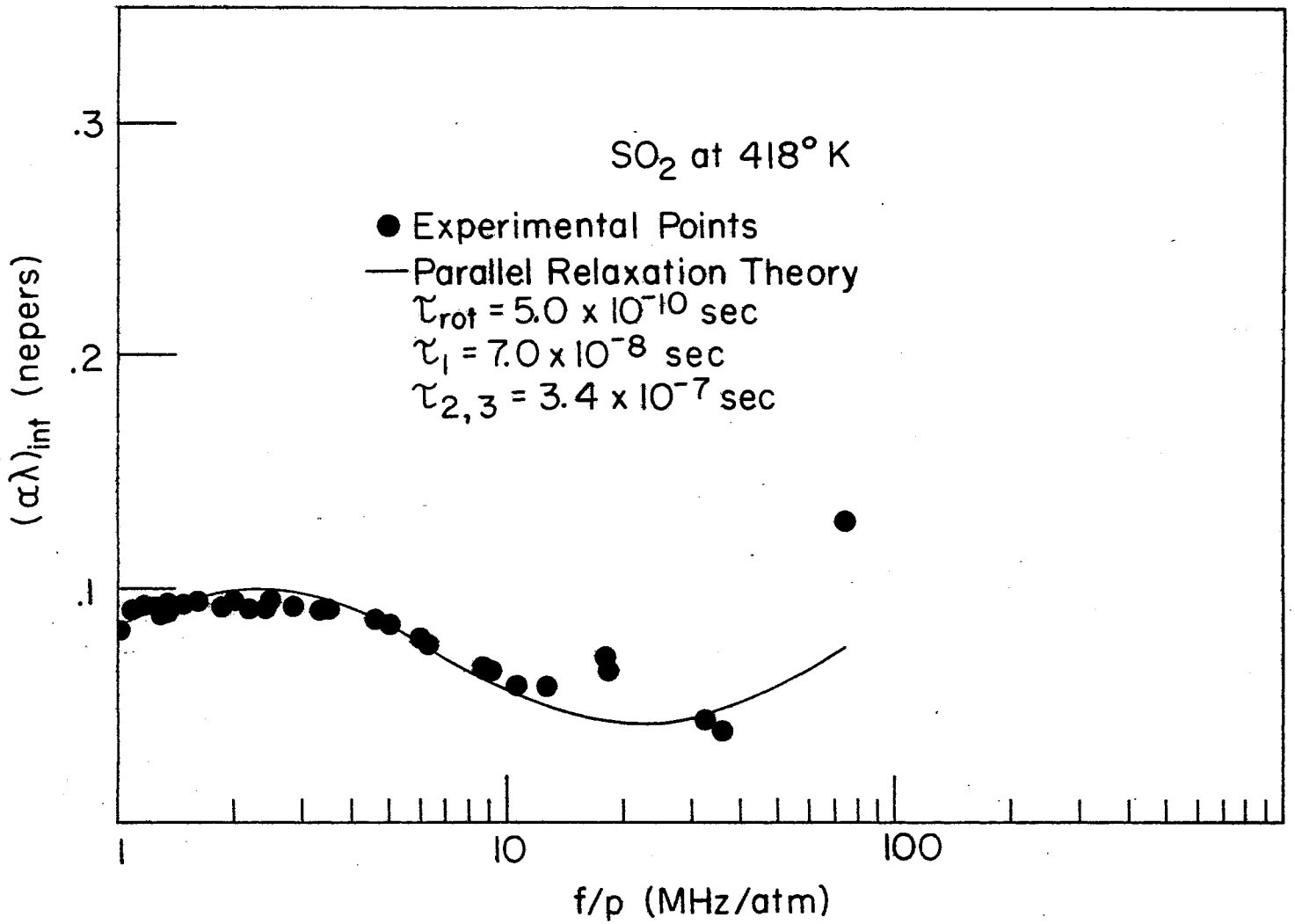

Figure 37. Absorption in Sulphur Dioxide at 418°K With Parallel Curves

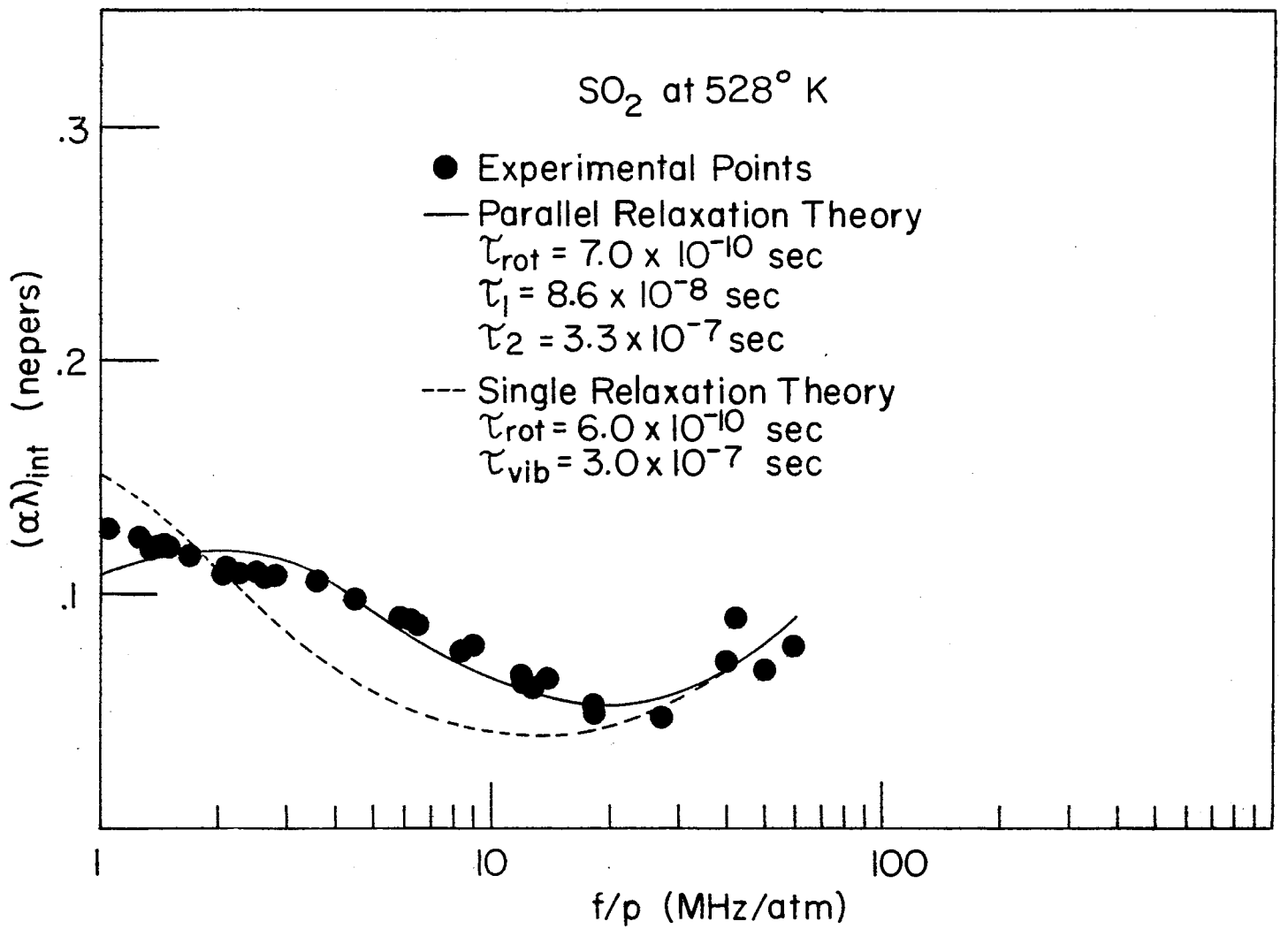

Figure 38. Absorption in Sulphur Dioxide at 528°K With Parallel and Single Relaxation Curves

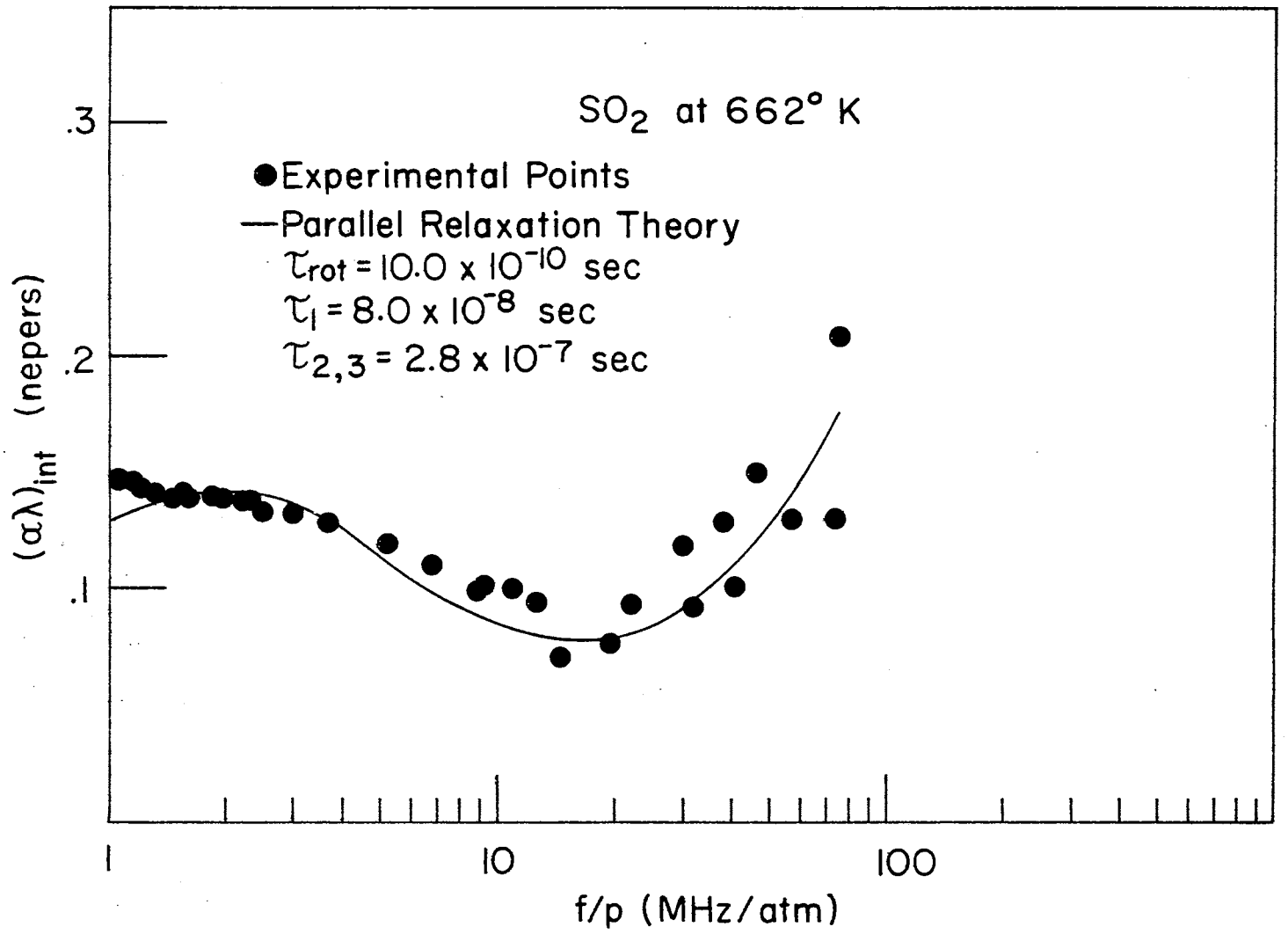

Figure 39. Absorption in Sulphur Dioxide at 662° K With Parallel Relaxation Curves

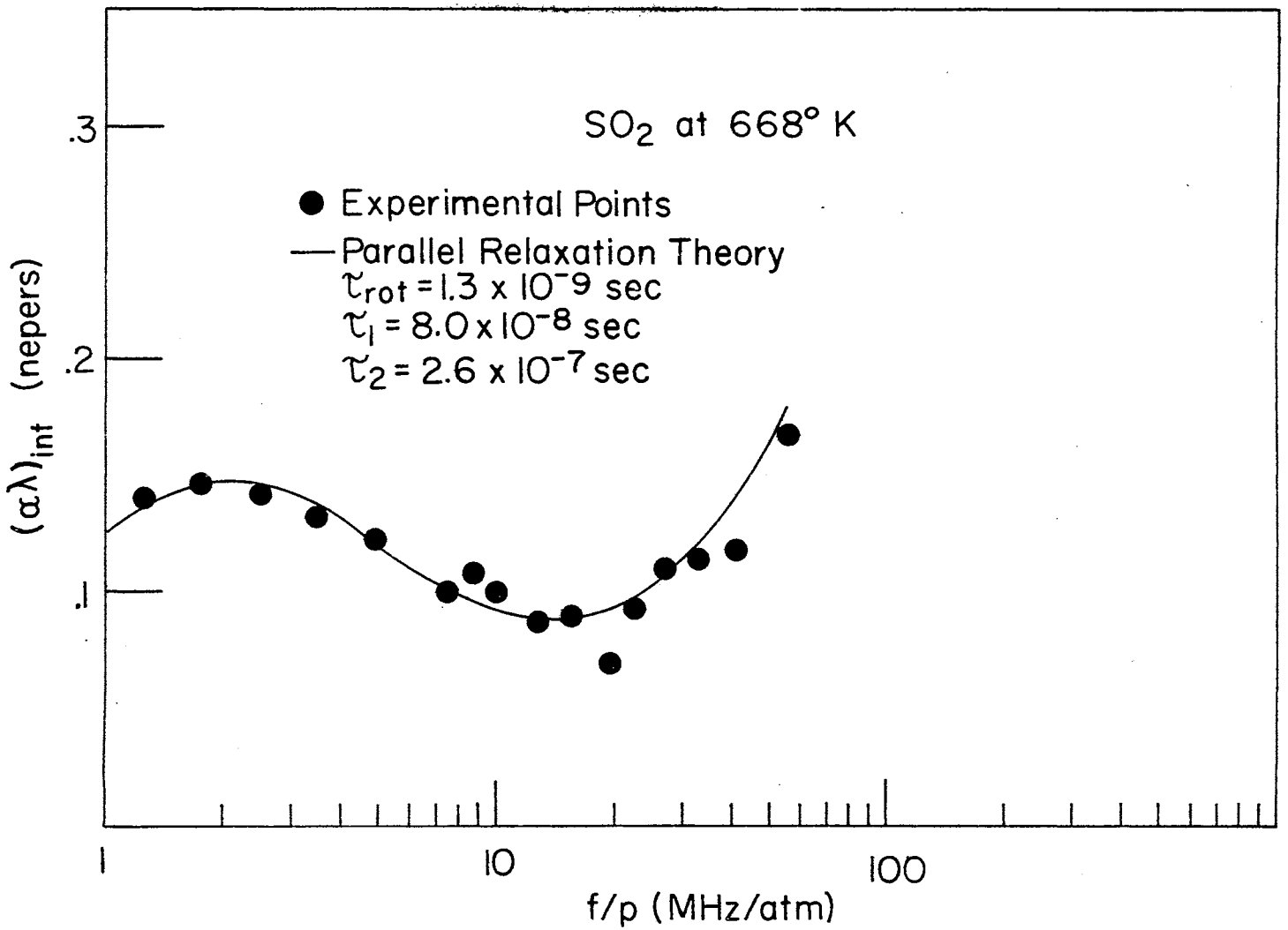

Figure 40. Absorption in Sulphur Dioxide at 668°K With Parallel Relaxation Curves

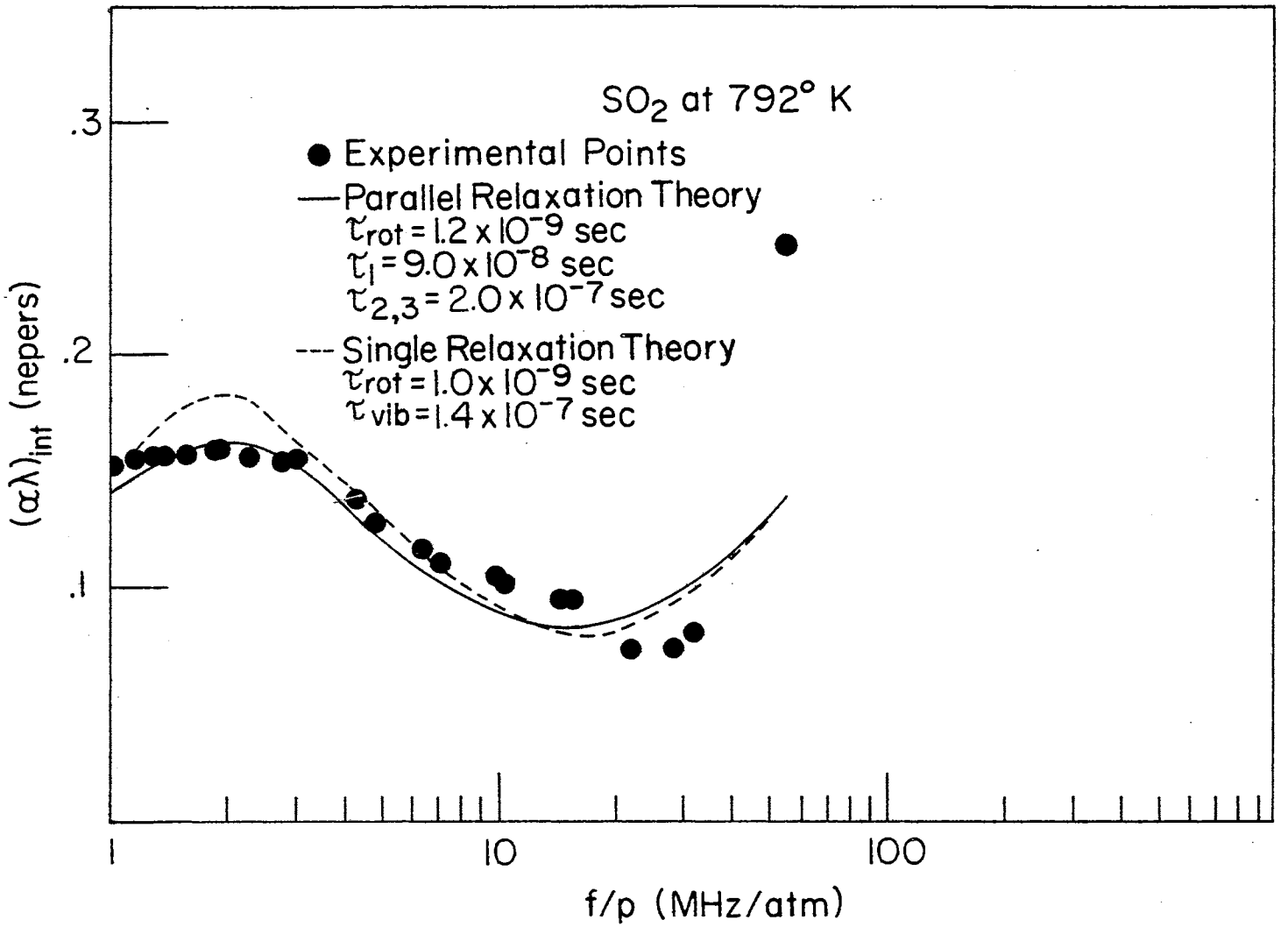

Figure 41. Absorption in Sulphur Dioxide at 792°K With Parallel and Single Relaxation Curves

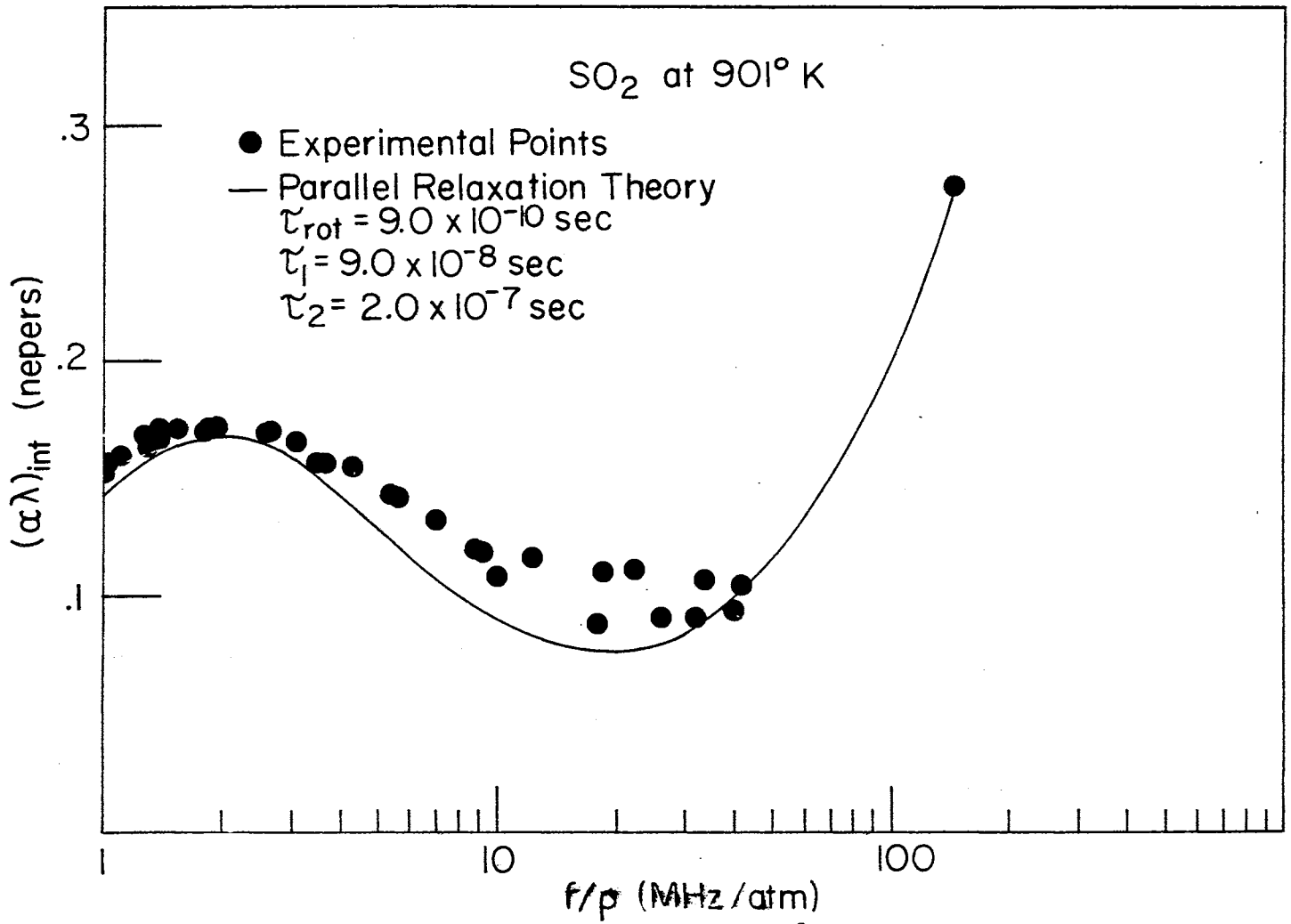

Figure 42. Absorption in Sulphur Dioxide at 901°K With Parallel Relaxation Curve

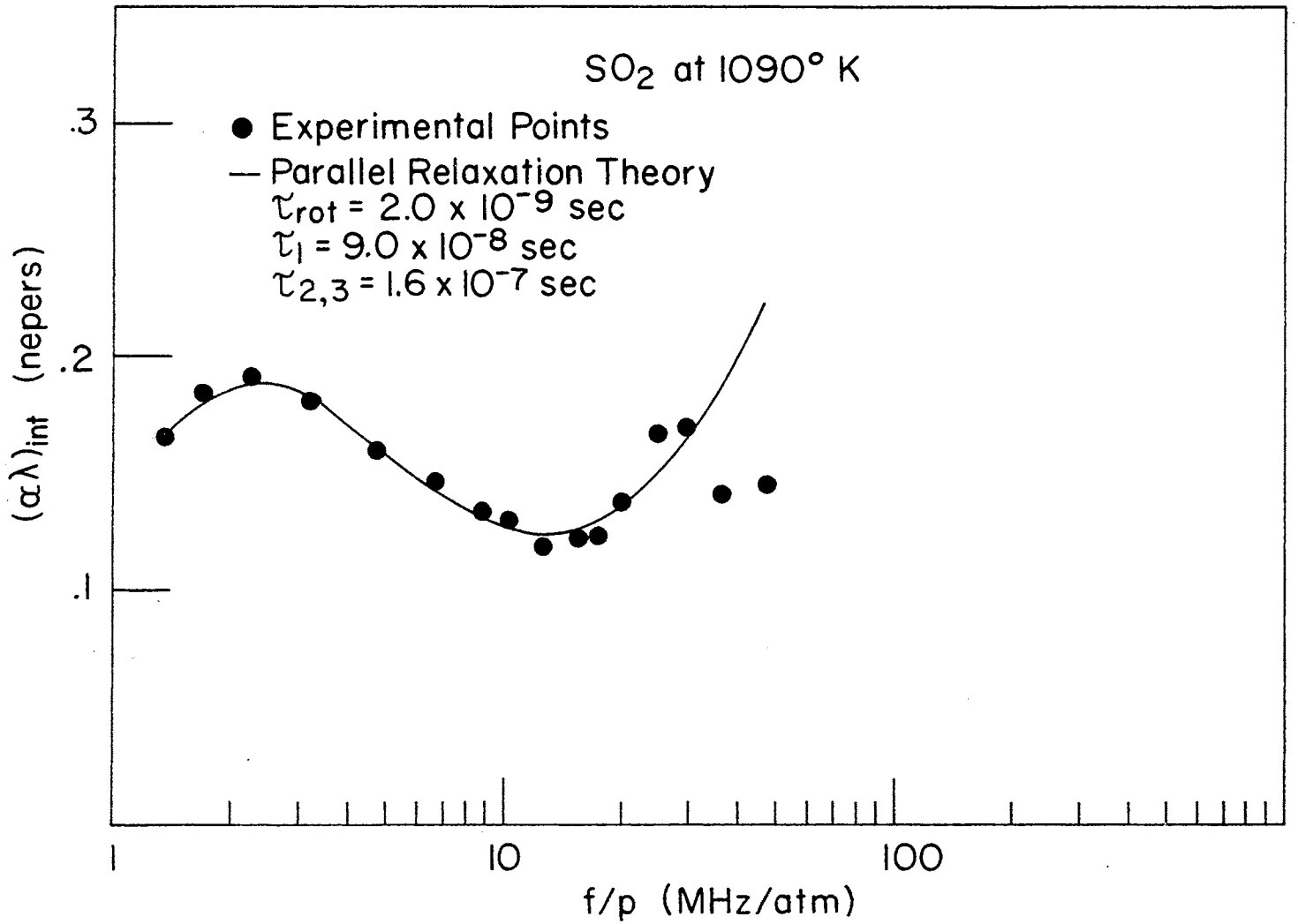

Figure 43. Absorption in Sulphur Dioxide at 1090°K With Parallel Relaxation Curve

temperatures, not only do the vibrational collision numbers approach the linear dependence predicted by L-T theory but the slope of ln Z_{vib} vs $T^{-1/3}$ for Z_1 approaches that for Z_2.

Fluoroform

Vibrational relaxation in Fluoroform has been measured by Fogg, Hanks, and Lambert (46) and Levgold and Amme (47). The only rotational collision number in the literature is that obtained from the thermal conductivity data of Crapo and Flynn (48). Their value seems much too low as is typical with collision numbers obtained from thermal conductivity data. An explanation for these small collision numbers has been formulated by Zeleznik (10) who questions the entire procedure for obtaining collision numbers from thermal conductivity data.

There seems to be some question in the literature whether CHF_3 is a symmetric top with $I_A = I_B = I_C$ (32) or with $I_A = I_C = I_B$ (10). The latter seems more reasonable which leads to $I_A = 5.52 \times 10^{-40}$ gm cm^2 and $I_B = 32.854 \times 10^{-40}$ gm cm^2. The lowest vibrational mode is doubly degenerate with $\theta = 731^{\circ}$K. Other parameters used for evaluation of the experimental data are given in Table VII. The gas used was purchased from Matheson with a stated purity of 98%.

The vibrational relaxation times are in excellent agreement with the results of Levgold and Amme (Figure 44). The temperature dependence is very classical closely following V-T transfer theory. This result demonstrates that a large dipole moment does not assure the collision numbers will behave anamalously with temperature. The rotational collision numbers seem to at first decrease then increase with temperature (Figure 45). This odd dependence is probably due to experimental error in the

rotational relaxation times which is quite large in this molecule due to the very high classical absorption associated with the large vibrational specific heat (Figures 46 through 50). Measurements at $f/P > 60$ MHz/atm were not possible due to this high absorption.

TABLE VII

EXPERIMENTAL RESULTS AND MOLECULAR PARAMETERS FOR FLUOROFORM

Thermodynamic Properties of Fluoroform (31)

Mass = 70.02 a.m.u. Frequency = 1 MHz

T (^{o}K)	$\eta \times 10^{3}$ (poise)	γ	C_p/R
299	.1448	1.192	6.221
373	.1784	1.165	7.304
473	.2266	1.142	8.254
573	.2575	1.126	9.200
723	.3101	1.113	10.00

Vibrational Frequencies (32)

ν_1 (cm^{-1})	ν_2 (cm^{-1})	ν_3 (cm^{-1})	ν_4 (cm^{-1})	ν_5 (cm^{-1})	ν_6 (cm^{-1})
3035	1140	700	1378	1152	508

Experimental Results for Fluoroform

T (^{o}K)	$\tau_{vib} \times 10^{7}$ (sec)	$\beta_{vib} \times 10^{7}$ (sec)	Z_{vib}	$\tau_{rot} \times 10^{9}$ (sec)	Z_{rot}
299	2.6	1.9	1600	1.0	8.9
373	3.5	1.8	1300	1.2	8.4
473	3.1	1.3	760	1.3	7.4
573	3.2	1.2	580	2.7	14.
723	2.4	.77	320	3.8	16.

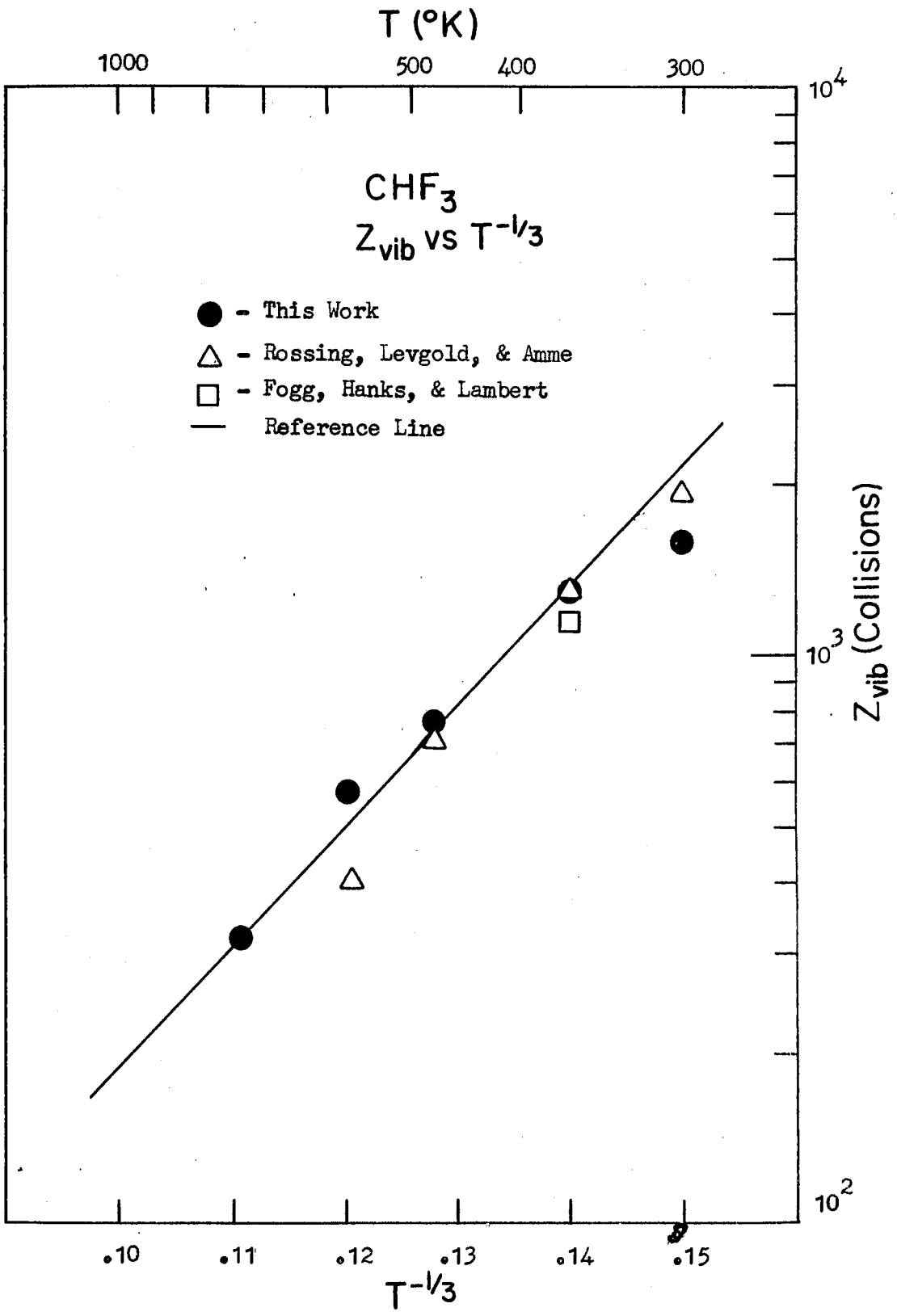

Figure 44. Vibrational Collision Numbers in Fluoroform

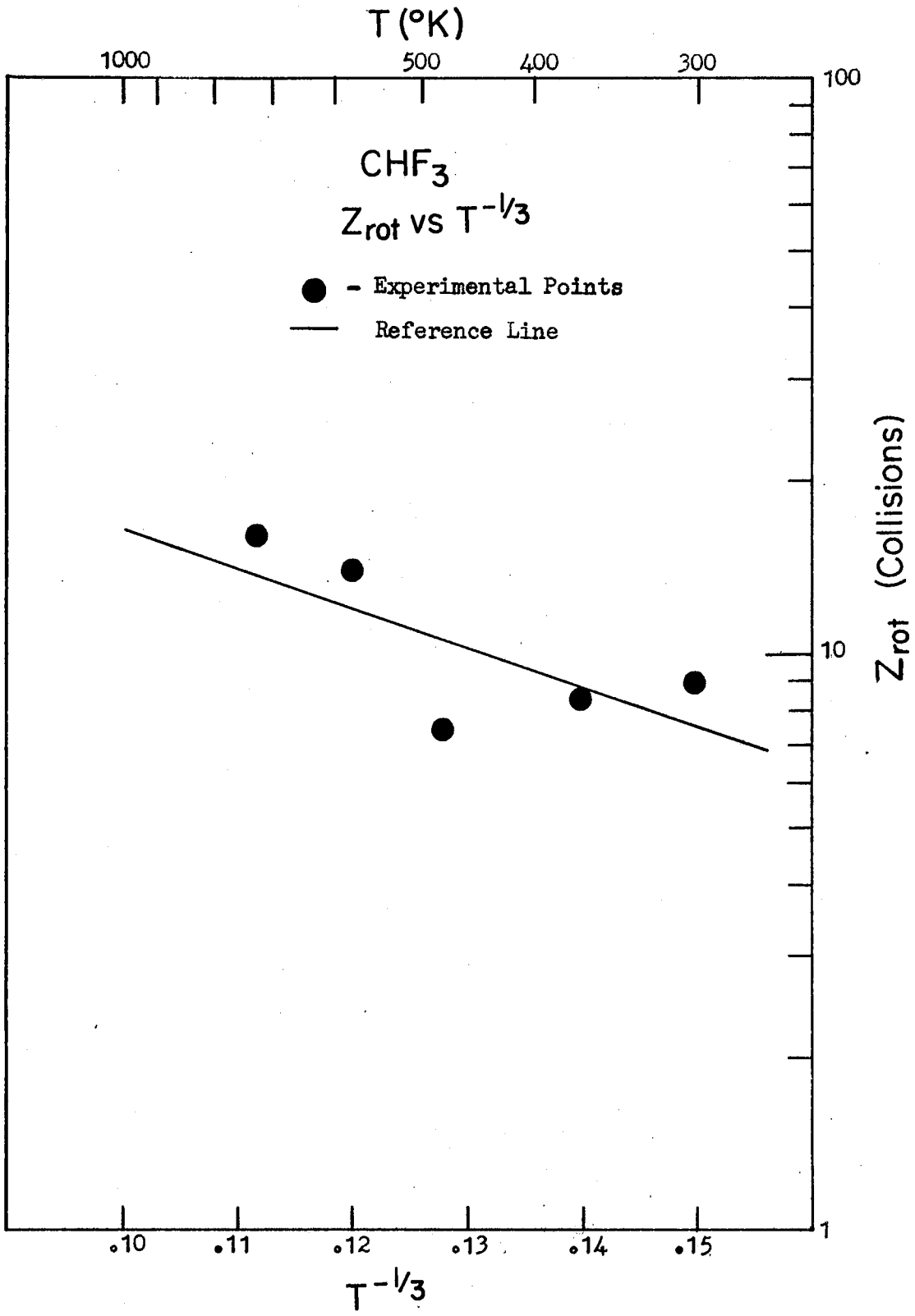

Figure 45. Rotational Collision Numbers in Fluoroform

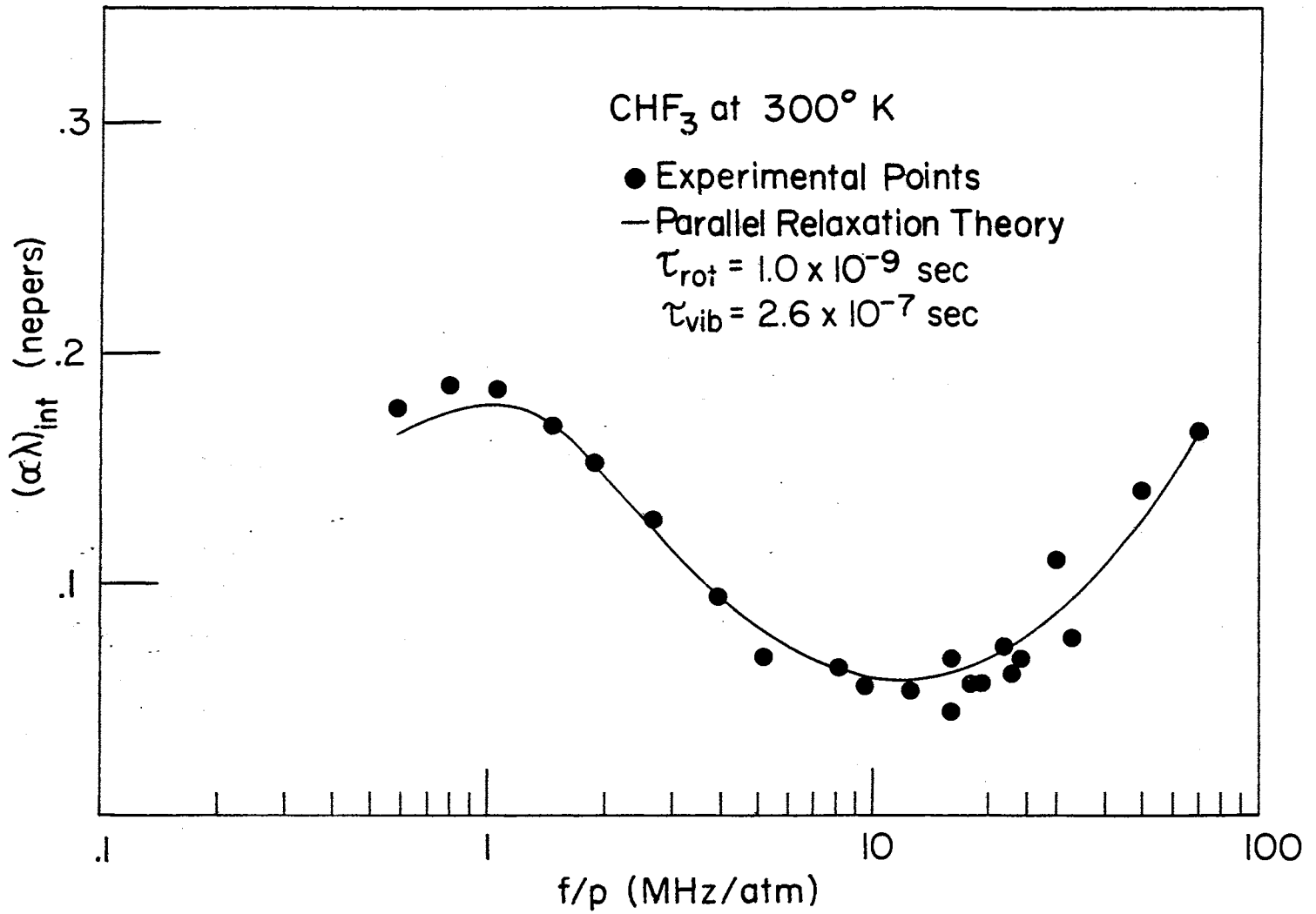

Figure 46. Absorption in Fluoroform at 300°K With Parallel Relaxation Curve

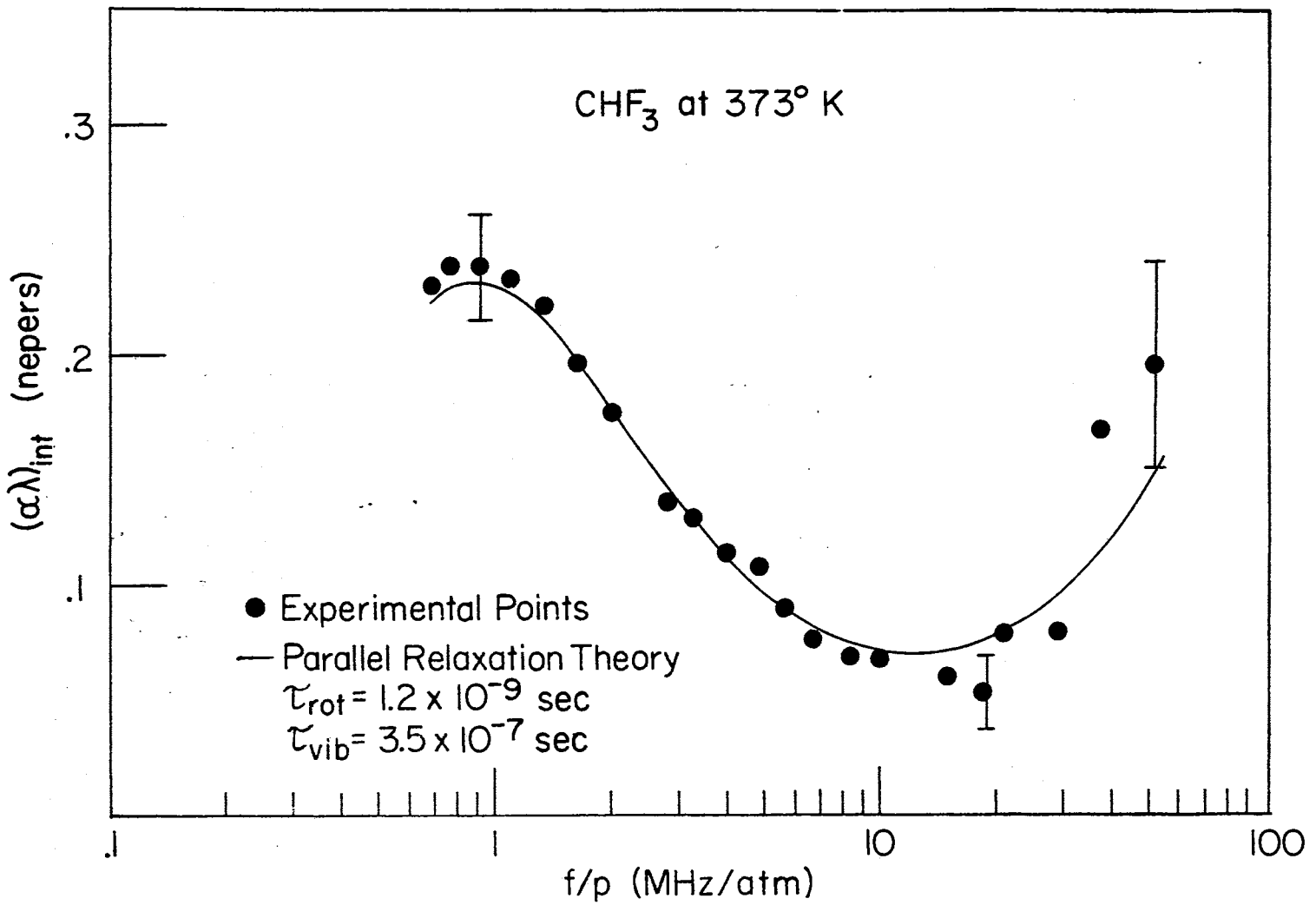

Figure 47. Absorption in Fluoroform at 373°K With Parallel Relaxation Curve

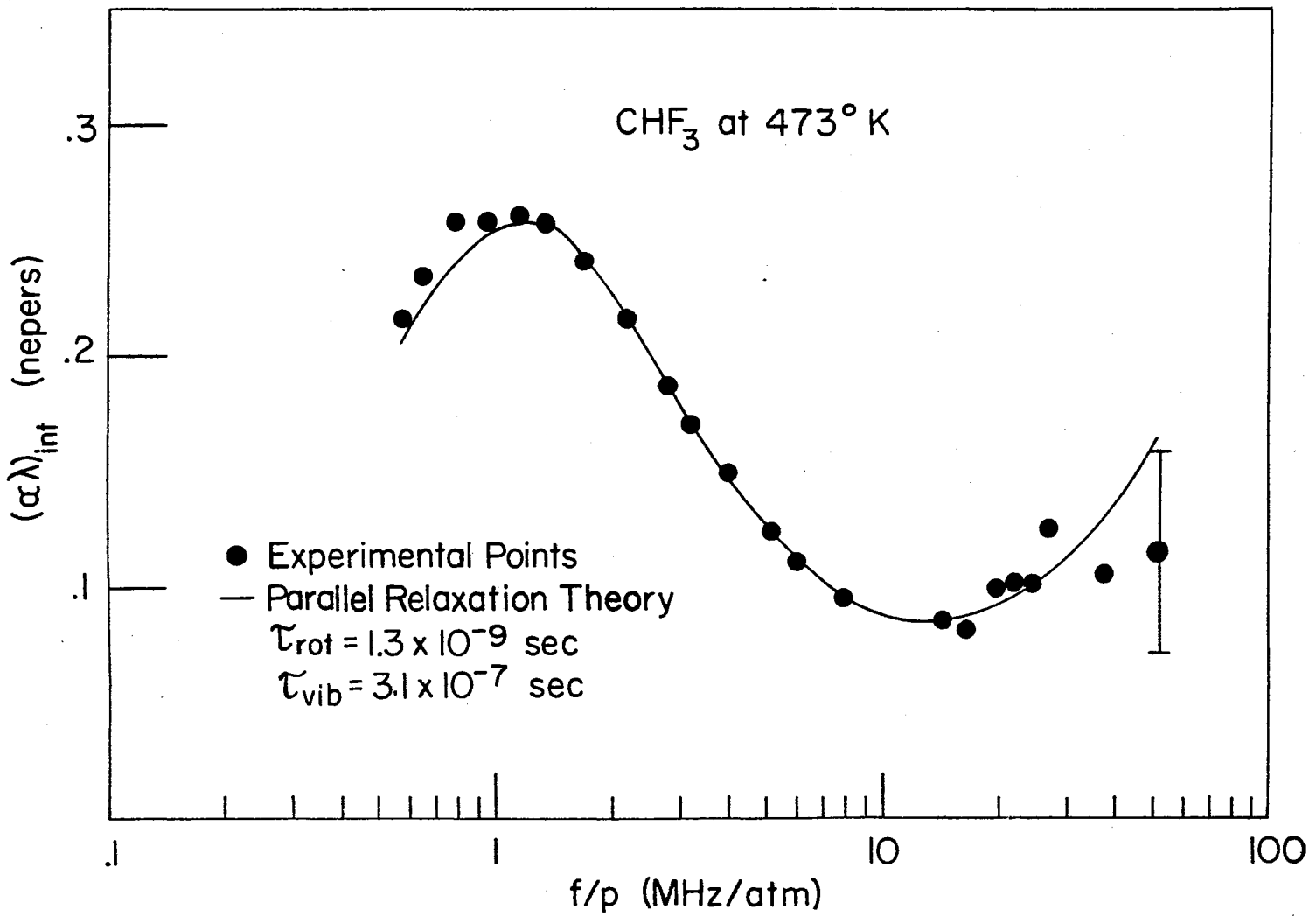

Figure 48. Absorption in Fluoroform at 473°K With Parallel Relaxation Curve

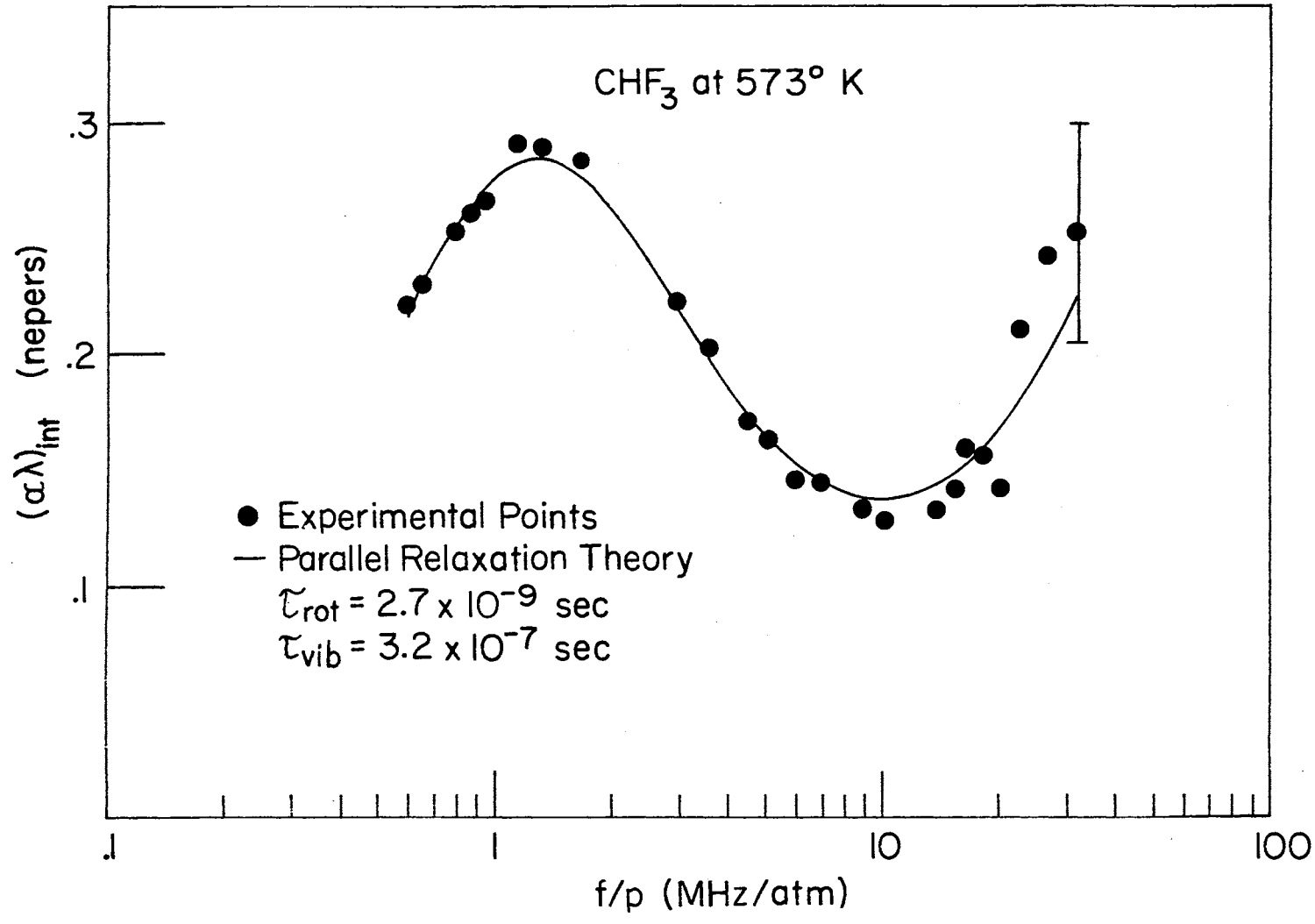

Figure 49. Absorption in Fluoroform at 573°K With Parallel Relaxation Curve

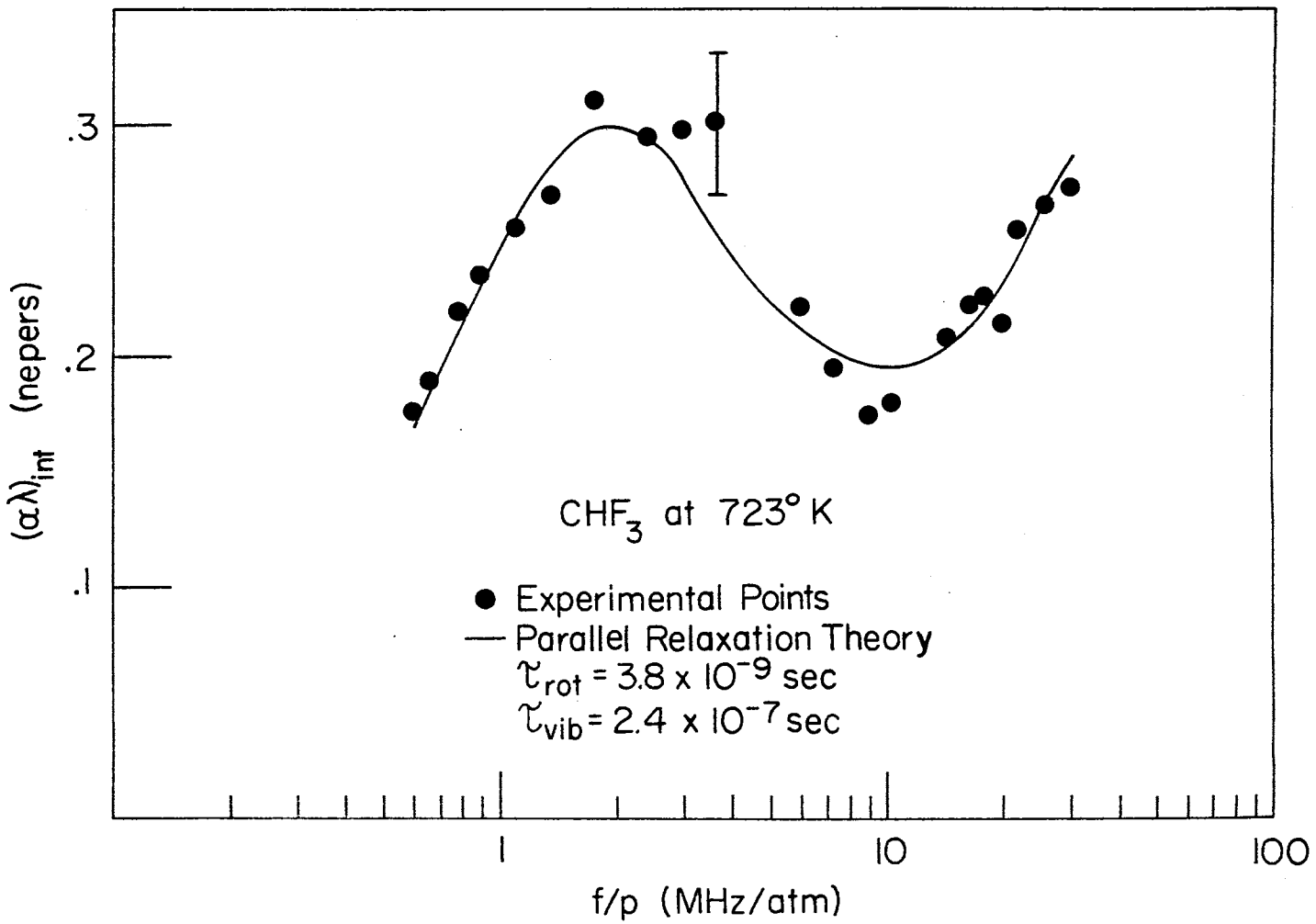

Figure 50. Absorption in Fluoroform at 723°K With Parallel Relaxation Curve

CHAPTER IV

SUMMARY OF RESULTS

Discussion of Vibrational Relaxation Results

The primary purpose of this investigation was to investigate the role of v-r energy transfer and intermolecular potentials in determining the temperature dependence of the vibrational relaxation times. With this general objective in mind, the experimental results for individual molecules will now be examined to determine what each contributes to this investigation.

The dominance of v-r energy transfer has been most firmly established in CH_4. This determination was made by Cottrell and Matheson (5) and later by Moore (7) without the benefit of this investigation. At the present time, the only reason other than v-r energy transfer which might explain the variation of $\tau(CH_4)/\tau(CD_4)$ from v-t theory is a difference in multipole moments between CH_4 and CD_4. In the absence of a better explanation, v-r energy exchange will be assumed. For CH_4, the variation of the vibrational collision numbers with temperature is the same as that predicted by v-t energy transfer theory. A v-r theory using the same exponentially repulsive potential assumed by Landau and Teller for v-t energy transfer gives the same temperature dependence. The results in CH_4, then, demonstrate that not only does v-r energy exchange not assure an anomalous temperature dependence of vibrational collision numbers, the correct temperature dependence is determined by an expo-

nentially repulsive intermolecular potential.

Once the dominance of v-r energy exchange has been assumed for CH_4, a similar assumption seems valid, even required, for H_2S and NH_3 due to the ratio of I/d^2 divided by M which is small for all these molecules. H_2S and NH_3 constitute the second group of molecules studied, that is, molecules which seem to exchange energy v-r and have large dipole moments. By comparing dZ/dT for these molecules with dZ/dT for CH_4, the effect of the large dipole moment can be isolated since v-r energy transfer has been assumed for all three. Ammonia is not an ideal molecule for this comparison. Cottrell and Matheson (39) have proposed that the vibrational energy exchange in NH_3 is primarily due to an easily excited inversion of the molecule. If this is the case, and the results of this investigation do not prove otherwise, the factors studied in this investigation (v-r energy transfer and large intermolecular forces) may not determine the energy transfer probability. For this reason, H_2S will be considered the best example of a molecule which has a large dipole moment and exchanges energy v-r studied in this investigation.

The vibrational collision numbers for H_2S at first increase then decrease with temperature. Comparing this behaviour with that of CH_4 which also is presumed to exchange energy v-r, one can conclude that the effect of the large dipole moment is to establish an anamalous temperature dependence of the vibrational collision numbers. Such a conclusion is, for now, based only on the results for one molecule and can not be considered to be true in general. Even the fact that the vibrational collision numbers in NH_3 do not decrease as rapidly with temperature as predicted by L-T theory can not give broader support to this conclusion since other factors may lead to the observed temperature dependence in

NH_3. All that can be said at this stage is that v-r energy transfer coupled with large angle dependent intermolecular forces and possible other factors results in a vibrational collision number in H_2S which at first increases then decreases with temperature.

The third group of molecules considered do not meet Moore's criteria for v-r energy transfer but do have a large dipole moment. The vibrational collision numbers of the lowest energy mode in SO_2 behave somewhat like the vibrational collision numbers in H_2S. Although a definite maximum in the vibrational collision numbers for SO_2 was not observed in this investigation, variation form simple L-T theory was definitely observed. In the case of H_2S, v-r theory was used to explain this anamalous behaviour, however, such an explanation is not so readily available for SO_2. The results in Fluoroform which is also in the third group of molecules studied, establishes that the presence of a large dipole moment does not in itself insure that the vibrational collision numbers will vary from the temperature dependence predicted by L-T theory. The vibrational collision numbers in Fluoroform do, in fact, follow the temperature dependence predicted by L-T theory.

The results of this investigation seem to end with a puzzle. Basically, the problem is as follows. H_2S which exchanges energy v-r and SO_2 which exchanges energy v-t both have large dipole moments and their vibrational collision numbers both depart from the temperature dependence predicted by L-T theory. The results in H_2S can be explained in terms of v-r exchange. A similar explanation might also hold true for SO_2 since it has one low moment of inertia. This is only supposition, however, since there are at least two other explanations. The first of these is that both H_2S and SO_2 vibrational collision numbers are the re-

sult of the preferred alignment postulated by Corran, Lambert, Salter, and Warbutton. This investigation certainly does not disprove such a hypothesis. The results in CHF_3 could be explained as the result of a non-preferred orientation. The temperature dependence of the vibrational collision numbers of all three of these polar molecules could then be explained in a qualitative manner using this explanation. Another possible explanation is that the results in SO_2 and those in H_2S are in no way related. The results in H_2S could then be explained using v-r theory and the results in SO_2 might be explained in terms of preferred orientation. The problem for a theoretician is to determine which of these explanations, if any, can lead to correct quantitative results.

Before leaving the discussion of vibrational relaxation, one other facet must be pointed out. That is, just because τ increases with temperature doesn't mean the collision number increases with temperature. An example is Ammonia. The increase in the relaxation time in Ammonia is due to the presence of several relaxation processes. As the specific heats of the vibrations with longer relaxation times increase, the observed relaxation time will increase even though the collision numbers of all the processes are decreasing with temperature. This phenomena might explain the peculiar temperature dependence observed by Harris (49) in air where the processes are the relaxation of N_2 and O_2 by H_2O. As the temperature increase, the absorption due to the relaxation of N_2 by H_2O may become more and more important. Another possible explanation is the v-r theory of Shields and Burks (3) which has been given further experimental confirmation by this investigation.

Discussion of Rotational Relaxation Results

The secondary purpose of this investigation was to investigate the temperature dependence of the rotational relaxation times of polyatomic polar molecules. Even though rotational and vibrational relaxation should be independent, one interesting aspect should be noted concerning their relaxation times. That is, d ln τ_{vib}/dT is very nearly equal to d ln τ_{rot}/dT for those molecules where d ln τ_{vib}/dT > 0 (H_2S, SO_2, and NH_3). This result can not be explained at the present time other than to point out that plotted vs $T^{-1/3}$ the ln of the relaxation times of most molecules will not vary greatly from any other. The agreement between d ln τ_{vib}/dT and d ln τ_{rot}/dT is very probably fortuitous.

The remainder of this discussion will be divided into two parts. First, the results of Żeleznik's theory (10) will be compared to the experimental results. Second, since a great deal of data has now been collected on the rotational relaxation times of numerous molecules (11, 25,27,29), a qualitative determination of the factors affecting Z_{rot} will be made. The limited applicability of Zeleznik's theory makes such a determination desirable until such time as a more general theory can be formulated which can be readily applied to any polyatomic molecule. For the purposes of this discussion, the assumption will be made that $dZ_{rot}/dT \propto T^{1/3}$. Based on the experimental results to date, this assumption, though not exact, does give a good indication of the temperature dependence of Z_{rot}.

Zeleznik's theory has been applied to the polar polyatomic molecules examined in this investigation. With the exception of SO_2, this theory gives fair agreement with the observed temperature dependence as shown in Table IX. The dipole dependence predicted by theory is not nearly so

good as is shown in Table X. Since Zeleznik's theory is strictly classical, the temperature dependence agreement clearly indicates that for molecules with strong intermolecular forces, these forces dominate the temperature dependence of Z_{rot}. This does not indicate or even imply that the increasing energy level spacing characteristic of rotation does not affect Z_{rot} since all the polar molecules examined have about the same energy level density near 300°K. This density is about .3 energy states/°K for each.

There are two factors which might be expected to affect the rate at which Z_{rot} increases with temperature. These are the energy level density and the intermolecular forces. The former effect has been established by Raff and Winter. Their results show that as the energy level density increases, $|dZ/dT|$ increases. The latter effect has been theoretically established by Zeleznik and experimentally by Evans. Considering only the non-polar molecules in Figure 51, the effect of the energy level spacing is as expected without exception. The effect of intermolecular potential on dZ/dT is not so obvious. For example, SO_2 has a greater energy level density than O_2 as well as larger intermolecular forces which leads to the conclusion that large intermolecular forces decreases $|dZ/dT|$. If this is the case, then $|dZ/dT|$ for HCl and NO should not be greater than that of N_2 and $|dZ/dT|$ for H_2S should not be greater than that for CHF_3.

Failing to find a correlation between dZ/dT and the total intermolecular potential (implied by the boiling points of the molecules), a term by term examination of the intermolecular potential was made. The strength of the dipole-dipole forces clearly can not account for the large difference between SO_2 and NH_3 or between CHF_3 and H_2S. If dipole-

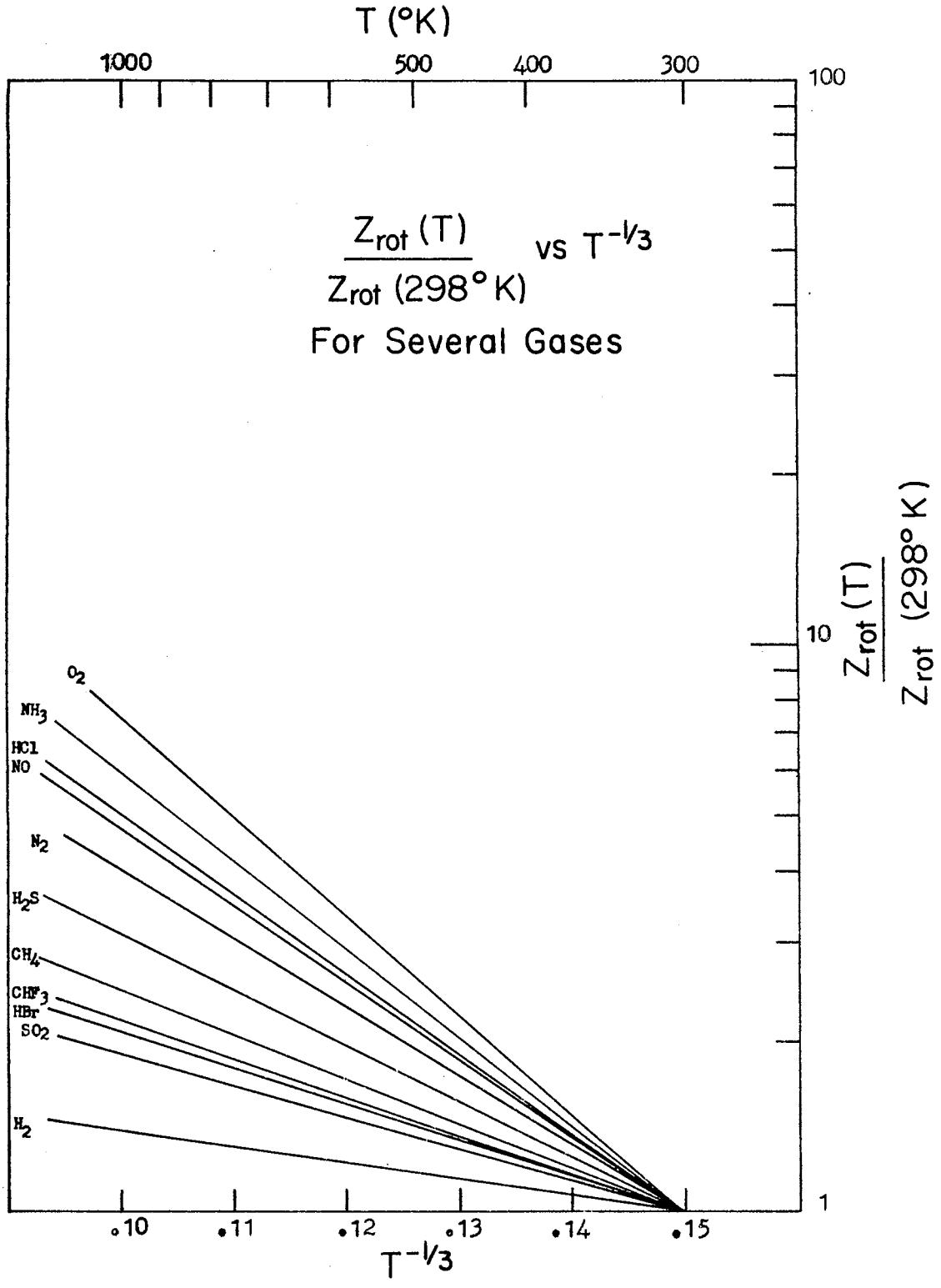

Figure 51. Temperature Dependence of Rotational Collision Numbers for Several Gases

TABLE VIII

MOLECULAR PARAMETERS USED IN R-T THEORY

Ammonia

$M = 17.032$, $\delta_{max} = .7$, $\sigma = 3.15A$, $\epsilon/k = 358\ ^{o}K$, $I = 3.348 \times 10^{-40}$ $gmcm^2$, $\mu = 1.477 \times 10_2^{-18}$ esu·cm

T	T*	Ω(2,2)	E*
300	.839	1.89	.871
415	1.16	1.57	.874
490	1.37	1.46	.883
612	1.71	1.34	.885
773	2.16	1.21	.904

Hydrogen Sulfide

$M = 34.08$, $\delta_{max} = .21$, $\sigma = 3.49A$, $\epsilon/k = 343\ ^{o}K$, $I = 3.869 \times 10^{-40}$ $gmcm^2$, $\mu = .92 \times 10^{-18}$ esu·cm^2

T	T*	Ω(2,2)	E*
298	.855	1.74	.871
383	1.13	1.50	.877
473	1.38	1.36	.889
578	1.67	1.26	.900
683	1.99	1.18	.910

Sulphur Dioxide

$M = 64.063$, $\delta_{max} = .42$, $\sigma = 4.04A$, $\epsilon/k = 347\ ^{o}K$, $I = 63.49 \times 10^{-40}$ $gmcm^2$, $\mu = 1.63 \times 10^{-18}$ esu·cm^2

T	T*	Ω(2,2)	E*
290	.836	1.79	.873
298	.860	1.76	.873
418	1.20	1.50	.881
528	1.52	1.36	.893
662	1.91	1.23	.907

TABLE VIII (Continued)

T	T*	Ω(2,2)	E*
668	1.92	1.23	.907
792	2.28	1.16	.919
901	2.60	1.11	.923
1090	3.14	1.01	.933

Fluoroform

$M = 70.09$, $\delta_{max} = .5$, $\sigma = 4.33$ Å, $\varepsilon/k = 240$ °K, $I = 103.6 \times 10^{-40}$ gm·cm^2, $\mu = 1.645$ debye

T (°K)	T*	Ω(2,2)	E*
299	1.24	1.32	.881
373	1.55	1.25	.890
473	1.93	1.16	.904
573	2.39	1.06	.918
723	3.02	.985	.929
873	3.64	.930	.937

TABLE IX

COMPARISON OF EXPERIMENTAL AND CALCULATED Z_{rot}s

T (^{o}K)	$Z(A,T)/Z(A,T_o)$ Exp	$Z(A,T)/Z(A,T_o)$ Calc
	Ammonia	
300	1.00	1.00
415	.91	1.24
490	.91	1.46
612	2.1	1.88
773	2.0	2.36
	Sulphur Dioxide	
290	1.00	1.00
298	.89	1.03
418	1.0	1.44
528	1.1	1.86
662	1.5	2.34
668	1.7	2.38
792	1.3	2.96
901	1.3	3.49
1090	1.6	4.18
	Hydrogen Sulfide	
298	1.00	1.00
383	1.0	1.15
473	1.4	1.38
578	1.9	1.73
683	2.2	2.07
	Fluoroform	
299	1.00	1.00
373	.94	1.39
473	.83	1.91
523	1.6	2.32
723	1.8	3.18
873		4.12

TABLE X

RATIOS OF ROTATIONAL COLLISION NUMBERS FOR
POLAR MOLECULES AT ROOM TEMPERATURE

Molecule A	Molecule B	$Z(A,T_o)/Z(B,T_o)$ Exp	$Z(A,T_o)/Z(B,T_o)$ Calc
SO_2	NH_3	.34	2.52
SO_2	H_2S	.46	.324
SO_2	CHF_3	.37	.378
H_2S	NH_3	.73	7.78
H_2S	CHF_3	.96	7.97
NH_3	CHF_3	1.0	.625

dipole forces are assumed to increase $|dZ/dT|$, the slope for O_2 compared to H_2S, and SO_2 can not be explained. If this force is assumed to decrease $|dZ/dT|$ as predicted by Zeleznik, the large slope for NH_3 can not be explained when compared to SO_2 or H_2S. Next, the quadrapole moments were examined to try to find some correlation. This comparison gave much better results. Assuming a large quadrapole moment decreases $|dZ/dT|$, one would order the slopes as $O_2 > H_2 > NH_3 > N_2 > HCl > SO_2$:HBr. With the exception of H_2, this correlation is exact and H_2 can readily be explained by the large energy level spacing. Quadrapole moments for H_2S and CHF_3 are not available so a comparison could not be made. The slope of CH_4 can not be explained since it has zero quadrapole moment, however, it does have significant higher order poles.

Conclusions

Based upon the experimental results of this investigation, several conclusions can be drawn. When doing so, however, the reader should keep in mind that only five molecules were examined in this study. As a result, the conclusions, especially those concerning vibrational energy transfer, can not be considered to be true in general.

With respect to vibrational energy transfer, the following conclusions can be drawn. First, the presence of v-r energy transfer or large dipole moments do not guarantee that the vibrational collision numbers will not follow the temperature dependence predicted by Landau and Teller. Second, the vibrational collision numbers in H_2S increase then decrease with increasing temperature. Shields and Burks' theory for v-r energy exchange can reproduce experimental results in H_2S provided suitable parameters are chosen and provided v-t energy transfer is pre-

sumed dominant at high temperatures. Third, the vibrational collision numbers of SO_2 do not follow Landau-Teller theory at low temperatures but do appraoch L-T theory at high temperatures. The behaviour of Z_{vib} with T in SO_2 can be explained qualitatively in terms of a preferred orientation during collisions. Fourth, the vibrational collision members in Ammonia decrease only slightly with temperature. This result is not inconsistent with Cottrell and Matheson's theory for an easily excitable inversion of the NH_3 molecule.

The rotational relaxation investigation results in the following conclusions. First, Zeleznik's theory is fair at predicting the temperature dependence of the rotational collision numbers of polyatomic polar molecules. Second, the dependence of the rotational collision numbers on the dipole moment predicted by Zeleznik's theory is too great for NO and H_2S which have dipole moments of less than 1 debye. Third, there seems to be some correlation between the molecular quadrapole moments and the temperature dependence of the rotational relaxation times. Fourth, acoustically derived rotational collision numbers can agree with those collision numbers derived from thermal transpiration measurements.

BIBLIOGRAPHY

1. L. D. Landau and E. Teller, Phys. Z. Sowjetunion 10, 34 (1936).

2. B. Nidom and S. H. Bauer, J. Chem. Phys. 21, 1670 (1953).

3. F. D. Shields and J. A. Burks, J. Acous. Soc. Am., 43, 510 (1968).

4. R. C. Milikan and L. A. Osburg, J. Chem. Phys. 41, 2196 (1964).

5. T. L. Cottrell and A. J. Matheson, Proc. Chem. Soc. 17, (1962).

6. T. L. Cottrell, R. C. Dobbie, J. McLain and A. W. Read, Trnas. Faraday Soc., 60, 241 (1964).

7. C. Bradley Moore, J. Chem. Phys., 43, 2979 (1965).

8. R. D. Sharma and C. A. Brau, J. Chem. Phys., 50, 924 (1969).

9. R. D. Sharma, J. Chem. Phys., 50, 919 (1969).

10. Frank J. Zeleznik, J. Chem. Phys., 47, 3410 (1967).

11. Landon B. Evans, 1969, Ph.D. Thesis, Oklahoma State University, unpublished.

12. T. L. Cottrell and J. C. McCoubrey, Molecular Energy Transfer in Gases, (Butterworths, London, 1961).

13. K. F. Herzfeld and T. A. Litovitz, Absorption and Dispersion of Ultrasonic Waves, (Academic Press, New York, 1959).

14. L. M. Raff and T. G. Winter, J. Chem. Phys., 48, 3992 (1968).

15. F. Douglas Shields, J. Chem. Phys., 46, 1063 (1967).

16. R. Holmes and M. A. Stah, Brit. J. Appl. Phys., 1, 607 (1968).

17. J. O. Hirshfelder, C. F. Curtiss, and R. B. Byrd, Molecular Theory of Gases and Liquids, (John Wiley and Sons, New York, 1954).

18. Francis Weston Sears, Thermodynamics, The Kinetic Theory of Gases, and Statistical Mechanics, (Addison-Wesley Publishing Co., Reading, Mass., 1959).

19. F. Douglas Shields, J. Acous. Soc. Am., 47, 1262 (1970).

20. R. N. Schwartz, Z. I. Slowsky, and K. F. Herzfeld, J. Chem. Phys. 20, 1591 (1952).

21. Hyung Kyu Shin, Chem. Phys. Letters, 1, 635 (1968).

22. Hyung Kyu Shin, Chem. Phys. Letters, 1, 443 (1967).

23. L. Monchick and E. A. Mason, J. Chem. Phys., 35, 1676 (1961).

24. Yahei Fujii, Papers of Ship Research Institute, No. 15 (1966).

25. G. L. Hill and H. E. Bass, unpublished results.

26. F. Douglas Shields and George P. Carney, J. Acous. Soc. Am., 47, 1269 (1970).

27. Garnett L. Hill, 1968, Ph.D. Thesis, Oklahoma State University, unpublished.

28. Linberg Hevi-Duty Furnace Operators Manual.

29. G. L. Hill and T. G. Winter, J. Chem. Phys., 49, 440 (1968).

30. J. L. Stretton, Trans. Faraday Soc., ____, 1053 (1965).

31. Roger A. Svehla, NASA Tech. Report R-132 and JANAF Thermochemical Tables (PB 168 370) (1966).

32. AIP Handbook, (McGraw-Hill Book Co., New York, 1963).

33. K. Geide, Acustica, 13, 31 (1963).

34. F. Douglas Shields, J. Acous. Soc. Am., 45, 481 (1969).

35. A. Das Gupta and T. S. Storvick, J. Chem. Phys., 52, 742 (1970).

36. S. C. Wang, Phys. Rev., 34, 243 (1929).

37. F. J. Krieger, USAF Research Memorandum RM-646 (1951) and NASA Tech Note D-481.

38. P. G. Corran, J. D. Lambert, R. Salter, and B. Warburton, Proc. Roy. Soc., 244A, 212 (1958).

39. T. L. Cottrell and A. J. Matheson, Trans. Faraday Soc., 59, 824 (1963).

40. J. G. Strauch and J. C. Decius, J. Chem. Phys., 44, 3319 (1966).

41. D. G. Jones, J. D. Lambert, M. P. Saksena, and J. L. Stretton, Trans. Faraday Soc., 65, 965 (1969).

42. S. Petralia, Nuovo Cimento, 10, 817 (1953).

43. H. H. Keller, Physik. Z., 41, 386 (1940).

44. Gerhard Herzberg, Infared and Raman Spectra of Polyatomic Molecules, (D. Van Nostrand Co., New York, 1945).

45. J. D. Lambert and R. Salter, Proc. Roy. Soc., A243, 78 (1957).

46. P. G. T. Fogg, P. A. Hanks, and J. D. Lambert, Proc. Roy. Soc., 219A, 490 (1953).

47. R. Amme and S. Legvold, J. Chem. Phys., 26, 514 (1957).

48. L. M. Crapo and G. W. Flynn, J. Chem. Phys. 43, 1443 (1965).

49. C. Harris, J. Acous. Soc. Am., 40, 148 (1966).

50. Metals Handbook, Vol. 1, (American Society for Metals, Metals Park, Ohio, 1961).

51. Martin Greenspan, Physical Acoustics, Vol. II, Part A (Academic Press, New York, 1965).

52. A. B. Bhatia, Ultrasonic Absorption (Clavedon Press, Oxford, 1967).

53. L. B. Evans, H. E. Bass, and T. G. Winter, J. Acous. Soc. Am., 47, 0000 (1970).

APPENDIX A

PREPARATION AND PROCEDURE USED FOR TAKING VELOCITY AND ABSORPTION MEASUREMENTS

Due to the toxic nature of most of the gases used in this investigation, along with the explosiveness of H_2S, several steps were taken before each series of measurements to insure the operator's safety and to give the best possible experimental results. The following discussion gives the step by step procedure followed in this investigation.

First, several weeks before an anticipated measurement, the system was evacuated. The system was heated to facilitate the removal of moisture. The tubing could not always be heated so several days were required for optimum pump down of 5μ. During this period the system was frequently checked for leaks. A leak rate of 1μ/hr. was considered acceptable. This procedure was followed each time the vacuum system was exposed to the atmosphere. In addition, the system was checked for leaks immediately before and after each series of measurements.

Second, all available information on the gas to be used was read. The Chemistry-Physics Instrument Shop has a copy of Metals Handbook, Vol. 1 (50) which indicates how reactive the proposed gas is with the stainless steel tube. If the gas reacts too violently (greater than 50 my), it was not used in the stainless steel tube. Safety precautions given in the Matheson catalog were followed. This required purchasing a gas mask and installing an explosive gas regulator for use with Hydro-

gen Sulfide. The first aid suggestions in the Matheson catalog were placed in an obvious location. The gas in use was written on the chalk board. If the gas to be used was explosive, a NO SMOKING sign was placed on the laboratory door.

Two or three days before the measurements began, the gas cylinder was placed in the hood and a regulator was installed while the exhaust fan was on and the furnace off. The regulator was first checked for leaks on a Helium bottle using soap bubbles then rechecked on the test gas bottle. The regulator outlet was connected to the vacuum system and checked for vacuum leaks up to the check valve on the regulator. Next, a small amount of gas was introduced into the system, usually 10 to 20 mm Hg. The gas cylinder was turned off and the pressure was observed for several hours. If no reaction was indicated, the system was filled to near atmospheric pressure and allowed to stand overnight. The pressure was again checked for any indication of leaks or reactions. In the absence of leaks or reactions, the system was again evacuated for at least 24 hours. When using H_2S, a gas mask was worn whenever the cylinder valve was open.

Third, on the day measurements were to begin, the electronic equipment was turned on and gas introduced into the system. The system was evacuated and refilled to flush the system. The entire apparatus was then allowed to set one hour. At the end of this time period measurements were begun. The amount of attenuation required to maintain a predetermined signal level was recorded for five different rod separations. Usually, the change in attenuation was predetermined at 3db, 4db, or 5db and the change in rod separation required to produce this attenuation was recorded. The velocity measurements were obtained as suggested by

Hill. The absorption data was plotted on a graph with attenuation on one coordinate and rod separation on the other. The absorption in db/in was then found. The absorption could be determined by measuring the change in attenuation between only two points, however, additional points served to establish a more accurate straight line on the graph reducing the experimental error. Attenuation data was collected for about 15 values of the pressure between atmospheric and 5 mm Hg by evacuating the system in steps. The system was filled with new gas and this process repeated for another 15 data points. The system was again evacuated and the next temperature to be used was dialed into the control console. The data was then analyzed making a new graph for each different pressure, calculating the absorption and velocity and entering this information on IBM cards. Analyzing the data took the remainder of a day so the chamber had about 20 hours to come into equilibrium at the new temperature. At temperatures above 250^{o}C, air was forced through the cooling jackets to protect the Viton O-Rings. Whenever the temperature was increased, the gas was checked for dissociation and reactions with the tube. Dissociation was evidenced by a pressure rise, and an increase in velocity. This was confirmed by taking a mass spectrometer sample. Reactions with the stainless steel were detected by unexpected pressure drops.

After the series of measurements were complete, the entire system was flushed with Nitrogen. The pump oil was changed, the gas regulator removed, the gas cylinder recapped and the regulator flushed while wearing a gas mask. The entire system was again evacuated awaiting a new series of measurements.

APPENDIX B

COMPUTER PROGRAMS USED TO ANALYZE DATA

Five programs were used to analyze the absorption and velocity data and to make the theoretical calculations reported. These programs are described below. The numbers refer to the numbers actually on the programs.

Program 17 - This program is used to calculate the parameters $\theta(\zeta^2)$ and $Z(1,T)/Z(1,T_o)$ required in Zeleznik's theory. The input consists of M(s.u.), σ(cm), I(cm^2gm), T(^oK), $\Omega(2,2)$, and E*.

Program 18 - This program corrects the experimental velocity data for non-idealality. For a complete discussion of this correction, see Evan's Ph.D. Dissertation (11). The input consists of T(^oK), γ, C_p/R, B, R = .831E 08, M(a.u.), y = 0.0, and F(Hz).

Program 27 - This program was used to analyze absorption data. The "best" relaxation times are found provided they lie within the range of TalMIN - TAlMAX and TA2MIN - TA2MAX. The theoretical curve used for comparison is a parallel relaxation curve with two relaxation times. Input is as follows.

1. Card 1 - Number of data points plus four and the name of the gas.

2. Card 2 - Maximum and minimum values of τ_1 and τ_2 in microseconds and the increment by which they are changed while searching for the best set of τ's.

3. Card 3 - Viscosity (poises), γ, k = 0.0, C_p/R, T(^oK), and F(Hz).

4. Card 4 - Mass (a.u.)

5. Remaining cards are data cards with Pressure (mmHg), Velocity (cm/sec), and Absorption (db/in).

Program 30 - This program is similar to Program 27 except a third relaxation process is considered. The data is first run through Program 27 then the rotational relaxation time is entered on card 4 as a constant and two τ's are used to fit the vibrational relaxation peak. The vibrational specific heats are calculated from the characteristic temperature of vibration. The input is the same as Program 27 except for Card 3 which has Mass (a.u.), $\theta(^oK)$ for the mode associated with τ_1, $\theta_2(^oK)$, and τ_{rot} in microseconds.

Program 30 is used to generate simulated data sets with up to ± 10% experimental error. The experimental data is used as input and the computer prepares five new sets of data with card output.

APPENDIX C

ABSORPTION AND DISPERSION OF ULTRASOUND IN GASES

Consider an infinitesimal cube of material as shown subjected to a stress represented by a stress tensor T_{ij}.

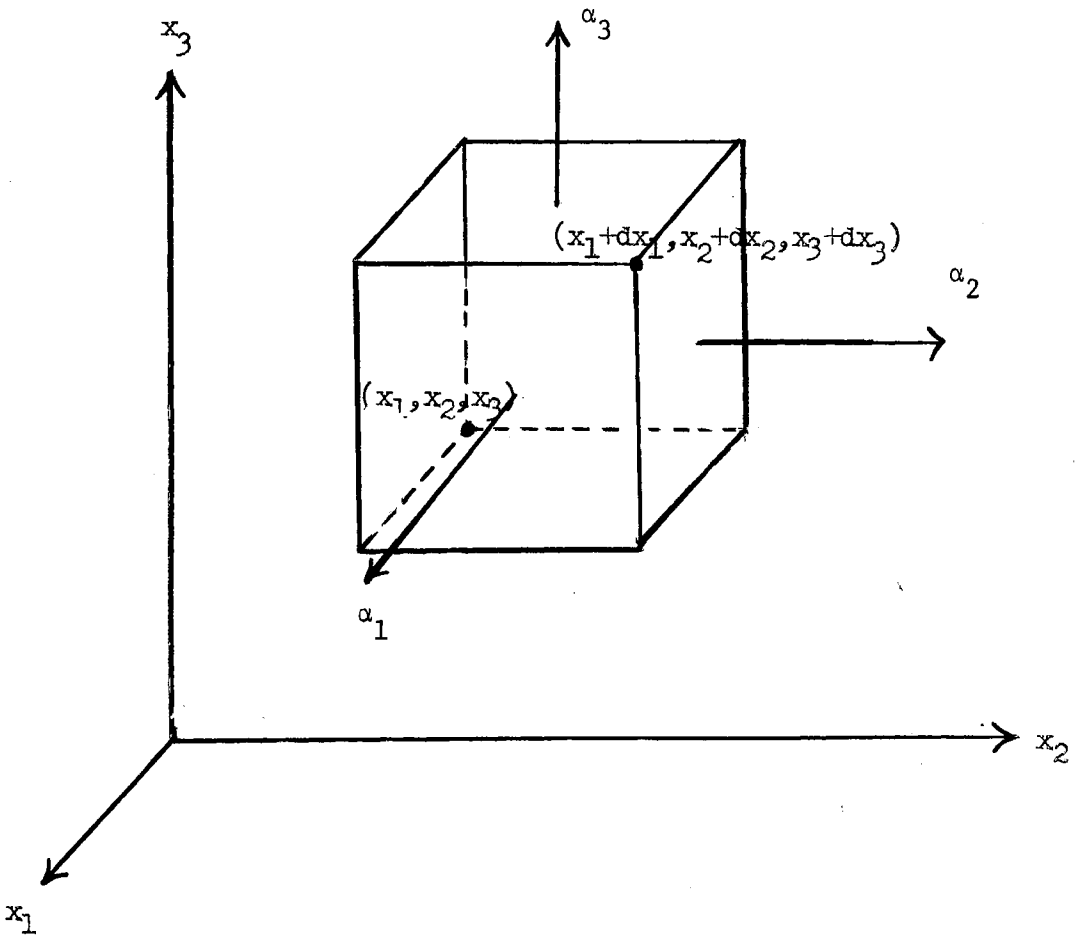

Let T_1 be the force per unit area acting in the $\vec{\alpha}_1$ direction on the front surface of the cube, T_2 be the force per unit area acting in the

$\vec{\alpha}_2$ direction on this surface, and T_3 be the force per unit area acting in the $\vec{\alpha}_3$ direction on the same surface. By definition of T_{ij},

$$\begin{aligned} T_1 &= T_{11}\ (x_1 + dx_1) \\ T_2 &= T_{21}\ (x_1 + dx_1) \\ T_3 &= T_{31}\ (x_1 + dx_1). \end{aligned} \tag{1}$$

On the rear surface, the force per unit area in the $\vec{\alpha}_1$, $\vec{\alpha}_2$, and $\vec{\alpha}_3$ directions respectively are

$$\begin{aligned} T_1 &= T_{11}\ (x_1) \\ T_2 &= T_{21}\ (x_1) \\ T_3 &= T_{31}\ (x_2). \end{aligned} \tag{2}$$

Expanding Equations (1) about x_1, subtracting Equations (2), and multiplying by the area gives for the total force on the front and rear surfaces,

$$\left(\frac{\partial T_{11}}{\partial x_1}\right) dx_1dx_2dx_3 \cdot \vec{\alpha}_1 + \left(\frac{\partial T_{21}}{\partial x_1}\right) dx_1dx_2dx_3 \cdot \vec{\alpha}_2 + \left(\frac{\partial T_{31}}{\partial x_1}\right) dx_1dx_2dx_3 \cdot \vec{\alpha}_3 \tag{3}$$

Similar expressions are obtained for the remaining four faces of the cube. Vectorially adding the forces on all faces gives

$$F_i = \sum_{j=1}^{3} \frac{\partial T_{ij}}{\partial x_j}\, dx_1dx_2dx_3, \tag{4}$$

where F_i is the force on the cube in the $\vec{\alpha}_i$ direction. Using Newton's Second Law, $\vec{F} = m\,\vec{a}$, Equation (4) can be written as

$$\rho \frac{d^2 \xi i}{dt^2} = \sum_{j=1}^{3} \frac{\partial Tij}{\partial xj} . \tag{5}$$

Equation (5) is the equation of motion for the cube of material in Figure 1.

The change in the amount of gas contained in our differential volume element $dx_1 dx_2 dx_3$ in a time interval dt must be equal to the amount flowing into the faces less the amount flowing out. The mass flowing into the $-\vec{\alpha}_1$ face is $\rho u_1(x_1) \cdot dx_2 dx_3$ where u_j denotes the component of velocity in the $\vec{\alpha}_j$ direction. The mass flowing out of the $\vec{\alpha}_1$ face is $\rho u_1(x_1 + dx_1) \cdot dx_2 dx_3$ hence the net increase in mass due to contributions from these two faces is

$$= \rho u_1(x_1 + dx_1) \cdot dx_2 dx_3 + \rho u_1(x_1) \cdot dx_2 dx_3 . \tag{6}$$

Expansion of $\rho u_1(x_1 + dx_1)$ about $\rho u_1(x_1)$, and adding the contributions from the other faces gives the net increase of mass in the volume,

$$\frac{\partial m}{\partial t} = - \sum_{i=1}^{3} \frac{\partial (\rho uj)}{\partial xj} dx_1 dx_2 dx_3 . \tag{7}$$

The mass, m, is the density, ρ, times the volume, $dx_1 dx_2 dx_3$, so Equation (7) can be written as

$$\frac{\partial \rho}{\partial t} + \sum_{i=1}^{3} \frac{\partial}{\partial xj} (\rho uj) = 0. \tag{8}$$

Let $\rho = \rho_o + \delta\rho$ and assume $\delta\rho << \rho_o$ which is the acoustic approximation. Using this approximation, Equation (8) becomes

$$\frac{\partial \rho}{\partial t} = - \sum_{i=1}^{3} \rho_o \left(\frac{\partial uj}{\partial xj}\right) . \tag{9}$$

Equation (9) is the equation of continuity of mass as it will be used in this dissertation.

Before proceeding further some assumptions must be made as to the mathematical form of the stress tensor, T_{ij}. Ideally, this tensor would be obtained by solving the Boltzmann equation and several such attempts have been made. Greenspan (51) discusses several successive approximate solutions and experimentally shows that the second order approximation is accurate at frequencies below 10^8 Hz at one atmosphere of pressure. The remaining derivations in this section will be based on this approximation. The results of the third order approximation will be discussed later. Using the form used by Bhatia (52),

$$T_{ij} = (-P + \eta' \nabla \cdot u)\, \delta ij + 2\, \eta\, \dot{e}_{ij}, \tag{10}$$

where P = hydrostatic pressure,

η' = second coefficient of viscosity,

Δ = dilitation = $\nabla \cdot \vec{\xi}$

η = shear viscosity, and

e_{ij} = strain = $\frac{1}{2}\left(\frac{\partial \xi i}{\partial xj} + \frac{\partial \xi j}{\partial xi}\right)$.

Combining Equations (5) and (10),

$$\rho \frac{dui}{dt} = - \frac{\partial P}{\partial x_i} + \{\eta \nabla^2 u_i + (\eta + \eta') \frac{\partial}{\partial x_i} \left(\frac{\partial u_j}{\partial xj}\right)\}. \tag{11}$$

Using the acoustic approximation,

$$\rho_o \frac{\partial u_j}{\partial t} = - \left(\frac{\delta P}{\delta \rho}\right) \frac{\partial \rho}{\partial x_i} + \{\eta \nabla^2 U_i + (\eta + \eta') \frac{\partial}{\partial x_i} \left(\frac{\partial u_j}{\partial x_j}\right)\}. \tag{12}$$

Differentiating with respect to time, and combining with Equation (9),

$$\rho_o \frac{\partial^2 u_i}{\partial t^2} = \rho_o \left(\frac{\delta P}{\delta \rho}\right) \frac{\partial}{\partial x_i} \left(\frac{\partial u_j}{\partial x_j}\right) + \frac{\partial}{\partial t} \{\eta \nabla^2 u_i + (\eta + \eta') \frac{\partial}{\partial x_i} \left(\frac{\partial u_j}{\partial x_j}\right)\} \tag{13}$$

For one-dimensional motion, $u_2 = u_3 = 0$, and

$$\rho_o \frac{\partial^2 u_1}{\partial t^2} = \rho_o \left(\frac{\delta P}{\delta \rho}\right) \frac{\partial^2 u_1}{\partial x_1^2} + (\eta' + 2\eta) \frac{\partial}{\partial t} \left(\frac{\partial^2 u_1}{\partial x_1^2}\right). \tag{14}$$

Assume the motion is plane harmonic, so

$$u_1 = A \cdot \exp[i \cdot \omega t - k x_1)] . \tag{15}$$

Combining Equations (14) and (15) gives

$$k^2 = \omega^2 \left(\frac{\delta P}{\delta \rho}\right)^{-1} \{1 + i\omega (\eta' + 2\eta) \frac{1}{\rho_o} \left(\frac{\delta P}{\delta \rho}\right)^{-1}\}^{-1} . \tag{16}$$

Next consider the effects of heat conduction. According to Kirchhoff's law, the heat flow into our volume in the $\vec{\alpha}_1$ direction is

$$m \frac{dq}{dt} = - \nu \left(\frac{\partial T}{\partial x 1}\right)_{x=x_1} dx_2 dx_3 \tag{17}$$

where ν = thermal conductivity.

The heat flowing out of the volume is this same term evaluated at $x = x_1 + dx_1$ so the net heat flow in the $\vec{\alpha}_1$ direction is the difference or

$$\rho_o \cdot dx_1 dx_2 dx_3 \cdot \frac{dq}{dt} = -\nu \cdot \frac{\partial T}{\partial x_1} dx_2 dx_3 + \nu \frac{\partial T}{\partial x_1} dx_2 dx_3 + \nu \cdot dx_2 dx_3 \cdot \frac{\partial^2 T}{\partial x_1^2} dx_1. \tag{18}$$

Multiplying by the mass of one mole, and dividing by the mass, gives

$$\frac{\partial Q}{\partial t} = \frac{\nu M}{\rho_o} \frac{\partial^2 T}{\partial x_1^2} \tag{19}$$

Using the First and Second laws of thermodynamics,

$$Tds = C_v dT + T(\partial P/\partial T)_V dV \tag{20}$$

Using the acoustic approximation and further assuming that the acoustic wave is adiabatic,

$$dQ = C_v dt - \frac{TM}{\rho_o^2} \cdot (\partial P/\partial T)_\rho d\rho. \tag{21}$$

Differentiating Equation (21) with respect to time and substituting into Equation (19) gives

$$C_v \frac{\partial T}{\partial t} = \frac{\nu m}{\rho_o} \cdot \frac{\partial^2 T}{\partial x_1^2} + \frac{TM}{\rho_o^2} \left(\frac{\partial P}{\partial T}\right)_\rho \left(\frac{\partial \rho}{\partial t}\right). \tag{22}$$

Let the temperature and density variations associated with the sound wave vary harmonically, so

$$\begin{aligned} \delta T = T - T_o &= B \cdot \exp\left[i(\omega t - kx_1)\right], \; T_o >> \delta T \\ \delta\rho = \rho - \rho_o &= C \cdot \exp\left[i(\omega t - kx_1)\right], \; \rho_o >> \delta\rho \end{aligned} \tag{23}$$

Substituting Equations (23) into Equation (21) gives

$$i\omega C_v \delta T = - \frac{\nu M}{\rho_o} k^2 \delta T + i\omega \frac{TM}{\rho_o^2} \left(\frac{\partial P}{\partial T}\right)_\rho \delta\rho \ . \tag{24}$$

Writing P as a function of ω and T, and differentiating with respect to time gives,

$$\frac{\partial P}{\partial t} = \left(\frac{\partial T}{\partial \rho_T}\right) \frac{\partial \rho}{\partial t} + \left(\frac{\partial P}{\partial T}\right)_\rho \frac{\partial T}{\partial t} \ . \tag{25}$$

Let P vary harmonically with time and space, so

$$\delta P = P - P_o = D \exp[i(\omega t - kx_1)]. \tag{26}$$

Substituting Equations (23) and (26) into Equation (25) and eliminating δT using Equation (24) gives

$$\left(\frac{\delta P}{\delta \rho}\right) = (\partial P/\partial \rho)_T \left(\frac{C_p - ik^2 \nu M/\rho_o \omega}{C_v - ik^2 \nu M/\rho_o \omega}\right). \tag{27}$$

Substituting Equation (27) into Equation (16) gives the propagation constant in a medium where no relaxation processes are involved,

$$k^2 = \{1 + i\omega (\eta' + 2\eta) \frac{1}{\rho_o} \left(\frac{\partial P}{\partial \rho}\right)_T^{-1} \left(\frac{C_p - ik^2 \nu M/\rho_o \omega}{C_v - ik^2 \nu M/\rho_o \omega}\right)^{-1} \}^{-1} \tag{28}$$

Next, the effects of thermal relaxation will be introduced into the equation for the propagation constant. Consider the volume of gas being compressed and allowed to expand in one dimension due to an ultrasonic wave. Upon compression, the local temperature of the gas increases from its equilibrium value of T_0 to an instantaneous value T_{tr}. If the compressional wave is of long duration (low frequency), the in-

ternal energy of the gas associated with the molecular vibrations and rotations will come into equilibrium with the instantaneous temperature T_{tr}. The time required for an internal degree of freedom to come within e^{-1} of its equilibrium value is defined as the "relaxation time" (τ).

The frequency of the ultrasonic wave determines how close the internal degrees of freedom are allowed to approach their equilibrium values. That is, if the frequency of the wave is large compared to $1/\tau$, the internal degrees of freedom associated with τ will be very nearly in equilibrium with T_{tr} at any time. If $1/f \cong \tau$, the internal energy will differ from its equilibrium value by a factor of e^{-1}. If $1/f << \tau$, the internal degrees of freedom associated with τ are never excited, and the acoustic wave will behave as though those degrees of freedom are not possible. When this situation occurs, the degrees of freedom so affected are said to be "relaxed".

The effect of a "relaxing" degree of freedom may be incorporated into an analytical discussion by using the value of the specific heat of the system which changes as the number of effective degrees of freedom changes. The specific heat can be written as

$$(C_v)_{eff} = C_{trans} + C_{int} \tag{29}$$

The effects of relaxation can now be introduced into Equation (28) by writing $(C_v)_{eff}$ in place of C_v and $(C_p)_{eff}$ in place of C_p. An alternative method involves writing the bulk viscosity, b, as a function of frequency where $b = \eta' + 2/3\eta$. Choosing the first method, Equation (28) becomes

$$\frac{k^2}{\omega^2} = \frac{\rho_o}{B_T} \frac{\{(C_v)_{eff} - iWk^2\}\{(C_p)_{eff} - iWk^2\}^{-1}}{1 + i\omega\cdot(4/3\ \eta/B_T)\cdot\{(C_v)_{eff} - iWk^2\}\{(C_p)_{eff} - iWk^2\}^{-1}} \quad (30)$$

where $B_T = \rho_o(\partial P/\partial\rho)_T$

$W = \nu M/\rho_o\omega$

and $b = 0.$

This is Bhatia's Equation (5.10.2)(52). Bhatia further shows that by expanding $\frac{k^2}{\omega^2}$ in powers of ν and η and retaining at most linear terms gives

$$\frac{k^2}{\omega^2} = \frac{\rho_o}{B_T}\frac{(C_v)_{eff}}{(C_p)_{eff}} - \frac{\rho_o}{B_T}\frac{(C_v)_{eff}}{(C_p)_{eff}}\left[\frac{1}{(C_v)_{eff}} - \frac{1}{(C_p)_{eff}}\right] iWk^2$$

$$- i\omega\cdot\frac{4}{3}\eta\frac{\rho_o}{B_T}\cdot\left[\frac{(C_v)_{eff}}{(C_p)_{eff}}\right]^2. \quad (31)$$

Bhatia next assumes that except for the first term, replacing the effective specific heats with the static specific heats is a good approximation. Evans, Winter, and Bass (53), have shown experimentally that such an approximation is good only when $\nu << \eta$. This is generally true only for heavy gases.

The next step in the development of the absorption and dispersion equations is the derivation of an expression for $(C_p)_{eff}$ as a function of frequency, pressure, relaxation times, and molecular constants of the gas. Let E_1' be the instantaneous energy associated with the ith degree of freedom and E'(Tr) be the value this energy would have in equilibrium at a temperature T_{tr}. The relaxation time for the ith internal mode can then be defined by the equation

$$-\frac{dE'_i}{dt} = \frac{1}{\tau_i}[E'_i - E'(T_{tr})] \quad . \tag{32}$$

If the specific heat of the ith mode, C'_i, doesn't vary significantly with temperature over the range of δT associated with the acoustic wave,

$$E'_i - E'_{oi} = C'_i(T'_i - T_o) \tag{33}$$

where T_o is the static temperature, and E'_{oi} = the equilibrium energy at that temperature. T'_i is the temperature associated with the instantaneous energy E'_i and is defined by Equation (33). Combining Equations (32) and (33),

$$T'_i - T_o + \tau \frac{d}{dt}(T'_i - T_o) = T_{tr} - T_o. \tag{34}$$

$T_{tr} - T_o$ varies harmonically in time from Equation (23) so $T'_i - T_o$ will also vary harmonically with time which leads to

$$T'_i - T_o = \frac{T_{tr} - T_o}{1 + i\omega\tau_i} \tag{35}$$

or

$$\frac{dT'_i}{dT_{tr}} = \frac{1}{1 + i\omega\tau_i} \tag{36}$$

The total energy of the system is $(C_v)_{eff} \cdot dT_{tr}$ so

$$dE = (C_v)_{eff}\, d\,T_{tr} = \bar{C}_v\, d\,T_{tr} + \sum_{i=1}^{n} C'_i\, d\,T'_i = (\bar{C}_v + \sum_{i=1}^{n} C' \frac{dT'_i}{dT_{tr}})dT_{tr} \tag{37}$$

where $\bar{C}_v = C_{trans}$

n = number of internal modes

Combining Equations (36) and (37),

$$(C_v)_{eff} = \bar{C}_v + \sum_{i=1}^{n} \frac{C_i'}{1 + i\omega\tau_i} . \qquad (38)$$

This value of $(C_v)_{eff}$ is substituted into Equation (31) to give the final expression for the propagation constant,

$$\frac{k^2}{\omega^2} = \frac{\rho_o}{B_T} \left\{ \frac{\bar{C}_v + \sum_{i=1}^{n} \frac{C_i'}{1+i\omega\tau_i}}{\bar{C}_p + \sum_{i=1}^{n} \frac{C_i'}{1+i\omega\tau_i}} \right\} - \frac{\rho_o}{B_T} \left\{ \frac{\bar{C}_v + \sum_{i=1}^{n} \frac{C_i'}{1+i\omega\tau_i}}{\bar{C}_p + \sum_{i=1}^{n} \frac{C_i'}{1+i\omega\tau_i}} \right\} \cdot \left\{ \frac{1}{\bar{C}_v + \sum_{i=1}^{n} \frac{C_i'}{1+i\omega\tau_i}} \right.$$

$$\left. - \frac{1}{\bar{C}_p + \sum_{i=1}^{n} \frac{C_i'}{1+i\omega\tau_i}} \right\} iWk^2 - i\omega \cdot \frac{4}{3} \eta \frac{\rho_o}{B_T^2} \left\{ \bar{C}_v + \sum_{i=1}^{n} \frac{C_i'}{1+i\omega\tau_i} \Big/ \bar{C}_p + \sum_{i=1}^{n} \frac{C_i'}{1+i\omega\tau_i} \right\}^2$$

This is the form used in all calculations in the following sections. Although this equation is easily manageable on a computer, the physical meaning of this result is not clear. In order to put this equation in the form used in most books, set $k = \omega/v - i\alpha$ where $\alpha \equiv$ coefficient of absorption. Assume $(C_p)_{eff}$ and $(C_v)_{eff}$ in all but the first term in Equation (39) are approximately equal to C_p and C_v. Further, assume $k^2 \cong \omega^2/v^2 - 2i\frac{\omega\alpha}{v}$ and $\tau_i = 0$ for all $i \neq 1$, then

$$\alpha = \tfrac{1}{2} \frac{v}{v_o^2} \frac{(C_p - C_v)\omega^2\tau_1}{C_v(C_p - C')(1+\omega^2\tau_1^2)} + \frac{2}{3} \frac{\omega^2}{v^3\rho_o} \left[\eta + \frac{3}{4} (\gamma - 1) \frac{\nu}{C_p} \right] \qquad (40)$$

where $\tau' = \frac{C_p - C'}{C_p} \tau_1$, and C_p and C_v are the values of the specific heats at frequencies slightly lower than the frequency at which C' begins to relax. Equation (40) is frequently written as

$$\alpha\lambda = \pi \frac{v^2}{v_o^2} \frac{(C_p - C_v)\omega\tau'^2}{C_v(C_p - C')(1+\omega^2\tau'^2)} + \frac{8\pi^2}{3} \frac{f}{P} \left[\eta + \frac{3}{4}(\gamma-1)\frac{\nu}{C_p}\right] \cdot \frac{1}{\gamma} \quad (41)$$

For experimental purposes, the quantity f/P is the quantity of importance. In Equation (41), ω can be replaced by 2π f/P without changing the result provided the relaxation process involves only binary collisions. This will not be obvious until after the discussion of probability of energy transfer.

So far, the thermal conductivity has been considered a constant as has the viscosity. Mason and Monchick (23) have shown that the thermal conductivity is a rather complicated function of the relaxation times τ_i and the relaxing specific heats. Using the simpler Eucken (17) approximation,

$$\frac{\nu M}{\eta} = 1 + \frac{9}{4}\frac{R}{C_v} \quad (42)$$

and replacing C_v with $(C_v)_{eff}$ gives

$$\nu = \frac{\eta}{M}\left\{1 + \frac{9}{4} R \left[\bar{C}_v + \sum_{i=1}^{n} \frac{C_i}{1+i\omega\tau_i}\right]\right\} \quad (43)$$

Equation (45) was used for the thermal conductivity in all calculations reported in his dissertation.

Before closing this section and proceeding to theoretical expressions for the τ_i's, a word should be said about the results of using a more accurate stress-strain relation. Greenspan (51) has shown that the best relation to use for some monatomic gases is the Burnett expression. He also derives an expression for the propagation constant in terms of the frequency, pressure, specific heats, and other molecular

constants. The effects of relaxation can be introduced by means of a frequency dependent specific heat as was done here for the Navier-Stokes relation. Next, the expression would have to be expanded in powers of ν and η to get an expression analagous to Equation (39). Such a development is beyond the scope of this investigation.

VITA

Henry Ellis Bass

Candidate for the Degree of

Doctor of Philosophy

Thesis: ENERGY TRANSFER IN POLAR POLYATOMIC GASES

Major Field: Physics

Biographical:

Personal Data: Born at Tulsa, Oklahoma, August 31, 1943, the son of Henry U. and Hazel A. Bass.

Education: Graduated from McLain High School, Tulsa, Oklahoma, in 1961; received the Bachelor of Science degree from Oklahoma State University, Stillwater, Oklahoma, in May, 1965, with a major in Physics; completed requirements for the Doctor of Philosophy degree in May, 1971.

Other: General Motors Corporation Scholar, 1962-1965; National Science Foundation Trainee, 1967-1970; member Sigma Pi Sigma Physics Honor Society; student member of the Acoustical Society of America; co-author of a letter entitled "Capacitor Microphone With Ceramic Diaphragm", published in the Journal of the Acoustical Society of America, 1966; co-author of a letter entitled "Precautions With Classical Absorption", published in the Journal of the Acoustical Society of America, October, 1970; co-author of a paper entitled "Vibrational and Rotational Relaxation in Sulphur Dioxide", to be published in the Journal of Chemical Physics; co-author of a paper entitled "Ultrasonic Absorption in Hydrogen Sulfide", to be published in the Journal of the Acoustical Society of America; co-author of a paper entitled "Ultrasonic Absorption in Ammonia", to be published in the Journal of the Acoustical Society of America, co-author of a letter entitled "Ultrasonic Absorption in Hydrogen", to be published in the Journal of the Acoustical Society of America.